UNIVERSIDADE DE SÃO PAULO
CENTRO DE ENERGIA NUCLEAR NA AGRICULTURA

MARCOS HENRIQUE FERESIN GOMES

Characterization of the foliar uptake of zinc sources by soybean (*Glycine max* L.)

Piracicaba
2021

MARCOS HENRIQUE FERESIN GOMES

Characterization of the foliar uptake of zinc sources by soybean (*Glycine max* L.)

Thesis presented to Center for Nuclear Energy in Agriculture of the University of Sao Paulo as a requisite to the Doctoral Degree in Sciences

Concentration Area: Chemistry in Agriculture and Environment

Advisor: Prof. Hudson Wallace Pereira de Carvalho

Piracicaba

2021

Dados Internacionais de Catalogação na Publicação (CIP)

Seção Técnica de Biblioteca - CENA/USP

Gomes, Marcos Henrique Feresin

Caracterização da absorção foliar de fontes de zinco pela cultura da soja (*Glycine max* L.) / Characterization of the foliar uptake of zinc sources by soybean (*Glycine max* L.) / Marcos Henrique Feresin Gomes; orientador Hudson Wallace Pereira de Carvalho. - - Piracicaba, 2021.

103 p.

Tese (Doutorado – Programa de Pós-Graduação em Ciências. Área de Concentração: Química na Agricultura e no Ambiente) – Centro de Energia Nuclear na Agricultura da Universidade de São Paulo, Piracicaba, 2021.

1. Adubação foliar 2. Espectroscopia de raio X 3. Fertilizantes 4. Microesferas de celulose 5. Nanopartículas 6. Nutrição vegetal 7. Soja 8. Zinco I. Título.

CDU (543.42 + 546.47) : 581.13

Elaborada por:
Marilia Ribeiro Garcia Henyei
CRB-8/3631
Resolução CFB Nº 184 de 29 de setembro de 2017

ACKNOWLEDGMENTS

I would like to begin thanking God for my physical and psychological health during all these years beginning with the master and PhD.

Secondly, I would like to thank to my family, my parents Margarete Feresin Gomes and Marcos Gonçalves Gomes and my sister Marilia Feresin Gomes for the incentive and support during the bad and good times.

I want to thank in special, Prof. Dr. Rafael Otto and Tiago Tezotto for the instructions on the beginning of my research carrier, without your advices I probably would not start a postgrad.

I would like to thank all the members of de Laboratory of Nuclear Instrumentation. Prof. Hudson and Eduardo Almeida, my advisors, friends, partners in business (and sometimes accomplices in my crazy ideas). I will be always grateful for all the knowledge, advices, technical discussions and happy hours on gas stations and Brahma cans. I am also grateful to my lab mates Daddy Eduardo Casca (my eternal fan number one), Bianca Bráci-k (the most intelligent country girl of the world), Gabriel Lãmbe (the future craziest and brilliant Brazilian researcher), João Paulo Rodrigues (our microscopy oracle), Camila Correa (tireless and sweet worker) and Thainara Rabelo (the grumpy carioca).

Special thanks to the undergrad students Marden Moraes, Fábio Corrêa, Laura Rodrigues, Marcela Góes, César Mendes for the opportunity to work and collaborate with you guys. I also would like to thank all others who helped me during this journey in special, Rafaela Migliavacca, Prof. José Lavres, Nádia Duran and Rizely Ferraz-Almeida.

I would like to thank the members of the biobeads group of the University of Bath, in special, my supervisors Prof. Davide Mattia and Prof. Karen Edler, and my workmate Ciaran Callaghan for the cultural and technical knowledge I got in Bath – UK.

Last, but not least, I would like to thank the University of São Paulo, the Center for Nuclear Energy in Agriculture (CENA), the Coordenação de Aperfeiçoamento de Pessoal de Nível Superior - Brasil (CAPES) - Finance Code 001, and the Brazilian Synchrotron Light Laboratory (LNLS), in special Dr. Carlos Alberto Perez, for providing me all the necessary facilities and funding for developing this work.

ABSTRACT

GOMES, M. H. F. **Characterization of the foliar uptake of zinc sources by soybean (*Glycine max* L.).** 2021. 103 p. Tese (Doutorado em Ciências) – Centro de Energia Nuclear na Agricultura, Universidade de São Paulo, Piracicaba, 2021.

Zinc (Zn) is an essential element for plant, animal and human nutrition. Around the world, *ca*. 800,000 children under 5 years die annually due to a Zn-deficient diet. The application of zinc in crops can be performed on plant leaves or in the soil, however, the low use-efficiency is remarkable. This study aims to understand and characterize the absorption, transport and metabolization of Zn when applied on soybean leaves by the most common fertilizers used by worldwide, *i.e*. inorganic salts, complexes/chelates, and concentrated suspensions, as well as evaluate possibility of the employment of new technologies, such as nanoparticles and cellulose microspheres. X-ray fluorescence (XRF) and X-ray absorption (XANES) spectroscopy were employed to perform *in vivo* analysis on soybean plants together with greenhouse trials. The absorption and transport of Zn depended on the type of Zn source. Zinc from $ZnSO_4$ was absorbed and transported faster than ZnO commercial suspension, while Zn applied as Zn-phosphite was transported faster than Zn-EDTA. The XANES analysis demonstrated that Zn from $ZnSO_4$ and Zn phosphite was transported bound with organic acids such as malate and citrate. Conversely, Zn supplied by Zn-EDTA was transported in its pristine form. In a short-term experiment, *i.e*. few days, cellulose microspheres were able to reduce the toxicity caused by $ZnSO_4$ salts and increase Zn transport trough leaf petiole. However, under longer evaluation, *i.e*. a couple of weeks, the root application of $ZnSO_4$ increased by 42% the Zn accumulation in soybean plants compared to the control (low Zn supply). Additionally, root uptake mechanism under hydroponics was more efficient than the foliar application of $ZnSO_4$, ZnO nanoparticles and $ZnSO_4$ + cellulose microspheres. The foliar and root application of Zn did not affect the activity of ezymes related to the metabolism of reactive oxygen species. Understanding the mechanisms ruling the foliar absorption and metabolization of nutrients is fundamental for the development of the next generation of fertilizers. Therefore, more studies on this subject are necessary.

Keywords: Zn. Foliar fertilization. X-Ray Fluorescence Spectroscopy (XRF). X-Ray Absorption Near Edge Spectroscopy (XANES). Cellulose microbeads. Nanoparticles.

RESUMO

GOMES, M. H. F. **Caracterização da absorção foliar de fontes de zinco pela cultura da soja (*Glycine max* L.).** 2021. 103 p. Tese (Doutorado em Ciências) – Centro de Energia Nuclear na Agricultura, Universidade de São Paulo, Piracicaba, 2021.

O zinco (Zn) é um elemento essencial para a nutrição vegetal, animal e humana. Em todo o mundo, aproximadamente 800.000 crianças menores de 5 anos morrem anualmente devido a deficiência de Zn em suas dietas. A aplicação de Zn nas lavouras pode ser realizada nas folhas ou no solo, porém, é notável a baixa eficiência de sua utilização. Este estudo buscou caracterizar e entender a absorção, transporte e metabolização de Zn quando aplicado em folhas de soja pelas fontes de fertilizantes mais utilizadas mundialmente, *i.e*. sais inorgânicos, complexos/quelatos e suspensões concentradas, bem como avaliar a possibilidade de utilização de novas tecnologias, tais como nanopartículas e microesferas de celulose. As espectrometrias de fluorescência (XRF) e absorção de raios X (XANES) foram empregadas na realização de análises *in vivo*, juntamente com ensaios em casa de vegetação. A absorção e transporte de Zn foram dependentes da fonte aplicada. O Zn aplicado como $ZnSO_4$ foi mais rapidamente absorvido e transportado do que aquele provindo de suspensão concentrada comercial, ao passo que o Zn aplicado como fosfito de Zn foi transportado mais rápido quando comparado ao Zn-EDTA. A ferramenta XANES demonstrou que o Zn aplicado como $ZnSO_4$ e fosfito de Zn foi transportado ligado a ácidos orgânicos, como malato e citrato, por outro lado, o Zn advindo do Zn-EDTA permaneceu em sua forma primitiva. Em um curto período, *i.e*. alguns dias, as microesferas de celulose foram capazes de reduzir a toxicidade causada pelo $ZnSO_4$ e aumentar o transporte de Zn no pecíolo das folhas. Contudo, em avaliações mais longas, *i.e*. na escala de semanas, a aplicação de $ZnSO_4$ na raiz aumentou em 42% o acúmulo de Zn nas plantas de soja em relação ao controle (baixo suprimento de Zn). A capacidade de transferência de Zn pela via radicular, em solução nutritiva, também foi maior do que aquela oferecida pela aplicação foliar de $ZnSO_4$, nanopartículas de ZnO e $ZnSO_4$ + microesferas de celulose. A aplicação foliar e radicular de Zn não afetou o a atividade das enzimas do sistema antioxidante. Compreender os mecanismos que regem a absorção foliar e a metabolização de nutrientes é fundamental para o desenvolvimento da próxima geração de fertilizantes, portanto mais estudos nesta temática são necessários.

Palavras-Chave: Adubação foliar. Espectroscopia por Fluorescência de Raios X (XRF). Espectroscopia de Absorção de Raios X Próximo da Borda (XANES). Microesferas de celulose. Nanopartículas.

SUMMARY

1 INTRODUCTION

Due to the high protein content, soybean [*Glycine max* (L.) Merrill] is an important crop for the global agricultural and food industry. Soybean is the legume with the highest amino acid score and closest to the standard set by the Food and Agriculture Organization (FAO) and World Health Organization.[1] Besides the nutritional value provided by its energy and protein content, the main advantage of soybean for human health is the high level of isoflavones which is several orders of magnitude higher than that found in other commercial legumes. These isoflavones can prevent cancer and work as antioxidants for vitamins regeneration.[1] Currently, Brazil occupies the spot of biggest soybean grower and exporter, cultivating a land size of 38,5 million hectares and exporting approximately 85 million ton in 2021.[2]

Zinc is an essential element for plant, animal and human nutrition. It is estimated that about 10% of all the proteins in the human body, are Zn-dependent.[3; 4] Therefore, clinical or subclinical Zn deficiency is associated with a wide range of physiological issues, especially in developing countries.[5] Around the world, ca. 800,000 children under 5 years die annually due to a Zn-deficient diet.[6] In plant metabolism, Zn is involved in several processes like maintenance of the cell membrane integrity, metabolism of carbohydrates, synthesis of protein and growth hormone.[7] However, the availability of Zn in most cultivated soils is low. A survey sampling performed on Brazilian agricultural areas revealed that approximately 35% of the soils were Zn deficient.[8]

The application of zinc in soybean crops is a well-established practice, being performed on plant leaves or in the soil, alone or together with NPK fertilizers.[9] However, the low use-efficiency of micronutrients agriculture is remarkable. According to Cunha et al.,[10] between 2009 and 2012, Brazilian agriculture applied 2.7 times the amount of Zn exported by crops. Increasing the efficiency of fertilizer is fundamental, not only from an economic perspective, but also from an environmental one.

Zinc can be sprayed on plant leaves as inorganic compounds, for example oxides, carbonates, sulfates, chlorides, nitrates, phosphites, synthetic chelates, *e.g*. ethylenediamine tetra-acetic acid (EDTA), and organic complexes.[11] The Zn absorption by plant leaves is directly influenced by physical-chemical characteristics of the source employed, such as solubility in water.[12] The soluble sources present faster absorption rates compared to the low solubility ones. However, since plant-nutrient demand is not linear, the employment of these regular sources can cause phytotoxicity by nutrient excess deposited on plant leaves or deficiency due to the low availability. Hence, one needs

to seek the development of Zn sources whose profile of release matches the plant needs. This is an alternative to improve nutrient use-efficiency and crops yields with low environmental impact.

1.1 Hypothesis

I. The Zn absorption and transport kinetics by soybean leaves change according to the fertilizer employed;

II. Zinc metabolization form varies according to the source applied on the leaves;

III. New sources such as nanoparticles and microcapsules can be used to supply Zn to soybean leaves more efficiently than the common sources used worldwide.

1.2 Objectives

The general objective of the thesis is to evaluate the absorption, transport and metabolization of Zn by soybean leaves when applied by the main used fertilizers worldwide and to develop new sources which are able to supply Zn for leaves more efficiently.

In the second chapter it was characterized the Zn foliar absorption and transport kinetics, as well as the metabolized form when applied by an inorganic salt (sulphate) and a concentrated suspension fertilizer (ZnO 480 nm).

The third chapter shows the evaluation of Zn foliar absorption, transport and metabolism by soybean leaves when applied by a chelated (Zn-EDTA) and a complexed (Zn-Phosphite) source.

The fourth chapter shows the development and characterization of a microsphere containing $ZnSO_4$ followed by the evaluation of Zn foliar absorption and transport when supplied by this new source and ZnO nanoparticles.

1.3 Structure of the thesis

This thesis comprises an introductory text (chapter 1) followed by three chapters. Chapters 2 & 3 were already published by a peer reviewed journal. The original texts were adapted to comply with institutional format requirements.

Chapter 2: GOMES, M. H. F. et al. In vivo evaluation of Zn foliar uptake and transport in soybean using X-ray absorption and fluorescence spectroscopy. **Journal of Agricultural and Food Chemistry**, v. 67, n. 44, p. 12172-12181, 2019.

Chapter 3: GOMES, M. H. F. et al. Foliar application of Zn phosphite and Zn EDTA in soybean (*Glycine max* (L.) Merrill): In vivo investigations of transport, chemical speciation, and leaf surface changes. **Journal of Soil Science and Plant Nutrition,** v. 20, p. 2731-2739, 2020.

Chapter 4: GOMES, M. H. F. et al. Soybean Zn absorption and development with nanoparticle and bead fertilizers. To be published.

References

1 BURSSENS, S. et al. Soya, human nutrition and health. In: EL-SHEMY, H. **Soybean and nutrition**. London: IntechOpen, 2011. p. 157-180.

2 COMPANHIA NACIONAL DE ABASTECIMENTO. **Acompanhamento da safra brasileira:** grãos, safra 2020/2021, 11º levantamento. Brasília, DF: Conab, 2021.

3 ANDREINI, C. et al. Zinc through the three domains of life. **Journal of Proteome Research,** v. 5, n. 11, p. 3173-3178, 2006.

4 KREZEL, A.; MARET, W. The biological inorganic chemistry of zinc ions. **Archives of Biochemistry and Biophysics,** v. 611, p. 3-19, 2016.

5 CAKMAK, I.; KUTMAN, U. B. Agronomic biofortification of cereals with zinc: a review. **European Journal of Soil Science,** v. 69, n. 1, p. 172-180, 2018.

6 CAULFIELD, L. E.; BLACK, R. E. Zinc deficiency. In: EZZATI, M. et al. (eds.). **Comparative quantification of health risks:** global and regional burden of disease attribution to selected major risk factors. Geneva: WHO, 2004. p. 257–279.

7 BROADLEY, M. et al. Function of nutrients: micronutrients. In: MARSCHNER, P. **Marschner's mineral nutrition of higher plants**. San Diego: Academic Press, 2012. p. 191-248.

8 GUILHERME, L. R. G. et al. Zinc availability in brazillian agroecosystems. In: International Zinc Symposium, 4., 2015, São Paulo. **Improving Crop Production and Human Health; proceedings.** São Paulo: Fertilizer Canada, 2015. p. 59-49.

9 LOPES, A. S. **Micronutrientes:** filosofias de aplicação e eficiência agronômica. São Paulo: ANDA, 1999.

10 CUNHA, J. F.; FRANCISCO, E. A. B.; CASARIN, V.; PROCHNOW, L. I. **Balanço de nutrientes na agricultura brasileira no período de 2009 a 2012**. Piracicaba: International Plant Nutrition Institute, 2018. (Informações Agronômicas, n. 145).

11 MONTALVO, D. et al. Agronomic effectiveness of zinc sources as micronutrient fertilizer. **Advances in Agronomy**, v. 139, p. 215-267, 2016.

12 FERNANDEZ, V.; STIROPOULOS, T.; BROWN, P. H. **Foliar fertilization:** scientific principles and field pratices. Paris: International Fertilizer Industry Association, 2013.

2 IN VIVO EVALUATION OF Zn FOLIAR UPTAKE AND TRANSPORT IN SOYBEAN USING X-RAY ABSORPTION AND FLUORESCENCE SPECTROSCOPY[1]

Abstract

Understanding the mechanisms of absorption and transport of foliar nutrition is a key step towards the development of advanced fertilization methods. This study employed X-ray fluorescence (XRF) and X-ray absorption near edge spectroscopy (XANES) to trace the in vivo absorption and transport of ZnO and $ZnSO_{4(aq)}$ to soybean leaves (*Glycine max*). XRF maps monitored over 48 h showed a shape change of the dried $ZnSO_{4(aq)}$ droplet, indicating Zn^{2+} absorption. Conversely, these maps did not show short movement of Zn from ZnO. XRF measurements on petioles of leaves that received Zn^{2+} treatments clarified that the Zn absorption and transport in the form of $ZnSO_{4(aq)}$ was faster that of ZnO. Solubility was the major factor driving $ZnSO_{4(aq)}$ absorption. XANES speciation showed that in planta Zn is transported coordinated with organic acids. Because plants demand Zn during their entire lifecycle, the utilization of sources with different solubilities can increase Zn use efficiency.

Keywords: zinc; foliar absorption; nutrient uptake; suspension; XRF; XANES

2.1 Introduction

Foliar fertilization is an important tool for the sustainable and productive management of crops. This approach is useful to supply nutrients to plants when soil conditions limit their availability to roots, as for example in the case of micronutrients under high pH conditions.[1] Additionally, foliar fertilization reduces application costs and nutrient losses that occur by adsorption and leaching, which are far more likely to occur through soil fertilization.[2] Foliar fertilization is also employed to elicit a quick response to correct a nutritional deficiency. Specific nutrients with lower mobility such as boron and zinc are often used complementing

---

[1] Reprinted (adapted) with permission from {GOMES, M. H. F. et al. In vivo evaluation of Zn foliar uptake and transport in soybean using X-ray absorption and fluorescence spectroscopy. **Journal of Agricultural and Food Chemistry**, v. 67, n. 44, p. 12172-12181, 2019}. Copyright {2019} American Chemical Society.

soil fertilization.[3] For instance, foliar fertilization of these nutrients during the "prebloom" stage of apples, resulted in very high crop yields.[4]

Nearly 10% of all proteins in the human body are Zn-dependent.[5] Zinc deficiency, along with other micronutrients especially in developing countries, is responsible for great economic losses and has a considerable effect on the gross domestic product by decreasing productivity and increasing the health care costs.[6; 7] Nearly 50% of world soils used for cereal production contain low levels of Zn, which reduces not only grain yield but also overall nutritional grain quality.[8] According to Brazilian agricultural practices, when concentrations of Zn in the soil are below 0.5 mg Zn kg^{-1} it's availability is considered low,[9] and therefore Zn has to be supplied as fertilizer.

Foliar Zn application is more effective at increasing grain Zn concentration than soil supply, and thus, this approach has become an important tool for grain biofortification.[10]

Many forms of Zn foliar fertilizers have been used, they can be applied as aqueous solutions of salts ($ZnSO_4$, $ZnCl_2$ or $Zn(NO_3)_2$), as chelates (Zn-EDTA), or as suspensions of finely ground minerals (*e.g* oxides and carbonates).[11] Although the soluble inorganic salt grants rapid absorption due to the fully availability of the nutrients, at high concentrations their field application may easily cause phytotoxicity in sprayed leaves and other organs.[12] On the other hand, low solubility sources, such as ZnO and $ZnCO_3$, even at high dosage did not demonstrate good leaf uptake results.[13; 14]

Once deposited on the leaf surface Zn^{2+} has to penetrate the cuticle or enter through the stomatal cavity, traverses the inner cells via apoplastic or symplastic pathways and then be loaded into the foliar vascular system.[1; 15] Du et al.[16] employed X-ray fluorescence microanalysis to investigate the movement of Zn in detached tomato and citrus leaves that were exposed for 24 h to Zn. They observed that once the Zn had moved through the leaf, three crucial processes were important for the subsequent redistribution of Zn within the leaf: (1) the redistribution of Zn within the interveinal tissues themselves, (2) the movement of Zn from the interveinal tissues into the adjacent lower-order veins, and (3) the movement of Zn into the higher-order veins for its subsequent redistribution through the leaf.[16] Accordingly, a more recent study on soybean and tomato showed also a rapid accumulation of Zn in leaf veins, observable as soon as of six hours after dripping a $ZnSO_4$ solution on the leaf surface.[17]

Nevertheless, the penetration mechanisms of hydrophilic polar solutes through the cuticle, the overall contribution of the stomatal pathway and the movement of newly absorbed Zn into the vascular system and its subsequent transport to the phloem are not fully understood yet.[1; 13; 18] Therefore, the comprehension of penetration mechanisms as well as the

nutrient transport, via foliar-applied nutrients, is crucial to the optimization of high performance fertilizers with better absorption rates and lower losses to the environment.

The properties of low solubility Zn sources, such as ZnO or $ZnCO_3$, can be explored to yield slow release fertilizers. Assuming that small particles, in the nanometer size range, can be entirely absorbed by plants, then can be slowly dissolved inside the bundles or cells. It would enable supplying higher loads of micronutrients while avoiding phytotoxicity. Same result would be achieved with nanoparticles sticking on the outside of leaves and slowly releasing ions that would be eventually absorbed through foliar feeding. These approaches can reduce both the costs of fertilizer application and losses due to leaching or strong adsorption of ions into soil colloidal particles.

X-ray fluorescence (XRF) spectroscopy is a well-known technique for qualitative and quantitative elemental evaluation. Unlike other techniques such as laser-induced breakdown spectroscopy (LIBS), atomic absorption spectroscopy (AAS), and inductively coupled plasma optical emission spectrometry (ICP OES), which are destructive, XRF allows the analysis of living materials.[19] It means that absorption and transport phenomena can be traced while they are happening. Assuming that plants have defense responses induced by stress conditions,[20] harvesting and sample processing (e.g., drying and grinding) can induce changes in plant metabolism and consequently distance the results obtained by the regular techniques from the field conditions. In this scenario, the XRF technique becomes an interesting tool to analyze plants metabolism in vivo.

Therefore, the goal of the present study was to explore foliar absorption and short distance transport from high and low solubility Zn sources, such as $ZnSO_4$ and ZnO, respectively. Soybean (*Glycine max* (L.) Merrill) was chosen as model plant species due to its economic importance. The differential of our study from previously X-ray based studies is the use of X-ray fluorescence (XRF) and X-ray absorption near edge spectroscopy (XANES) on whole plants rather than on detached leaves.

2.2 Materials and methods

The plants were grown in greenhouse in vermiculite watered daily with deionized water until the V3 phenological stage was reached. Then, they were assembled in a sample holder and received the foliar application of the fertilizers. Immediately after the application, the plants were transferred to a growth room at 27 ºC, air relative humidity of 80% and photoperiod of 12 h under 6500 K LED lamps illumination supplying 250 µmol photons m^{-2} s^{-1}.

The treatments consisted of aqueous solution of $ZnSO_4.7H_2O$ (Merck, Germany) and a ZnO aqueous dispersion (YARA, NO). The solutions and dispersions were prepared using deionized water. The concentrations employed and described below are presented as weight of Zn per volume of water.

Treatments were characterized by measuring the pH, contact angle on the leaf surface and droplet drying time. For the ZnO source we also registered X-ray diffraction pattern, scanning electron microscopy images, measured the fraction of soluble Zn and the hydrodynamic diameter by means of dynamic light scattering.

2.2.1 Characterization of ZnO suspension and $ZnSO_{4(aq)}$ solution

2.2.1.1 pH

The pH was determined using a pH meter (TEC-2, TECNAL, BRA). The fertilizers were transferred to 50 mL beckers and diluted up to 2,300 mg L^{-1} using deionized water. Then, the measurements were performed introducing the equipment electrode directly on the fertilizer suspension/solution.

2.2.1.2 Contact angle

The contact angle was measured to determine the contact surface between the fertilizer and the leaves, which influence directly the interaction between them and consequently the foliar uptake of nutrients.

It was performed on the University of São Carlos in Sorocaba - SP using a Goniometer/Tensiometer (Model 500 Advanced, Ramé-hart, USA, Figure 1 (A)). For analysis, 5 µl droplets of each fertilizer at 2,300 mg L^{-1} of Zn was applied up to the abaxial face of the leaf and elapsed one minute for stabilization (Figure 1 (B)), it was performed the measurements in triplicate. The results were analyzed on the DROP image Advanced software.

Figure 1 - (A) Ramé-hart Model 500 Advanced Goniometer/Tensiometer equipment; (B) Set up of the droplet for analysis; (C) Images of the $ZnSO_4$ and ZnO droplets dripped on the abaxial face of a soybean leaf

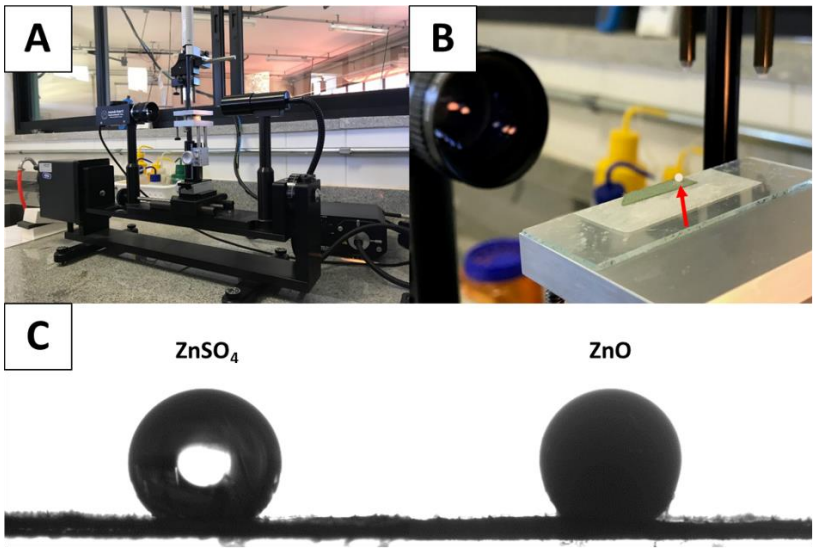

2.2.1.3 Droplet drying time

The drying time was determined taking pictures of droplets of the fertilizers applied on the abaxial face of a leaf each two minutes. Each droplet had 5 µl and 2.300 mg L^{-1} of Zinc. The pictures were taken by a D3100 Nikon camera with a 18-55 mm lengths.

2.2.1.4 X-ray diffraction spectroscopy

Aiming at determining the crystallite size of the ZnO tested, it was performed XRD analysis (PW3710, PHILLIPS, NL). The instrumental broadening was subtracted. These sizes were determined using the Scherrer equation (Equation 1).

$$D\ (nm) = \frac{K\lambda}{\beta \cos\theta} \quad (1)$$

D, crystallite size in nanometers

K, Scherrer constant (0.94 for spherical crystals with cubic symmetry);

λ, wavelength of light used for the diffraction (0.154184 nm to Cu);

β, FWHM (full width at half maximum) of the peak;

θ, angle measured.

2.2.1.5 Scanning electron microscopy

The scanning electron microscope images were taken on the Structural Characterization Laboratory of the University of São Carlos in São Carlos - SP. The fertilizer was dripped directly on an aluminum foil assembled on a sample holder and dried in air for 24 h. The readings were performed on the Magellan 400 L (EDAX Ametek, USA) facility.

2.2.1.6 Solubility

The partial of soluble Zn in the fertilizer was determined analyzing its concentration in the original fertilizer with and without centrifugation by XRF technique using thin film method. The fertilizer was transferred to two plastic vials of 1 mL, centrifuging one of them for one hour at 1.300 rotations per minute on a centrifuge machine (Mikro 120, Hettich Instruments). Then, 950 µL of each sample was transferred to other vials adding 50 uL of the 1,003 mg Ga L^{-1} internal standard (1:10 dilution from Aldrich 10,030 mg Ga L^{-1}). Fifteen mL of the final solutions were dripped up to a 6.3 mm window XRF cuvette (no. 3577 - Spex Ind. Inc., USA) sealed with 5 µm thick PP film (no. 3520 - Spex Ind. Inc., USA), and then analyzed on an energy dispersive X-ray spectrometry (EDX720, Shimadzu, Japan). Aiming at checking the results obtained, the procedure was repeated with $ZnSO_{4(aq)}$.

2.2.1.7 Dynamic light scattering

The DLS analysis was carried out on the Nanotechnology National Laboratory in Campinas - SP. The fertilizer was diluted up to 100 mg L^{-1} and an aliquot of approximately 30 mL was transferred to a Polystyrene Cuvette (DTS 0012, Malvern Company). Then the cuvette was loaded in the Zetasizer Nano Range (MALVERN PANALYTICAL, UK) equipment which operated using water as dispersant (viscosity of 0.8872 cP and refractive index of 1.33), reading time of 60 seconds and frequency of 398 k counts per second (kcps).

2.2.2 Foliar absorption

Foliar absorption was monitored by 2D X-ray fluorescence Zn maps around a 0.5 µL fertilizer droplet. Plants at the V3 phenological stage was assembled on an acrylic sample holder built specifically for this type of analysis (Figure 2 (A)). This facility aims at preserve the plants alive during the trial conduction. A $ZnSO_{4(aq)}$ or aqueous dispersed ZnO droplet containing 2.3 g Zn L^{-1} was dripped on the top of a vein located on the abaxial face of the leaf (Figure 2 (B)). Immediately after the application, the plants were transferred to an acrylic chamber located inside a growth room aiming at maintain the humidity, photoperiod and temperature

stable in 80%, 12 h and 27 ºC, respectively, during the analysis (Figure 2 (D)). Once 1, 12, 24 and 48 h had elapsed since the fertilizer application, the samples were loaded inside the equipment for mapping (Figure 2 (C)).

Figure 2 - (A) Soybean plant assembled on the acrylic sample holder; (B) Dripping of the fertilizers up to the vein on the abaxial face a soybean leaf; (C) Soybean plant loaded inside the EDAX Ametek Orbis PC µ-XRF equipment; (D) Plants inside the acrylic chamber maintained in high humidity

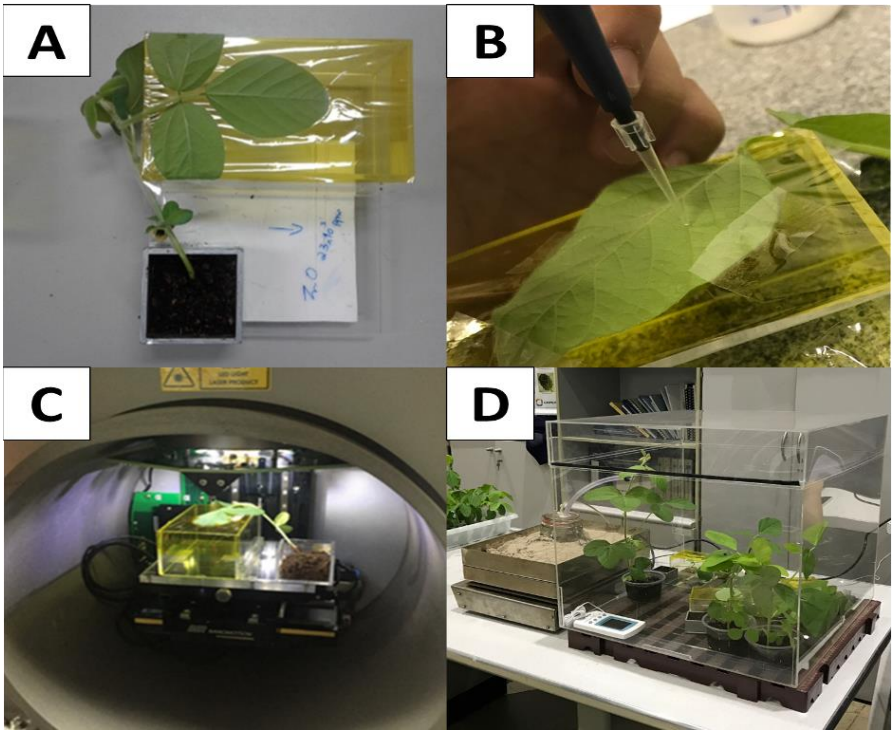

The analysis was performed using an Orbis PC EDAX AMETEK benchtop µ-XRF unity. We employed a 30 µm X-ray beam to map and area of nearly 0.8 mm^2 for the $ZnSO_4$ and 2.3 mm^2 for the ZnO using a matrix of 32 x 25 pixels. The X-ray beam was generated by a Rh anode operating at 40 kV and 900 µA, it was focused on the sample with a polycapillary optics. To improve the signal to noise ratio, a 25 µm thick Ni primary filter was used. X-ray fluorescence photons were detected by a 50 mm^2 silicon drift detector with dwell time of 3 s per point, the dead time was below 1%. The time to record each map was close to 1 h. The distance between the sample and the source was 10 mm. The limits of detection were calculated according to Equation 2.

$$\text{Limit of detection}_{(\text{mg kg}^{-1})} = \frac{3.3*\sqrt{\frac{BG_{mean})}{t(s)}}}{S\ (\text{cps } \mu g^{-1} cm^2)*A\ (\text{g cm}^{-2})}, \quad (2)$$

The average background counts (BG_{mean}) is the mean background value (cps) under the corresponding analyte Kα peak of the five randomly X-ray spectras selected in the analyzed region, and t (s) is the acquisition time. The sensitivity (S) for Zn was calculated using a Zn thin film Micro Matter™ standard (Serial Number 6330) containing 16.16 mg Zn cm^{-2}. The superficial density (A) was obtained weighing a piece of soybean leaf with 1 cm^2.

2.2.3 *In vivo* redistribution kinetics

The redistribution was traced by measuring Zn concentrations on the treated petiole. Nearly 0.4 mL of $ZnSO_{4(aq)}$ and ZnO based treatments containing 23 g Zn L^{-1} were spread on all leaf surface using a brush. The measurements were performed 2 mm away from the leaf edge using the μ-XRF ORBIS PC (Figure 3), once a day during a week. X-rays were generated by a Rh anode operating at 40 kV and 900 μA, using a 1 mm collimator and a 25 μm thick primary Ni filter. The X-ray fluorescence photons were detected by a 50 mm^2 silicon drift detector, the dwell time was 90 seconds and the dead time was smaller than 2%. The distance between the sample and the source was 10 mm. The Zn-Kα net counts and the Compton peak area were used to monitor the relative Zn concentration.

Figure 3 - Scheme of the analyzed region on the kinetics readings

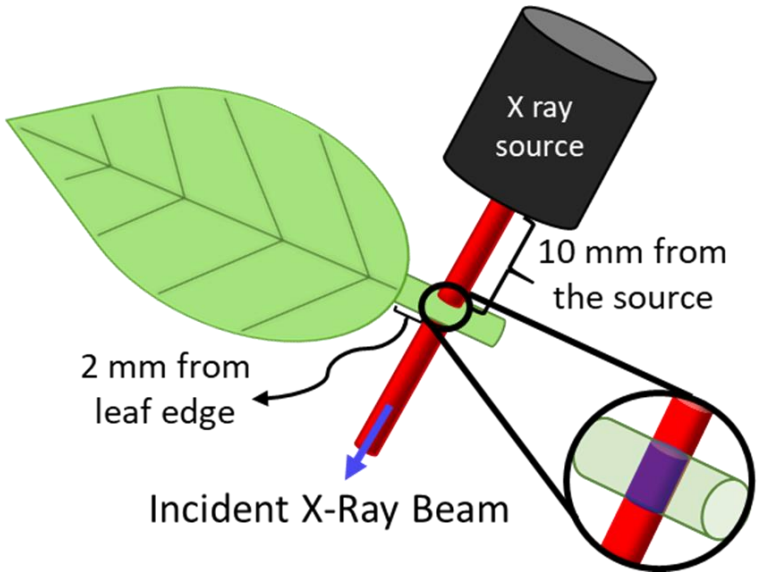

2.2.4 Evaluation of X-ray radiation damage

To evaluate the tissue damage induced by the X-day beam, the leaf surface was irradiated using the same equipment described above. The leaf surface was irradiated by a white beam without primary filter using 45 kV, 100 and 900 µA. The sample was exposed to successive exposure shots of 120 and 240 s summing up one hour of total exposure. These experiments were performed using two biological replicates.

2.2.4.1 Light microscopy analysis

Portions of petioles at the irradiated point and nearby were fixed and vacuum infiltrated for 15 min. in a modified Karnovsky (1965) solution (2% glutaraldehyde, 2% paraformaldehyde, 5mM $CaCl_2$ in 0.05 M sodium cacodylate buffer, pH 7.2) for 48 h at 4 °C. Dehydration was conducted in increasing ethanol series, for 1h each step (30%-100%, 10% increase). Samples were embedded in historesin from Leica. Sections (5-µm thick) were obtained in a rotatory microtome (Leica RM2155, Nussloch, Germany), subsequently stained with 0.05% (w/v) toluidine blue and mounted with Entellan® mounting media. Pictures were taken with a Zeiss Axioskop 40 HBO 50 A/C (Carl Zeiss, Jena, Germany).

2.2.5 Chemical speciation

The Zn chemical environment was investigated using Zn K XANES at the XRF beamline of the second-generation 1.37 GeV Brazilian Synchrotron National Laboratory (LNLS). During three distinct beamtime campaigns we monitored in which chemical form Zn was absorbed and transported. At the beamline the synchrotron radiation was generated by a bending-magnet dipole. The radiation was selected by a Si(111) monochromator and the beam was focused on the sample by a KB mirror system resulting in a spot of *ca*. 20 x 22 μm^2. The spectra were recorded in fluorescence mode using a 30 mm^2 silicon drift detector (KETEK GmbH, Germany). In addition to Zn Kα region of interest (ROI), we also recorded the ROI of the scattered radiation. For details on the sample environment during the measurements at the beamline see Figure 4. The XANES spectra were recorded from living plants that, because of the relatively low flux provided by the beamline (108 photons s^{-1} mm^{-2}) and the short exposure time, produced no radiation damage, scorching, or changes in successive recorded spectra. These results are in line with data obtained by da Cruz et al.,[21] who applied a flux density of 2.78 × 109 photons s^{-1} mm^{-2} to common bean plants.

The XANES measurements were recorded from two individual plants that received independent $ZnSO_{4(aq)}$ treatment. Treatments were performed dripping 0.5 μL of 2.3 g Zn L^{-1} $ZnSO_{4(aq)}$ on the abaxial surface of a leaf and letting it dry for three hours (Figure 4 (A)). Measurements were recorded at several points nearby the Zn spot, 3 h after the application.

Further XANES spectra were recorded on the petiole of three leaves treated with 0.4 mL of $ZnSO_{4(aq)}$ solution with a Zn concentration of 23 g L^{-1} Zn (Figure 4 (B)). Measurements were taken 15, 22, 35 and 59 h after treatment. Between three to five XANES spectra were merged to improve the signal-to-noise ratio. Spectra for various reference compounds, such as Zn-malate, Zn-citrate, Zn-histidine, Zn-succinate and Zn-cysteine, Zn-phosphate and Zn-phytate, were recorded according to Han et al.[22] For $ZnSO_4$, Zn-malate and Zn-citrate the spectra were recorded as cellulose pressed pellets (0.2 and 1 wt % Zn) and in aqueous solutions (1 wt % Zn). Spectra for solids were recorded in transmission and fluorescence geometry while for liquids they were registered at transmission mode. The measurements of solutions were carried out using a cell shown in Figure 4 (D) (25.4 μm polyamide window and 1 mm optical path). The pH of the liquid references was pH 5 for Zn-malate, pH 5 for Zn-citrate and pH 3.5 for $ZnSO_4$.

The Spectra were merged, energy calibrated using a Zn foil, and then normalized using the Athena software within the IFEFFIT package.[23]

Figure 4 - (A) Fertilizer droplet just after the applications; (B) Spreading of the fertilizer on the soybean leaf; (C) Soybean plant loaded in the beamline; (D) Set up of the cell used for measurements in liquids samples

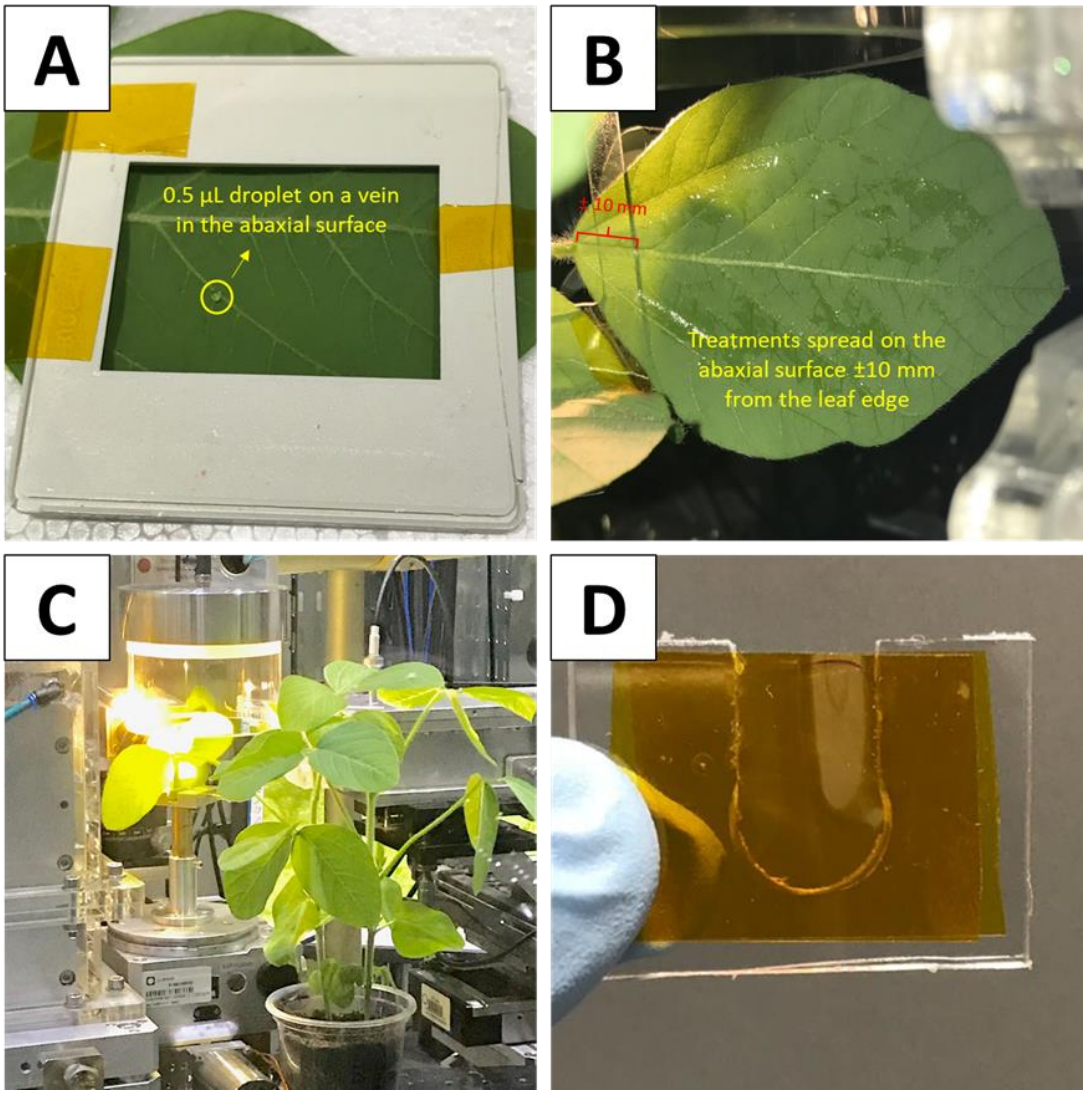

2.3 Results and discussion

2.3.1 Characterization of ZnO suspension and $ZnSO_{4(aq)}$ solution

Table 1 presents physical-chemical characterization for the ZnO suspension and $ZnSO_{4(aq)}$ solution applied to soybean leaves. Additionally, scanning microscopy showed that the ZnO suspension applied on the leaf surface was a disperse population of slab-shaped particles, mostly within submicron size range (Figure 5). X-ray diffraction identified that the crystal phase was wurtzite (Figure 6 and Table 2).

Table 1 - Physical-chemical characterization of ZnO suspension and $ZnSO_{4(aq)}$ solution applied on the leaves of soybean

Measured parameter	**ZnO**	**$ZnSO_{4(aq)}$**
pH†	7.0	6.1
Hydrodynamic diameter (nm)‡	480 ± 118	-
Recovery of soluble Zn (wt./v. %)†	0.2	99.5
Contact angle on leaf (°)†	142 ± 6	140 ± 2
Drying time on leaf (min)†	60	90

Concentration of Zn in the probed suspension and solution: † 2,300 mg Zn L^{-1}; ‡ 100 mg Zn L^{-1}.

Figure 5 - Scanning Electron Microscope images of the commercial ZnO fertilizer

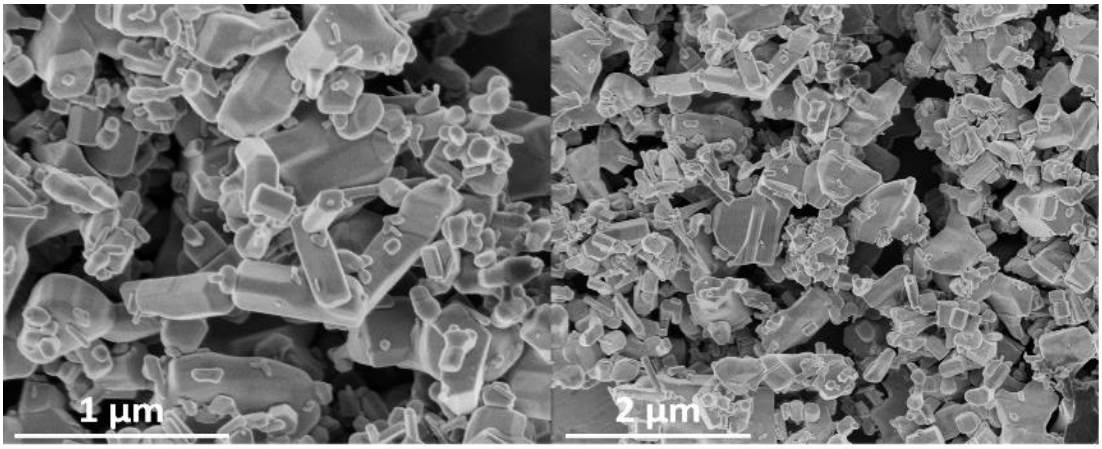

Figure 6 - XRD pattern of the commercial ZnO tested

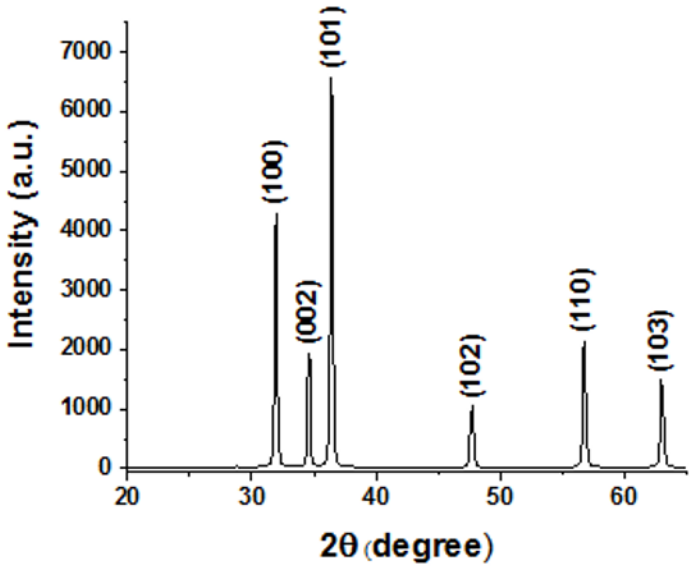

Table 2 - Crystallite size (D) in different planes for XRD data of the ZnO used in this study. The hkl stands for the Miller indexes

Plane (hkl)	D (nm)
100	34,72
002	24,85
101	33,39

2.3.2 Foliar absorption

Figure 7 presents chemical images revealing the spatial distribution of Zn as function of time. Figure 7 (A) shows the spot of the ZnO suspension and Figure 7 (B) shows the one for $ZnSO_{4(aq)}$ solution. The areas, *ca*. 2.3 mm^2 for the ZnO suspension and 0.8 mm^2 for the $ZnSO_4$ solution, were mapped after 1, 12, 24 and 48 h after Zn application. No measurable changes in the shape of the ZnO spot were detected. Conversely, for $ZnSO_4$, as time progressed, we observed spatial changes in the distribution of the droplet.

Figure 7 - μ-XRF chemical images unravelling the spatial distribution of Zn as a function of time. (A) Droplet of submicrometer ZnO. (B) Droplet of $ZnSO_4$. One can observe Zn flowing to the vein in the $ZnSO_4$ treatment as function of time, whereas movement was not detected for submicrometer ZnO

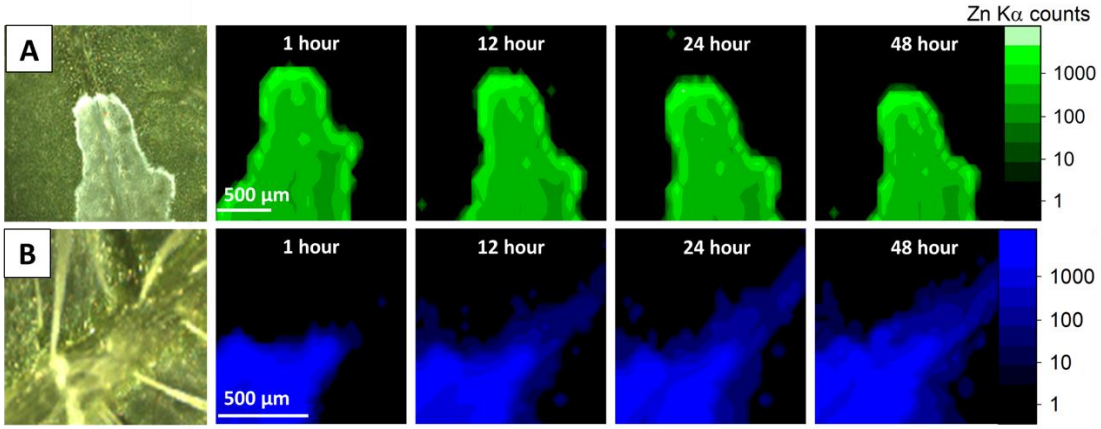

Figure 8 shows overlaid images of the Zn μ-XRF map and the leaf image, where $ZnSO_4$ was spotted and mapped. The combination of optical images and μ-XRF maps revealed Zn absorption and transport through the leaf vein. This phenomenon was observable only when Zn was applied in the form of $ZnSO_{4(aq)}$. In agreement to our procedure, chemical maps evidencing the movement of Zn in detached leaves have been previously reported.[16; 17]

Figure 8 - Overlap of the Zn µ-XRF map and the corresponding picture of mapped area

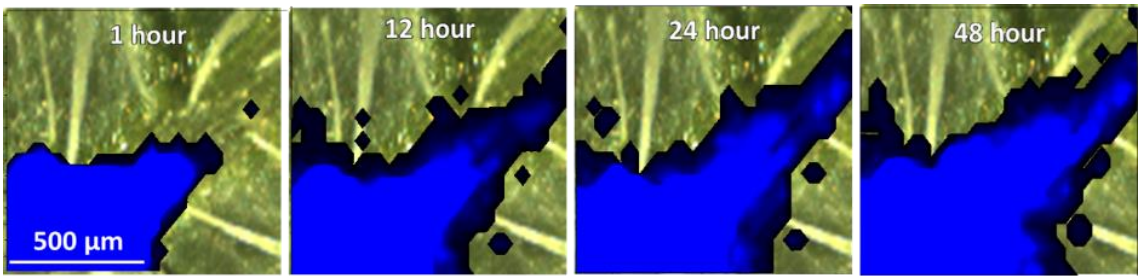

The concentration of 2.3 g Zn L^{-1} is normally used in field application. However, to accomplish the *in vivo* measurements of redistribution and speciation, we had to increase this dose to 23 g L^{-1} Zn. This compromise had to be made to meet the current state of the art of the X-ray spectroscopy techniques employed in this study.

Foliar nutrients can be absorbed either via stomata and ruptures of the leaf cuticle or through penetration of the cuticle via hydrophilic and lipophilic routes.[1] Figure 9 illustrates these pathways and the barriers involved. In case of stomatal uptake, the size exclusion limits range from 3.5 to 100 nm.[24; 25] In case of cuticular uptake via lipophilic pathways, the first obstacle is the cuticle. The cuticle is a porous layer (pore diameters ca. 0.45-4.8 nm) several micrometers thick. It is made of lipids, which display increasing polarity from the surface to the inner part of the leaf.[24; 26; 27] Then, nutrients must transpose the cell wall, which is mainly composed of cellulose. From this point, ions can either move through the apoplast, or they can enter the cell and subsequently be transported via the symplastic route.

Figure 9 - Scheme of a transversal view of a soybean leaf and the possible pathways of penetration of solutes

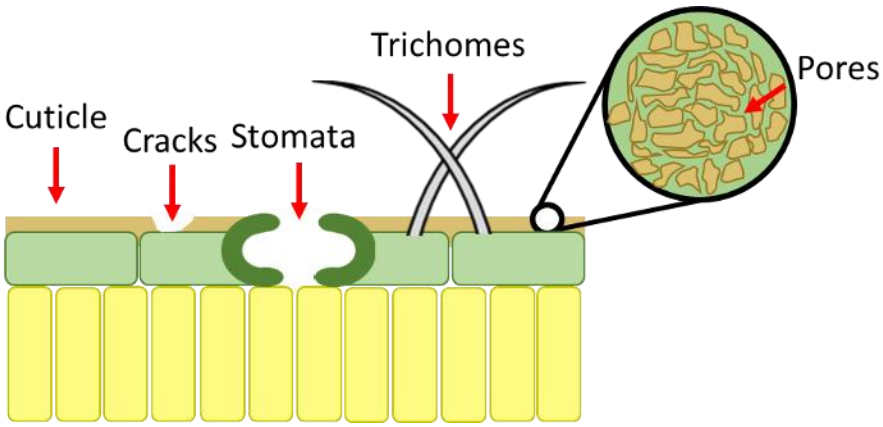

There are several physical-chemical factors known to influence foliar uptake of fertilizers. For example, pH, particle size, solubility, deliquescence point, surface tension and electric charge.[16; 17; 28-30] All these parameters, to a certain extent, influenced the Zn uptake from ZnO suspension and $ZnSO_{4(aq)}$.

The pHs for ZnO and $ZnSO_4$ were 7.0 and 6.1, respectively. At these pH ranges, Zn penetration can be reduced through cuticular fixation of cations by the cuticular membrane.[28; 31] The solubility of ZnO tends to increase as the particle size decreases.[21] $ZnSO_{4(aq)}$ was completely soluble, whereas the dissolved Zn fraction in the ZnO suspension was only 0.2% (Table 1).

Because ZnO was suspended in water by means of a surfactant, we expected that this component could influence both drying time and wettability of our experiment. However, the measurements showed that surface tension was similar in both cases since the contact angles (Figure 1) were 142 ± 6º and 140 ± 2º for ZnO and $ZnSO_{4(aq)}$, respectively. The additive did not increase the drying time (Figure 10), it was found approximately 60 and 90 min for ZnO and $ZnSO_{4(aq)}$, respectively. Altogether, among all factors discussed above, the one that played the major role on the Zn absorption was the solubility of the Zn source. However, the transport of entire particles along the phloem is limited to particles smaller than 5.4 nm.[32] Additionally, a higher mobility of Zn from a soluble source was also reported by Du et al.[16] and Li et al.[17] on tomato, citrus, and soybean.

Figure 10 - Pictures of the ZnO and $ZnSO_4$ droplets elapsed 1, 60 and 90 min of the application

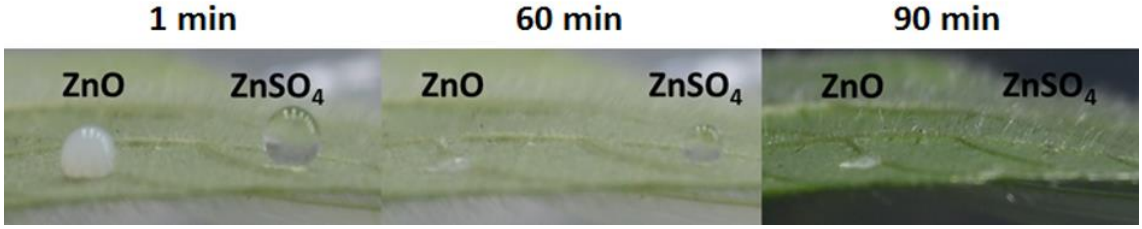

The results suggested that the uptake and transport of ZnO should occur only after its dissolution, either on the leaf surface, aided by the wetting agent, or in the polar regions of the cuticle during the inward diffusion process. The chemical images presented in Figure 7 showed that the movement of $ZnSO_{4(aq)}$ occurred within the vein towards the petiole. Therefore, one can infer that the absorbed Zn was moving through the phloem bundles.

Although no observable changes in the chemical images of the ZnO-treated plants were detectable, its absorption and movement cannot be discarded. If some ZnO was absorbed and transported, it's concentration should be below the limit of detection, i.e. below 135 mg Zn kg^{-1}. It is worth mentioning that the limit of detection could be improved at the expense of increasing the measurement time (see Equation 2). As we aimed to perform *in vivo* measurements, the dwell time was kept at 3 s per point. However, the results above clearly demonstrate that the absorption and transport of Zn from a $ZnSO_4$ source was significantly higher than from a ZnO source.

2.3.3 Redistribution kinetics

After observing local**,** short-range Zn absorption and transport, we decided to investigate long-range Zn transport, via redistribution of nutrients into the phloem.[33] Nutrients have necessarily to cross the petiole during withdrawal from leaves in order to reach other plant tissues. Therefore, we monitored Zn content through time in petioles, by X-ray fluorescence spectroscopy.

Figure 11 (A) presents the abaxial face of the leaf that received the ZnO treatment, whereas Figure 11 (B) shows the monitored part of the petiole. Figure 11 (C) represents the concentration of Zn as function of time, expressed as Zn Kα photon counts normalized by the Rh Kα Compton scattering counts, for the petioles whose leaves were treated with $ZnSO_{4(aq)}$, ZnO suspension and that of a control plant. The Compton scattering intensity is directly proportional to the probed petiole volume. The normalization ensures that the reported XRF signal is proportional to the concentration of Zn, instead being dependent on total Zn amount. This normalization was necessary due to slight changes in the thickness of the probed regions.

The plants were monitored for a week after they received the treatments. During this period, the plant roots were in contact with soil substrate and constantly irrigated. The Zn content in the petiole of the plants continuously increased in all treatments, probably due to the plant growth and consequently root to shoot Zn uptake. However, the Zn increase for the leaf that received $ZnSO_{4(aq)}$ was steeper, confirming that the foliar absorption and redistribution of Zn from this source was faster than that of ZnO. It is also important to mention that the $ZnSO_{4(aq)}$ scorched the leaf surface, whereas no damages were observed for ZnO treatment.

Figure 11 also suggests that the increase of Zn content followed two regimes. The analysis of the curve slopes reveals that the increase for $ZnSO_{4(aq)}$ was steeper during the first 30 h, and then decreased. Conversely, this statement does not hold for the ZnO and control plants. Table 3 shows that after 35 h, the rates of Zn increase in the petioles,

expressed in terms of the slopes, were control < ZnO < $ZnSO_{4(aq)}$. In these measurements, the XRF limit of detection was 7.5 mg of Zn per kilogram of plant tissue (Equation 2).

Figure 11 - XRF monitoring of the content of Zn in the petiole as a function of time. (A,B) Photographs showing the spread of the treatment on (A) down face of the leaf and (B) petiole. The red circle indicates the location of the X-ray beam. (C) Number of Zn photon counts normalized by the Compton scattering as a function of time. Zn contents were higher in the petioles of the leaves treated with $ZnSO_{4(aq)}$. The error bars are the standard deviations of means of three XRF measurements

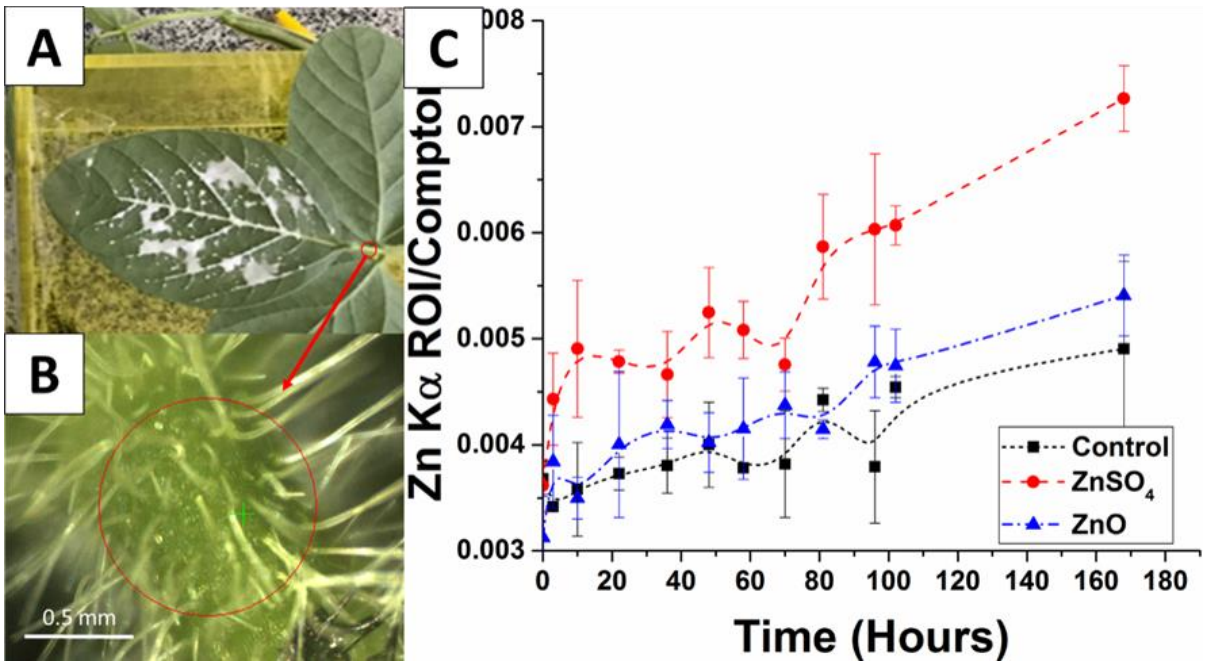

Table 3 - Analysis of the slope of Zn concentration curves on the petiole between 35 and 59 h after the application of the fertilizers

Sample	**Slope (Zn counts $hour^{-1}$) x 10^{-5}**	**Pearson's r**
Control	0.85 ± 0.25	0.807
ZnO	1.07 ± 0.17	0.937
$ZnSO_4$	1.97 ± 0.29	0.945

Using μ-XRF, we are able to monitor short distance and redistribution of nutrients in living plants. This procedure leads to the conclusion that besides leaf absorption and short distance transport, Zn from $ZnSO_{4(aq)}$ was available to be redistributed to other plant organs since it passed through the petiole. This confirms the mobility of Zn in the phloem as previously

described.[33] An increase in root to shoot transport might have been responsible for the higher Zn content found in petioles of control and ZnO treated plants.

2.3.4 Evaluation of X-ray radiation damage

One of the main concerns regarding spectroscopic chemical speciation, especially in biological tissues, regards the possibility of changes induced by the irradiation itself. Figure 12 shows a series of XANES spectra recorded at the leaf blade of two control plants. Despite the noise, due to intrinsic low Zn concentration, we could not register any noticeable spectral change for a series of spectra recorded at a certain point. Ergo, these data suggest that the Zn chemical species did not change during the irradiation.

Figure 12 - Series of XANES spectra recorded at the leaf blade of two control plants

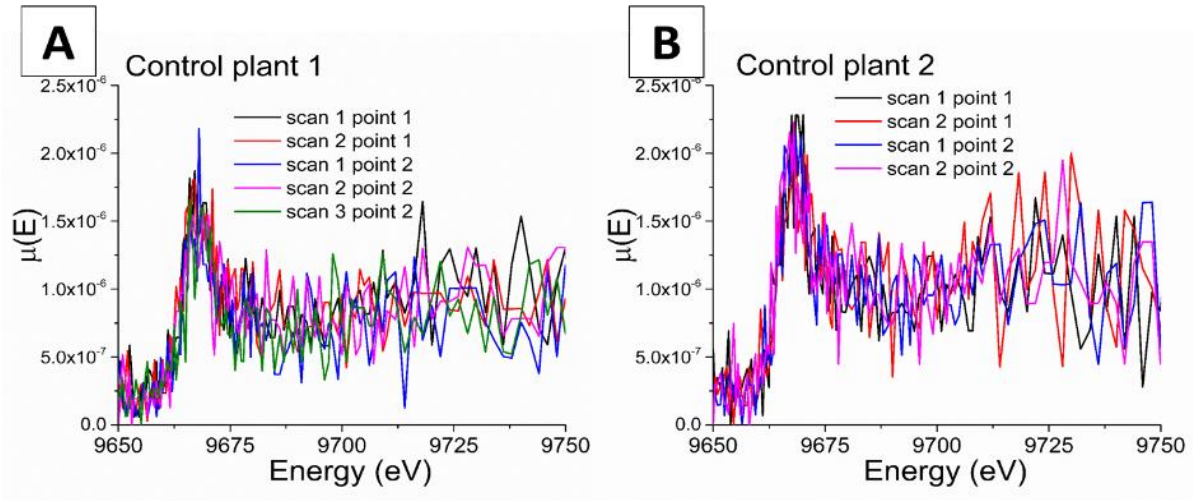

Other possible damage by X-ray exposure consists of tissue dehydration. Figure 13 presents the X-ray scattering intensity recorded during the XANES shown in Figure 12. The intensity of the scattered X-rays did not change during the XANES measurements. On the other hand, Figure 14 presents the X-ray scattering recorded at the Zn Kα ROI for leaf blades irradiated with an X-ray beam produced by a laboratory Rh anode operating at 900 μA and 100 μA. We observed that at higher currents (brighter beam), the scattering intensity decreased as function of time, until it reached stability after nearly 42 min of irradiation. Conversely, the beam generated at 100 μA did not influence the scattering intensity. We observed also that an exposure to a 900 μA X-ray beam produced a scorching damage on the irradiated area (Figure 14). On the other hand, we did not observe any damage at the points where the XANES spectra were recorded (Figure 15).

Figure 13 – Intensities of the X-ray scattering beams recorded during the XANES shown in Figure 12

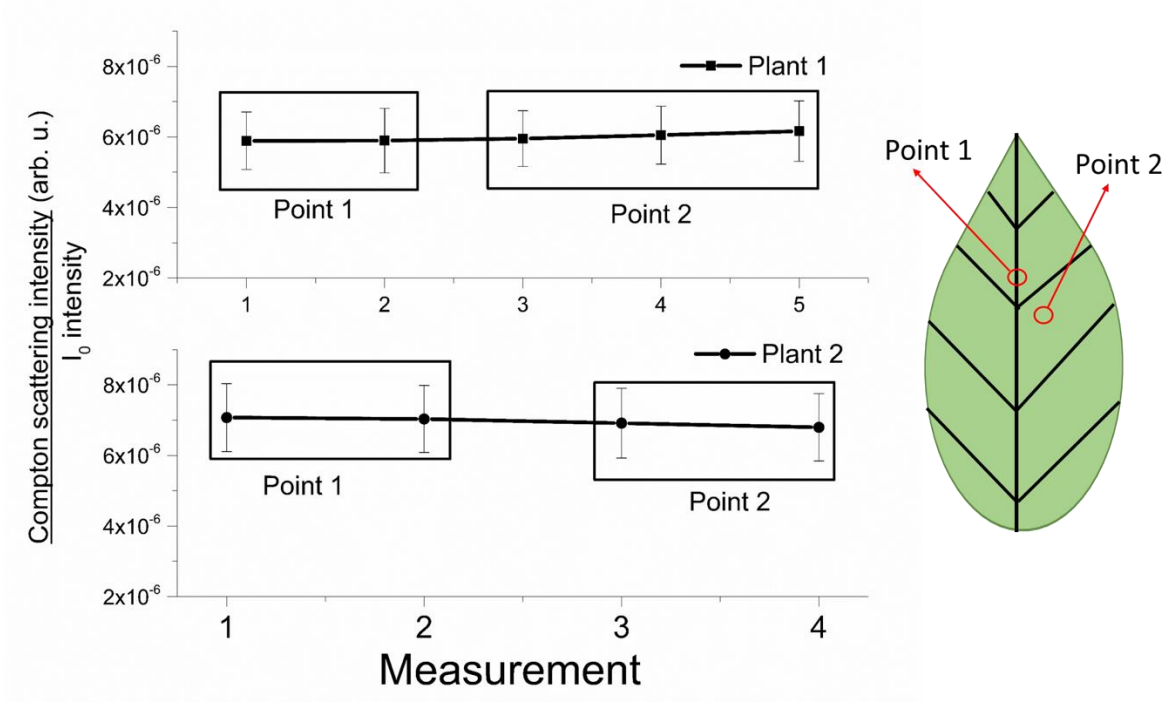

Figure 14 - X-ray bremsstrahlung scattering recorded at the Zn Kα ROI for leaf blades irradiated with an X-ray beam produced by a laboratory Rh anode operating at 900 μA and 100 μA

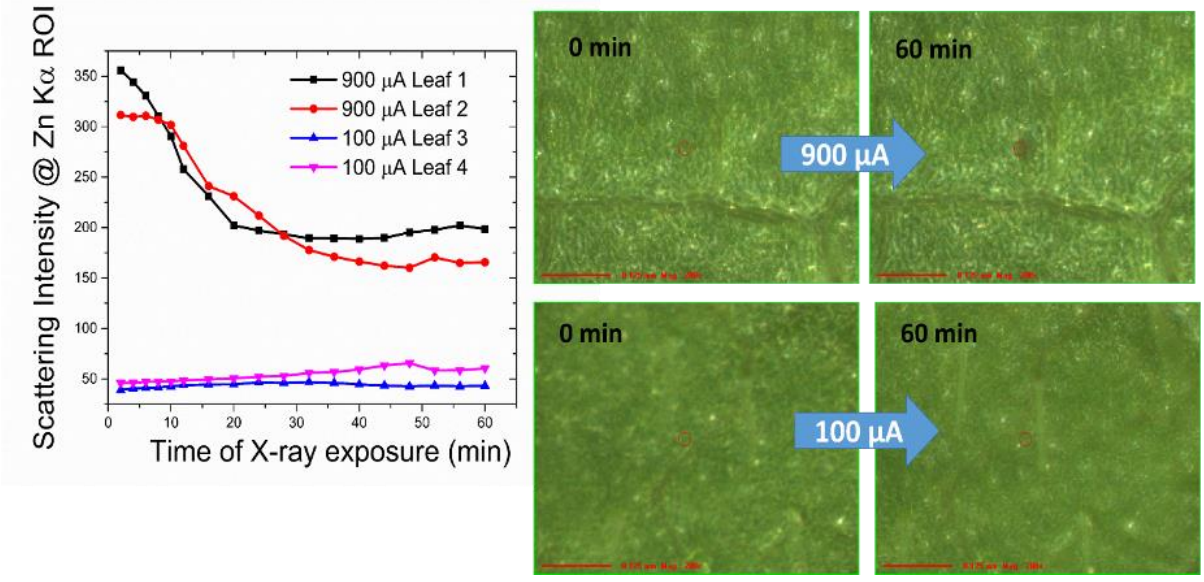

Figure 15 - Pictures of region where the XANES measurements were taken on the leaf blade

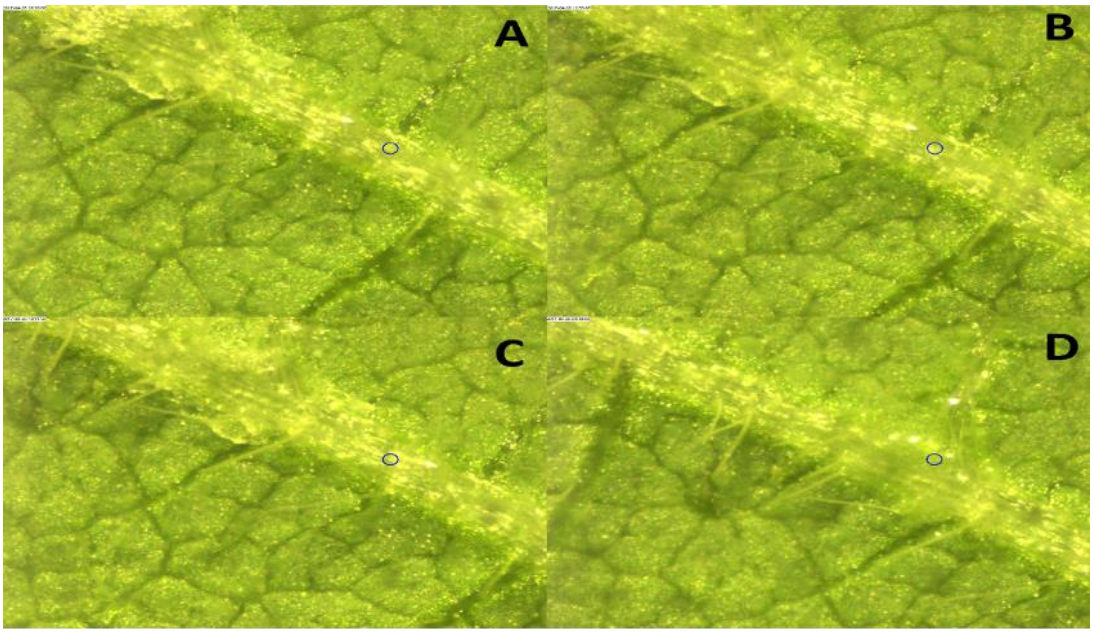

A similar set of measurements was carried out on petioles of control plants. The data presented in Figure 16 did not reveal changes on the XANES spectra recorded at the petiole and Figure 17 did not indicate any drop on the intensity of Compton scattering. Additionally, Figure 18 presents pictures of the location where measurements were taken of Plant 2 with no observable sign of scorching. Altogether, these results suggest that no radiation damage was caused by X-ray beam at XRF beamline of LNLS.

Figure 16 - Series of XANES spectra recorded at the petiole of two control plants

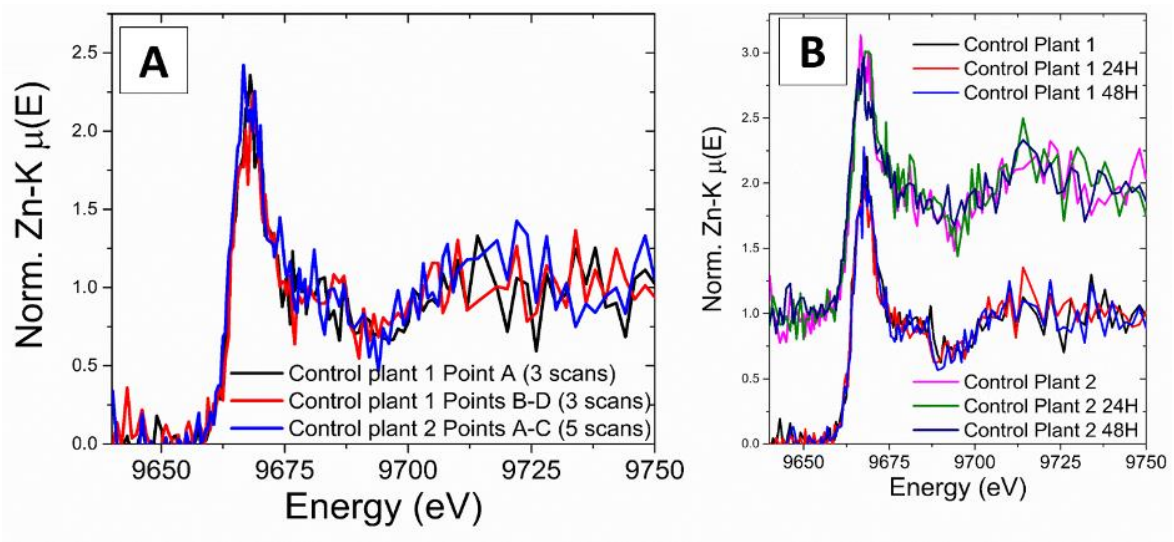

Figure 17 – Intensities of the X-ray scattering beams recorded during the XANES shown in Figure 16

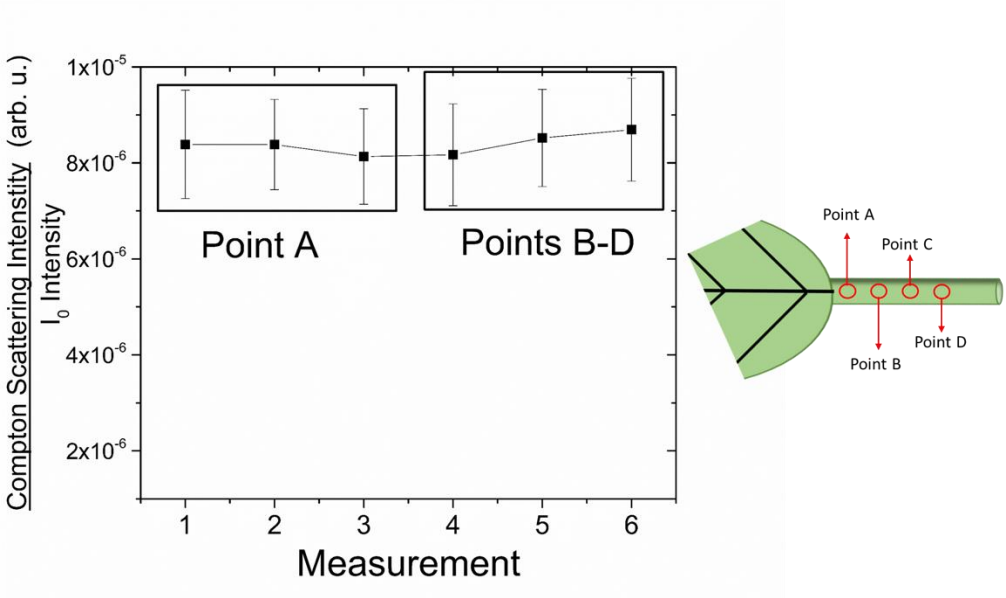

Figure 18 - Pictures of region where the XANES measurements were taken on the petiole

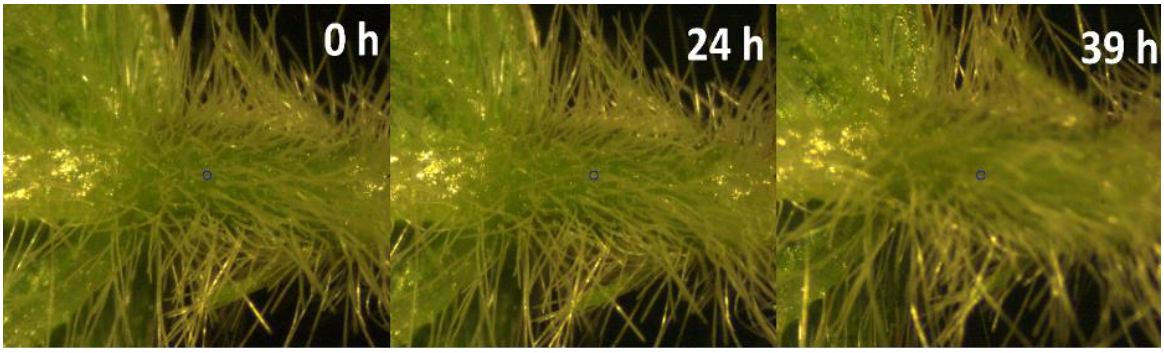

Aiming at characterizing possible changes in the structure of petiole cells caused by the irradiation, we performed morphological analysis by light microscopy. Figure 19 presents light microscopy images of the irradiated and control petioles. The data indicated that irradiation did not affect the structure of the petiole. On the other hand, Zn-treatments showed long-distance cell expansion defects, in a dose dependent manner, over parenchyma cells adjacent to the vasculature, affecting overall parenchyma diameter (Figures 20 and 21). All treatments display no significant difference in the number of parenchyma cells (data not shown), correlating the decrease of the parenchyma diameter only to cell expansion. Similar effect produced upon Zn-treatment were previously described by Sridhar et al.[34] in root cortical cells near the vasculature of barley plants.

Figure 19 - Cross-sections of petioles at the irradiated and adjacent sections; (A-D) non irradiated and non Zn-treated; (E-H) irradiated but not Zn-treated; (I-L) X-ray irradiated and treated with 2.3 g Zn L^{-1} $ZnSO_{4(aq)}$, (M-P) X-ray irradiated and treated with 23 g Zn L^{-1} $ZnSO_{4(aq)}$. The samples were irradiated by a 1 mm X-ray beam for 90 s and instrument operating at 40 kV and 900 µA. Bar l = 200 µm

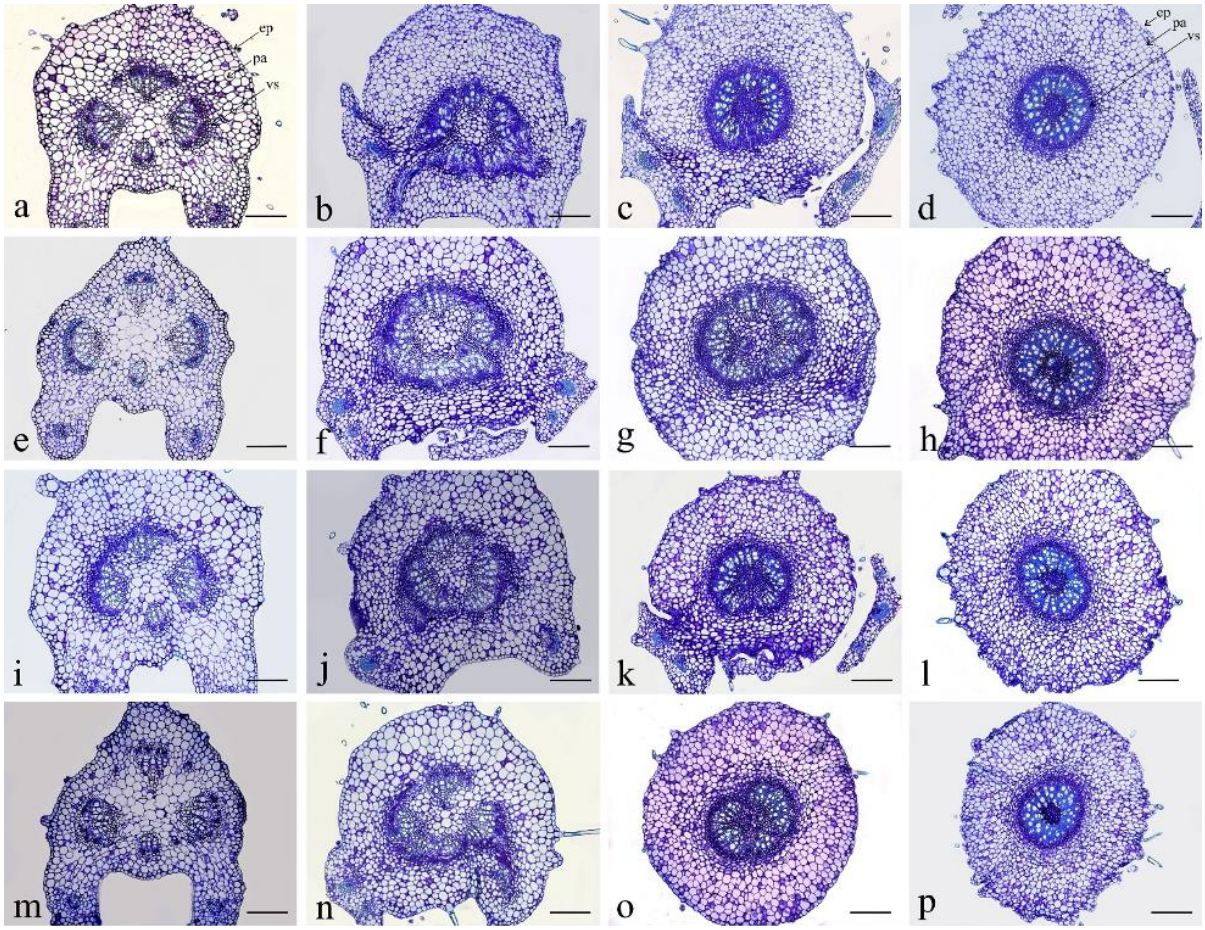

Figure 20 - Detailing of petiole parenchyma cells adjacent to stem junction. (A) Non-irradiated, non-treated control; (B) X-ray irradiated, but non Zn-treated; (C) X-ray irradiated and treated with 2.3 g Zn L^{-1} $ZnSO_{4(aq)}$; (D) X-ray irradiated and treated with 23 g Zn L^{-1} $ZnSO_{4(aq)}$. Alterations on cell expansion and shape of parenchyma cells close the endodermis (arrows). ep: epidermis; pa: parenchyma; vs: vascular system. Bars: 50 µm

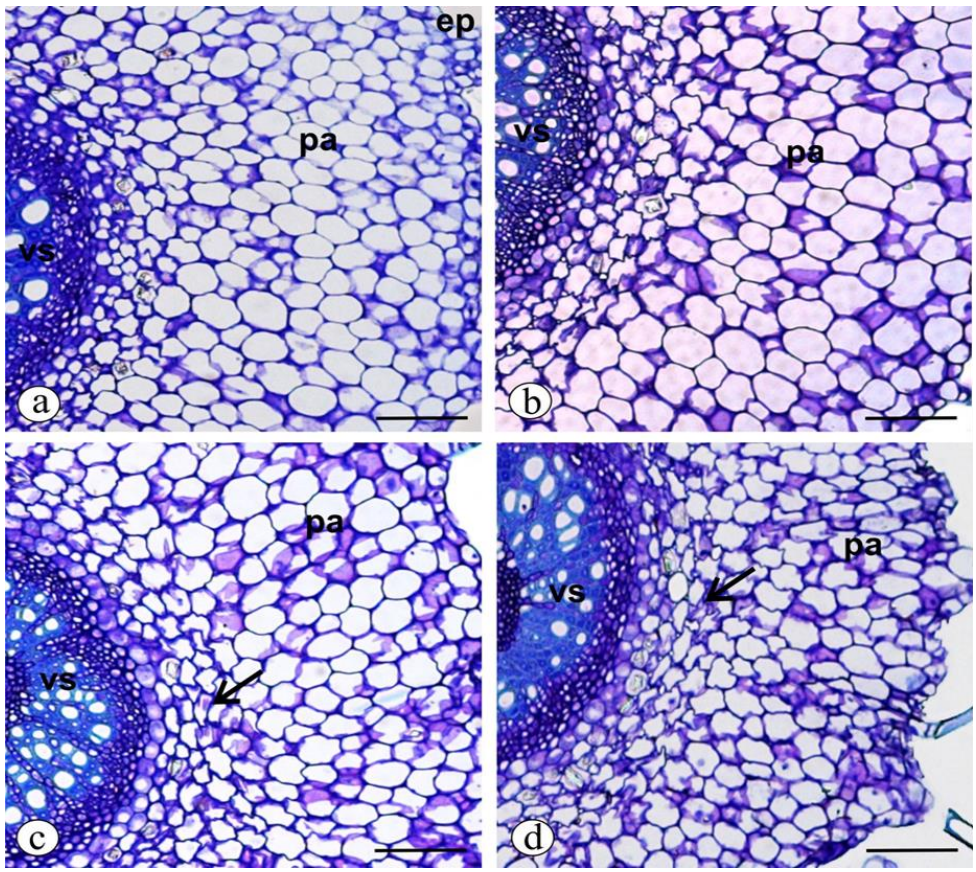

Figure 21 - Effects of Zn-treatments on petiole diameter

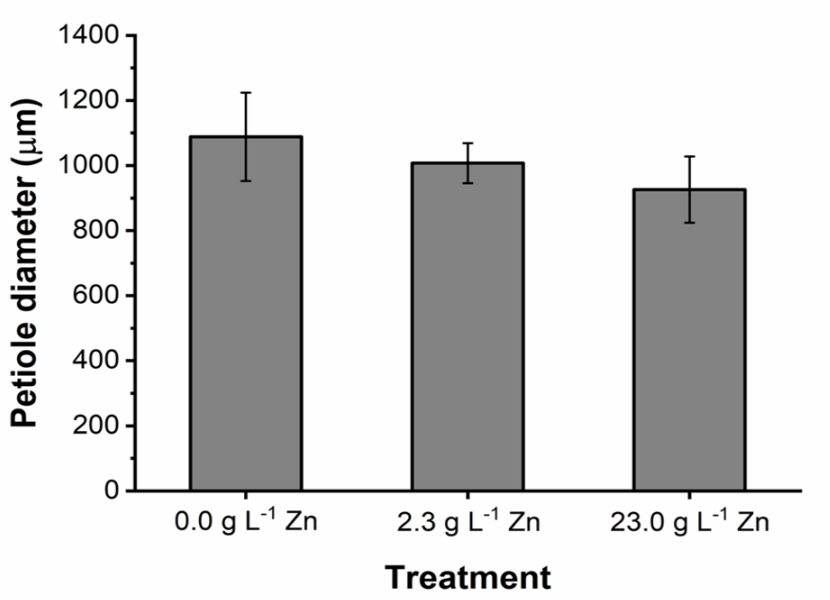

2.3.5 Chemical speciation

XANES was employed to uncover the evolution of Zn chemical species in the area surrounding the deposited $ZnSO_{4(aq)}$ droplet. Figure 22 (A) presents the spatial distribution of Zn in a $ZnSO_4$ droplet dried for three hours. Points A to D (arrows) highlight the locations where XANES spectra were recorded. The red spot in the center of the image indicates the highest Zn concentration, which decreased towards the edges. Figure 22 (B) shows the Ca chemical image of this same region, featuring the presence of leaf veins. The Ca signal discontinuity shown in the center of the image, is due to shielding of Ca Ka photons by the Zn layer on the top of the leaf blade.

Figure 22 (C) presents the XANES spectra recorded at the sites A-D indicated in Figure 22 (A), along with Zn-based reference compounds (Zn-malate, Zn-citrate, and $ZnSO_4$). The features of the spectra presented in Figure 22 (C) suggest that Zn chemical environment depended on the position where it was recorded.

Figure 22 - Combined synchrotron μ-XRF and XANES. μ-XRF chemical images for (A) Zn applied as $ZnSO_{4(aq)}$ on the abaxial face of a leaf and (B) Ca naturally present in the leaf. (C) XANES spectra registered for $ZnSO_4$, Zn−malate, and Zn−citrate reference compounds and spectra recorded at sites A−D highlighted in panel A. The Zn concentration was higher in the center of the stain. The Ca map shows the presence of veins, and the Zn chemical environment depended on the spot location

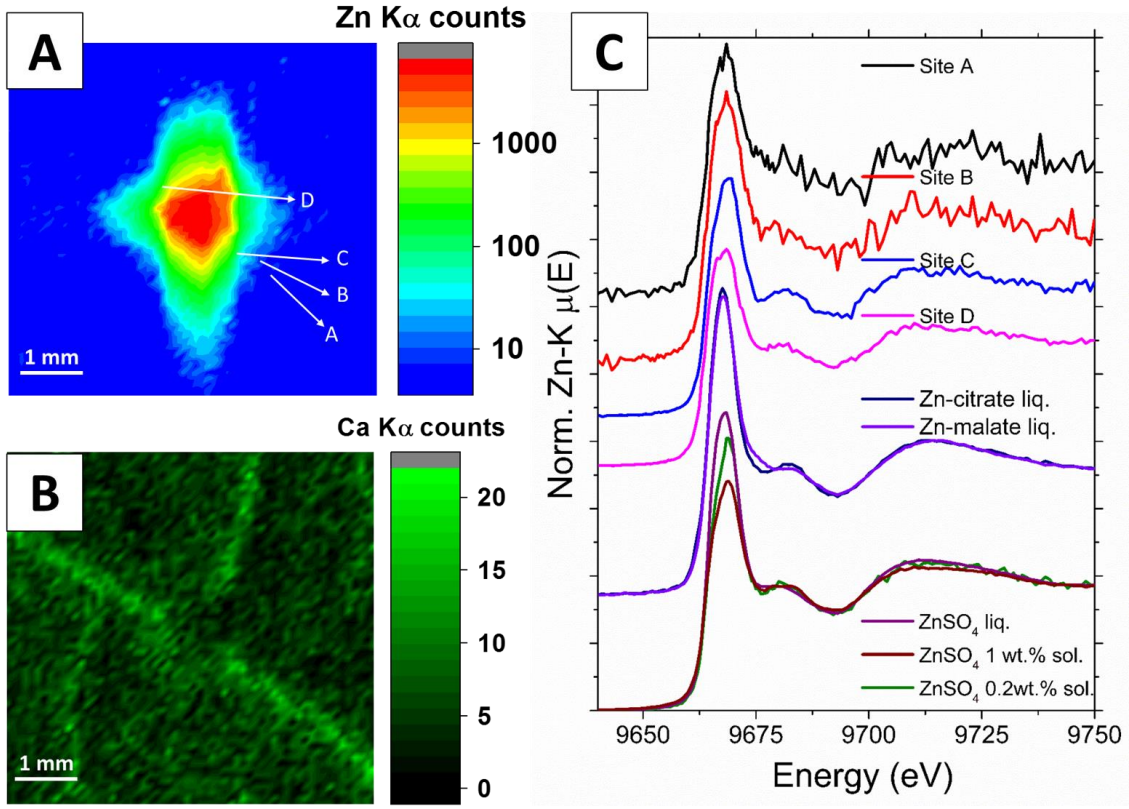

Figure 23 presents overlays of the spectra recorded on the leaf blade with those of reference compounds. A qualitative interpretation of this data set indicates that in sites A and B (Figures 23 (A) and (B), respectively) Zn is in a chemical environment similar to that of Zn-malate (i.e., coordinated by carboxyl groups). In sites C and D, the spectra are closer to that of $ZnSO_4$, showing a characteristic second absorption maximum at 9680 eV, which is also present in the reference compound. Figure 23 (C) and (D) also shows that the spectra recorded in sites C and D were slightly distorted by incident beam self-absorption (IBSA). Similar results were previously reported by Doolette et al.,[35] who observed Zn bound with citrate and phosphate the near where a $ZnSO_4$ droplet was applied on wheat leaves.

Figure 23 - Overlay between the spectra recorded on the leaf blade in sites A, B, C and D with those of reference compounds

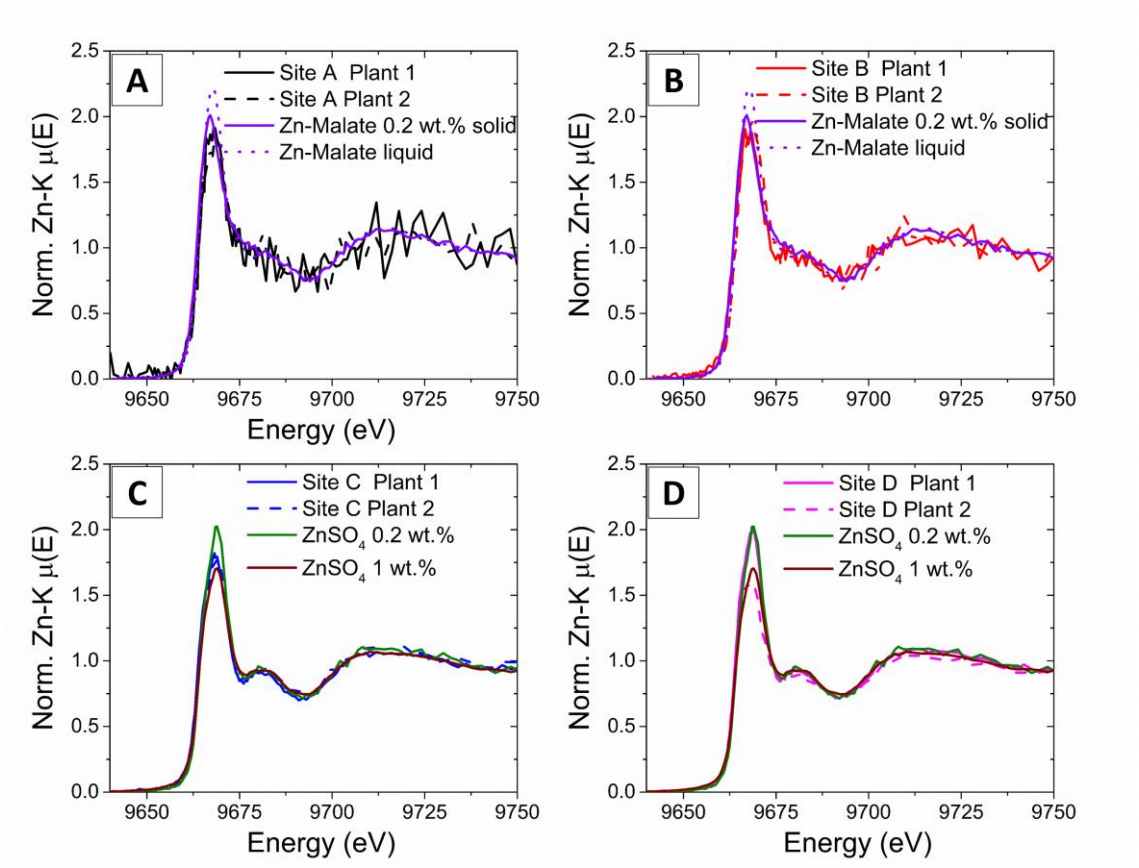

We also measured the Zn chemical environment in the petiole as function of time. The leaf received a $ZnSO_{4(aq)}$ treatment similar to that of Figure 11. The blue circle in Figure 24 (A) indicates the location of the X-ray beam. Figure 24 (B) shows the concentration of Zn in the spot of measurement as function of time. Figure 24 (C) presents the XANES spectra recorded for the reference compounds (Zn−malate and Zn− citrate). Figure 24 (D−F) presents the

XANES spectra recorded for three plants. For all treated plants, we observed increases in the signal-to-noise ratios of the XANES spectra as functions of time, which was a result of the increasing Zn content in the petiole. The spectra recorded for Plant 1 developed a slight shoulder at 9680 eV (more evident in the spectrum at 22 h), which might suggest a change of the Zn chemical environment. By contrast, this change was not clear in Plants 2 and 3.

Figure 24 - Combined synchrotron XRF kinetics and XANES on the petiole. (A) Picture highlighting (blue circle) the X-ray spot. (B) Content of Zn on the petiole of a treated leaf as function of time. (C) XANES spectra recorded for the reference compounds (Zn−malate and Zn−citrate). (D− F) XANES spectra recorded for Plants 1, 2, and 3, respectively, as functions of time. The Zn coordination environment depended on the content of Zn present on the petiole

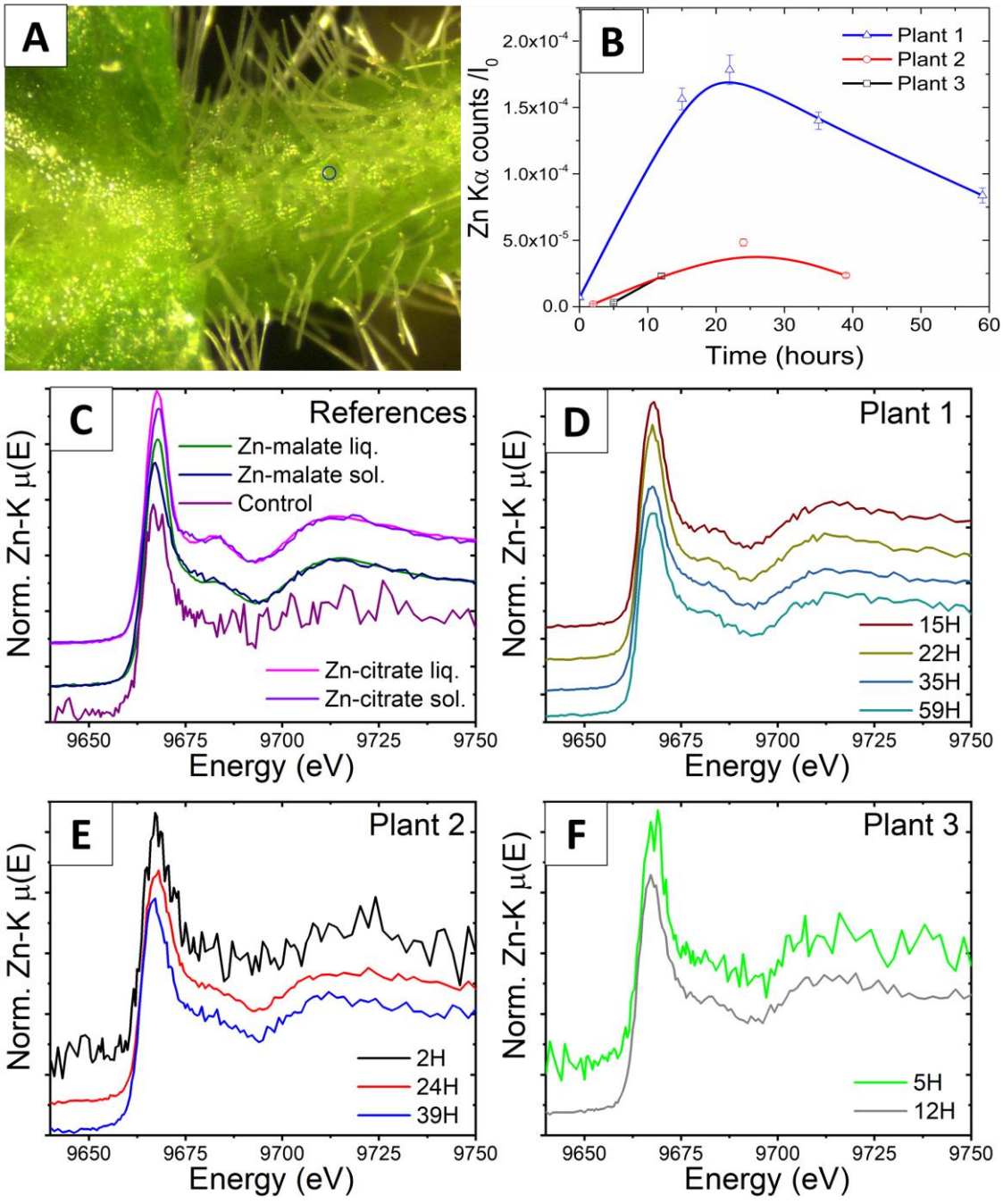

According to the spectra shown in Figures 22 and 23, the concentration of $ZnSO_4$ decreased as a function of distance from the treatment spot. This is consistent with fact that the center of the hotspot (red area) might be primarily constituted of dried $ZnSO_4$ deposited on the leaf surface. The spectra for $ZnSO_4$ reference compounds at 1 wt % Zn presented an attenuated whiteline caused by incident beam self-absorption (IBSA). This was observed in the spectra recorded at the Zn hotpots of the leaf blade (Figure 23 (C) and (D)).

Points A and B of the leaf blade (i.e., away from the Zn hotspot) showed spectral features closer to those of the Zn-malate solid reference than to those of Zn-malate in solution. The main difference exhibited by these two Zn-malate reference spectra regards the height of whiteline. However, unlike the $ZnSO_4$ at points C and D in Figure 22 (A), in the present case, the reduced intensity cannot be attributed to IBSA effect. Figure 25 shows that the spectra recorded in solution media presented higher whitelines than the solid counterparts. This figure did not show any ISBA for the 0.2 wt % Zn pressed pellets measured with fluorescence geometry. Preliminary measurements (data not shown), in addition to those presented in Figure 22, reveal that pellets containing 1.0 wt % Zn are not suitable for measurements in XRF geometry because of IBSA.

Figure 25 - XANES spectra of the Zn malate and sulphate standards, highlighting that the spectra recorded in solution media presented higher whiteline than the solid counterparts

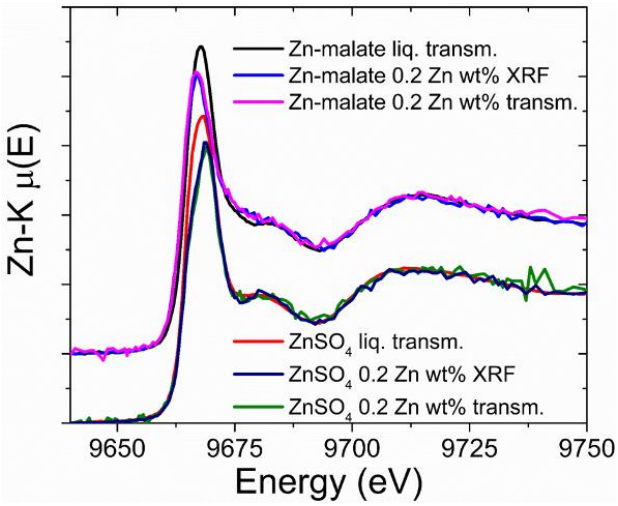

Specifically, the higher signal-to-noise ratio presented by the spectra recorded at the point B, attributed to the higher Zn concentration, suggests that the Zn short-range movement did not happen as $ZnSO_4$ chemical form. It was rather transformed to Zn bound organic molecules in an environment similar to that of the Zn-malate pellet.

It is known that anionic forms exert greater influence on Zn absorption rather than on transport.[36] Likewise, anions and cations are absorbed in equal amounts.[37] The chemical speciation nearby the Zn spot, combined to these latter statements from the literature, altogether suggest that the hydrated Zn^{2+} moves across the cuticular pores followed by the hydrated SO_4^{2-}. To keep the electric charge neutrality, the pair might also cross the cell wall coupled. The separation of the $Zn^{2+}_{(aq)}$-$SO_4^{2-}_{(aq)}$ pair might occur during the cell wall or membrane admission. Once Zn^{2+} enters the symplast or apoplast, it is coordinated by carboxyl groups of organic molecules.

In agreement to what was demonstrated by benchtop μ-XRF measurements (Figure 11 (C)), at the XRF synchrotron beamline we also observed that Zn migrated from the leaf to the petiole (Figure 24 (B)).

The spectra recorded at the petiole of Plant 1 developed an absorption maximum at 9864 eV as function of time. This feature was more evident at 22 h. However, this trend was not clear in Plant 2. Thus, the chemical speciation at the petiole, in agreement with data for the leaf blade, confirmed that Zn is not transported as $ZnSO_4$. The spectra recorded for the plants presented features similar to that of Zn-malate and Zn-citrate reference compounds. This fact, led us to conclude that Zn moves along the phloem complexed by organic groups.

The main differences exhibited by the XANES spectra between Zn-citrate and Zn-malate are the higher whiteline and the presence of a shoulder at 9684 eV for Zn-citrate (Figure 22 in aqueous phase and Figure 25 in solid state). These features were used to estimate how the fraction of Zn-malate and Zn-citrate like compounds changed along the transport. The similarity between the XANES is consequence of their alike chemical environment. At the first coordination shell both are surrounded by six oxygen atoms at nearly 2.07 Å.[38; 39] However, at second coordination shell Zn-citrate shows 3.9 carbon atoms whereas Zn-malate presents 2.8 carbon atoms, both at ca. 2.85 Å.[39] The K_f for Zn-citrate is 4.5 whereas that for Zn-malate is 2.8. Therefore, citrate is a stronger ligand than malate. Additionally, citrate was suggested as a chelate for Zn in the leaves of hyperaccumulators *Thlaspi Caerulescens*.[38] On other hand, Zn-malate is the main form of Zn transport through shoots of *Noccaea caerulescens* due to its lower stability.[40] We recently showed that Zn is transported in a chemical form similar to Zn-malate in the stem of *Phaseolus vulgaris*.[21]

2.4 Conclusions

Although foliar fertilization is a widespread practice that improves crop yields, the mechanism by which nutrients penetrate through the leaf surface and reach the vascular bundles remains to be fully understood.

Among the investigated physical-chemical parameters (pH, contact angle and drying time) for $ZnSO_4$ and a 480 nm ZnO dispersion, Zn solubility seemed to be most important factor controlling Zn uptake. In a previous study, we showed,[21] in agreement with other authors,[41] that the solubility of ZnO can be controlled by the particle size. Hence, despite the importance of performance additives, one of the keys to increase the uptake velocity of low solubility Zn sources such as ZnO or $ZnCO_3$ remains Zn solubility.

Two-dimension XRF maps showed that the absorption of Zn^{2+} from $ZnSO_{4(aq)}$ was faster than that of ZnO. Furthermore, single point XRF measurements, performed on the petiole of a leaflet that received the application of $Zn^{2+}{}_{(aq)}$, demonstrated that the transport of Zn through the vascular bundles was also faster consequent to $ZnSO_{4(aq)}$ treatment. In this context, benchtop XRF revealed itself a promising tool for *in vivo* nutrient uptake and redistribution studies. The limits of detection might be improved trough large area detectors or crystal analysers.

In vivo XANES chemical speciation showed that Zn was transported preferentially complexed with organic molecules, such as citrate and malate, rather than as $ZnSO_4$.

References

1 FERNANDEZ, V.; BROWN, P. H. From plant surface to plant metabolism: the uncertain fate of foliar-applied nutrients. **Frontiers in Plant Science,** v. 4, art. 289, 2013.

2 HAVLIN, J. L. et al. **Soil fertility and fertilizers:** and introduction to nutrient management. New Jersey: Pearson, 2005.

3 QUAGGIO, J. A. et al. Fertilização com boro e zinco no solo em complementação à aplicação via foliar em laranjeira Pêra. **Pesquisa Agropecuária Brasileira**, v. 38, p. 627-634, 2003.

4 STOVER, E. et al. Prebloom foliar boron, zinc, and urea applications enhance cropping of some 'Empire' and 'McIntosh' apple orchards in New York. **Hortscience,** v. 34, n. 2, p. 210-214, 1999.

5 ANDREINI, C. et al. Counting the zinc-proteins encoded in the human genome. **Journal of Proteome Research,** v. 5, n. 1, p. 196-201, 2006.

6 DARNTON-HILL, I. et al. Micronutrient deficiencies and gender: social and economic costs. **American Journal of Clinical Nutrition,** v. 81, n. 5, p. 1198S-1205S, 2005.

7 STEIN, A. J. Rethinking the measurement of undernutrition in a broader health context: Should we look at possible causes or actual effects? **Global Food Security-Agriculture Policy Economics and Environment,** v. 3, n. 3-4, p. 193-199, 2014.

8 GRAHAM, R. D.; WELCH, R. M. **Breeding for staple food crops with high micronutrient density**. Washington, DC: International Food Policy Research Institute, 1996. (Working Papers on Agricultural Strategies for Micronutrients).

9 RAIJ, B. et al. **Recomendações de adubação e calagem para o Estado de São Paulo.** Campinas: Instituto Agronômico de Campinas, 1996. (Boletim IAC, n. 100).

10 CAKMAK, I. et al. Biofortification and localization of zinc in wheat grain. **Journal of Agricultural and Food Chemistry,** v. 58, n. 16, p. 9092-9102, 2010.

11 MONTALVO, D. et al. Agronomic effectiveness of zinc sources as micronutrient fertilizer. **Advances in Agronomy**, v. 139, p. 215-267, 2016.

12 KROGMEIER, M. J.; MCCARTY, G. W.; BREMNER, J. M. Phytotoxicity of foliar-applied urea. **Proceedings of the National Academy of Sciences of the USA**, v. 86, n. 21, p. 8189-8191, 1989.

13 EICHERT, T. et al. Size exclusion limits and lateral heterogeneity of the stomatal foliar uptake pathway for aqueous solutes and water-suspended nanoparticles. **Physiologia Plantarum,** v. 134, n. 1, p. 151-160, 2008.

14 VU, D. T. et al. Quantitative methods for estimating foliar uptake of zinc from suspension-based Zn chemicals. **Journal of Plant Nutrition and Soil Science,** v. 176, n. 5, p. 764-775, 2013.

15 MARSCHNER, P. **Mineral nutrition of higher plants**. 3. ed. San Diego: Academic Press, 2012.

16 DU, Y. M. et al. In situ analysis of foliar zinc absorption and short-distance movement in fresh and hydrated leaves of tomato and citrus using synchrotron-based X-ray fluorescence microscopy. **Annals of Botany,** v. 115, n. 1, p. 41-53, 2015.

17 LI, C. et al. Absorption of foliar-applied Zn fertilizers by trichomes in soybean and tomato. **Journal of Experimental Botany**, v. 69, n. 10, p. 2717-2729, 2018.

18 FERNANDEZ, V.; EICHERT, T. Uptake of hydrophilic solutes through plant leaves: current state of knowledge and perspectives of foliar fertilization. **Critical Reviews in Plant Sciences**, v. 28, n. 1-2, p. 36-68, 2009.

19 RODRIGUES, E. S. et al. Laboratory microprobe X-ray fluorescence in plant science: Emerging applications and case studies. **Frontiers in Plant Science**, v. 9, art. 1588, 2018.

20 TOYOTA, M. et al. Glutamate triggers long- distance, calcium-based plant defense signaling. **Science**, v. 361, p. 1112−1115, 2018.

21 DA CRUZ, T. N. M. et al. Shedding light on the mechanisms of absorption and transport of ZnO nanoparticles by plants via in vivo X-ray spectroscopy. **Environmental Science: Nano**, v. 4, p. 2367−2376, 2017.

22 HAN, F. et al. Organic acids promote the uptake of lanthanum by barley roots. **New Phytologist**, v. 165, n. 2, p. 481-492, 2005.

23 RAVEL, B.; NEWVILLE, M. ATHENA, ARTEMIS, HEPHAESTUS: data analysis for X-ray absorption spectroscopy using IFEFFIT. **Journal of Synchrotron Radiation,** v. 12, p. 537-541, 2005.

24 EICHERT, T.; GOLDBACH, H. E. Equivalent pore radii of hydrophilic foliar uptake routes in stomatous and astomatous leaf surfaces - further evidence for a stomatal pathway. **Physiologia Plantarum,** v. 132, n. 4, p. 491-502, 2008.

25 EICHERT, T.; BURKHARDT, J. Quantification of stomatal uptake of ionic solutes using a new model system. **Journal of Experimental Botany**, v. 52, n. 357, p. 771-781, 2001.

26 POPP, C. et al. Characterization of hydrophilic and lipophilic pathways of *Hedera helix* L. cuticular membranes: permeation of water and uncharged organic compounds. **Journal of Experimental Botany**, v. 56, n. 421, p. 2797-2806, 2005.

27 SCHÖNHERR, J. Water permeability of isolated cuticular membranes: The effect of cuticular waxes on diffusion of water. **Planta,** v. 131, p. 159-164, 1976.

28 SCHÖNHERR, J. Plant cuticles are polyelectrolytes with isoelectric points around three. **Plant Physiology,** v. 59, n. 2, p. 145-150, 1977.

29 SCHONHERR, J.; LUBER, M. Cuticular penetration of potassium salts: Effects of humidity, anions, and temperature. **Plant and Soil,** v. 236, n. 1, p. 117-122, 2001.

30 GRIGNON, C.; SENTENAC, H. pH and ionic conditions in the apoplast. **Annual Review of Plant Physiology and Plant Molecular Biology,** v. 42, p. 103-128, 1991.

31 RICHARDSON, J. J.; LANGE, F. F. Controlling low temperature aqueous synthesis of ZnO. 1. Thermodynamic Analysis. **Crystal Growth & Design,** v. 9, n. 6, p. 2570-2575, 2009.

32 ETXEBERRIA, E. et al. Determining the size exclusion for nanoparticles in citrus leaves. **Hortscience,** v. 51, n. 6, p. 732-737, 2016.

33 EPSTEIN, E.; BLOOM, A. **Mineral Nutrition of plants:** principles and perspectives. Sunderland: Sinauer Associates, 2004.

34 SRIDHAR, B. B. M. et al. Effects of Zn and Cd accumulation on structural and physiological characteristics of barley plants. **Brazilian Journal of Plant Physiology,** v. 19, n. 1, p. 5-22, 2007.

35 DOOLETTE, C. L. et al. Foliar application of zinc sulphate and zinc EDTA to wheat leaves: differences in mobility, distribution, and speciation. **Journal of Experimental Botany**, v. 69, p. 4469−4481, 2018.

36 MALAVOLTA, E. **Manual de nutrição mineral de plantas**. São Paulo: Agronômica Ceres, 2006.

37 SCHÖNHERR, J. Foliar nutriton using inorganic salts: Laws of cuticular penetration. **Acta Horticulturae,** v. 594, p. 77–84, 2002.

38 SALT, D. E. et al. Zinc ligands in the metal hyperaccumulator *Thlaspi caerulescens* as determined using X-ray absorption spectroscopy. **Environmental Science and Technology,** v. 33, n. 5, p. 713-717, 1999.

39 SARRET, G. et al. Zinc distribution and speciation in *Arabidopsis halleri* x *Arabidopsis lyrata* progenies presenting various zinc accumulation capacities. **New Phytologist,** v. 184, n. 3, p. 581-595, 2009.

40 MONSANT, A. C. et al. In vivo speciation of zinc in *Noccaea caerulescens* in response to nitrogen form and zinc exposure. **Plant and Soil,** v. 348, n. 1-2, p. 167-183, 2011.

41 MUDUNKOTUWA, I. A. et al. Dissolution of ZnO nanoparticles at circumneutral pH: a study of size effects in the presence and absence of citric acid. **Langmuir,** v. 28, n. 1, p. 396-403, 2012.

3 FOLIAR APPLICATION OF Zn PHOSPHITE AND Zn EDTA IN SOYBEAN (*Glycine max* (L.) Merrill): IN VIVO INVESTIGATIONS OF TRANSPORT, CHEMICAL SPECIATION, AND LEAF SURFACE CHANGES[2]

Abstract

Due to a zinc-deficient diet, about 800,000 children die each year worldwide. This aspect is amended by exploiting foliar fertilization, a useful alternative to improve crop yield and nutritional quality of food crops. The aim of this study was then to investigate the leaf uptake and transport of zinc by soybean (*Glycine max* (L) Merrill). Plant leaves were treated with Zn phosphite and Zn ethylenediamine tetra-acetic acid (EDTA) commercial formulations. X-ray spectroscopy (XRF and XANES) was exploited to trace nutrient movement in the petiolule and scanning electron microscopy (SEM) to evaluate the influence of leaf surface treatments. No radiation damage, in terms of elemental redistribution, was observed during the XRF and XANES measurements. As an alternative to radioisotopes, XRF allowed to detect the movement of Zn from both sources in the plant petiolule. Both fertilizers disintegrated leaf epicuticular wax crystals, yet accumulation of sediments in the vicinity of stomata was noted only for Zn phosphite. Absorption and redistribution of Zn were higher for plants that received Zn phosphite. Zinc supplied as Zn phosphite was transported in a form different from that of the pristine Zn phosphite, whereas Zn supplied as Zn EDTA was transported in its chelated form.

Keywords: foliar fertilization; *Glycine max*; X-ray fluorescence (XRF); X-ray absorption near edge structure (XANES); Zn phosphite; Zn EDTA

3.1 Introduction

Although being required only as a trace element, zinc is essential for plant and animal (including humans) nutrition. In plants, Zn is involved in several metabolic processes like synthesis of protein and growth hormone, metabolism of carbohydrates, and maintenance of the cell membrane integrity.[1] However, the availability of Zn in most cultivated soils is low. A survey relying on approximately 38,000 soil samples from Brazilian agricultural areas revealed that ca. 35% of the soils were Zn deficient.[2] Around the world, ca. 800,000 children under 5 years die annually due to a Zn-deficient diet.[3]

Zinc deficiency in plants can be overcome by fertilization with zinc inorganic compounds (oxides, carbonates, sulfates, chlorides, or nitrates), synthetic chelates (e.g., ethylenediamine tetra-acetic acid—EDTA), natural organic complexes, or inorganic complexes.[4] However, the crop response is usually dependent on the Zn source[5] and on the fertilization method, usually employing soil or foliar application.[6] Once it crosses the cuticle, Zn reaches the foliar vascular system before being transported to the other parts of the plant. To this end, it should penetrate the leaf surface, for example, across the cuticle and/or through the stomatal cavity, and traverse the inner cells via apoplastic or symplastic pathways.[7; 8] Nevertheless, the models to explain the permeability of foliar-applied nutrients are still not conclusive.[9]

Foliar applications increased the Zn content in wheat, rice, and soybean grains,[6; 10-13] demonstrating that foliar fertilization is a useful strategy for grain biofortification and may thereby increase Zn content in the diet of human population. Foliar application of Zn EDTA leads to an increase in Zn concentration and bioavailability in rice grains.[14] In wheat, efficiency of this application was 1.4–1.7 times more effective relatively to $ZnSO_4$.[15] Zn EDTA is an effective foliar fertilizer also for triticale, increasing the grain yield during drought stress.[16] For chickpea, Zn EDTA increased the Zn concentration in the seeds.[17] The combination of soil and foliar fertilization with Zn EDTA led to enhancement of the Zn content in the wheat grain, which was more pronounced then that related to a single application in the soil.[18]

Phosphites are inorganic salts usually obtained by the reaction of cationic compounds and phosphorous acid, H_3PO_3,[19] which constitute themselves in an alternative to the widely used sulfates and chlorides as sources of foliar fertilizers. Despite the presence of phosphorous, the use of phosphites as the P source is controversial.[20] Hence, phosphite salts are traded as fertilizers due to the presence of the cations, such as Zn^{2+}. Besides supplying plant nutrients, phosphite-based compounds present also anti-fungal properties, in which the mechanism of control is not fully clarified.[19]

The performance of foliar fertilization may vary according to the physical-chemical properties of the formulation, the plant species, and the environmental conditions. The characteristics of the formulation such as molecular size, solubility, pH, surface tension, and spreading play a relevant role in the efficacy of nutrient uptake by the leaves.[8] We hypothesize that the uptake velocity as well as the chemical form of Zn during its transportation depends on the Zn source. A clear understanding on the uptake and transport of nutrients by the plants is then fundamental for the development of highly efficient fertilizers. Hence, the aim of this work was therefore to investigate the transport kinetics, the effect on the leaf surface, and the chemical environment of Zn in soybean leaves exposed to Zn EDTA and Zn phosphite. Soybean (*Glycine max* (L.) Merrill) was chosen as a model plant species due to its economic relevance, and the Zn sources due to their worldwide application by rural producers. Absorption kinetics was monitored in vivo by using X-ray fluorescence spectroscopy (XRF), and X-ray absorption near edge spectroscopy (XANES) uncovered the Zn chemical environment in the treated leaves. Moreover, the leaf structure was characterized by scanning electron microscopy (SEM) after foliar application of Zn.

3.2 Materials and methods

3.2.1 Plant growth and foliar treatments

Soybean plants were cultivated in a growth room at 27 ± 3 °C, with a relative humidity of 80 ± 5% and a photoperiod of 12 h under 6500 K LED lamp illumination supplying 250 μmol photons $m^{-2}s^{-1}$ (Figure 1 (A)). When the third trifoliate leaf started expanding, the plants were transferred to the sample holder shown in Figure 1 (B).

The treatments consisted of an aqueous solution of commercial Zn phosphite (8.0 wt% Zn and 1.25 g mL^{-1} density, Agrivalle, BR) and Zn EDTA (15.0 wt% Zn, Alternativa Agrícola, BR) at 23 g L^{-1} Zn diluted in deionized water. The final pHs of the solutions were 1.5 and 5.9 for Zn phosphite and Zn EDTA. Zn phosphite requires a pH lower than 3.0 to keep the solution stable. Approximately 70 μL of the solutions was spread on half part (from the middle to apex) of a leaflet abaxial surface, by using a brush. This volume was determined as the weight difference before and after the application. Immediately after application, the plants in the sample holder were returned to the growth room where they stayed for 3 days and then analyzed by XRF measurements. The plants were thereafter conditioned inside of a box with a similar environment and transported to the synchrotron facility.

3.2.2 Redistribution kinetics

The movement of Zn was monitored *in vivo* by evaluating the Zn content in the petiolule of the treated leaflet. Measurements were performed in the petiolule, 1 mm far from the leaf edge, before the application and after elapsing 12, 24, 48, and 72 h of it. Aiming at to distinguish possible changes on the Zn concentration in the petiolule due to plant growth, a control plant that did not receive application was analyzed.

The XRF spectra were registered using a benchtop X-ray fluorescence spectrometer (ORBIS PC, EDAX, USA). The experimental setup and the region of the petiolule probed by the X-ray beam are shown in Figure. S1b-d. X-ray was generated by a Rh anode operating at 40 kV and 900 μA, the beam was shaped by a 1 mm collimator. A 25 μm thick primary Ti filter was employed to improve the signal-noise ratio and reduce the intensity of low energy photons. The X-ray fluorescence photons were detected by a 50 mm2 silicon drift detector, the dwell time was 90 s (three shots of 90 s each) and the dead time was smaller than 2%. The distance between the sample and the source was 10 mm. The ratio between Zn-Kα net counts and the Compton peak determine the relative Zn content. Aiming at avoiding scattering of Zn photons from the fertilizers during the analysis, the leaves were covered with a 1 mm thickness Pb foil (Figure 1 (B)).

Figure 1 - Experimental setup for the redistribution kinetics analysis. (A) Soybean plant inside the growth room at the V3 phenological stage; (B) Soybean plant after to receive one of the tested foliar fertilizers and assembled on the acrylic sample holder. Leaves were covered with a 1 mm thickness Pb foil to avoid scattering of Zn photons; (C) Soybean plant and sample holder loaded inside the EDAX Ametek Orbis PC µ-XRF equipment; (D) Region of the petiolule probed by the X-ray beam during measurements

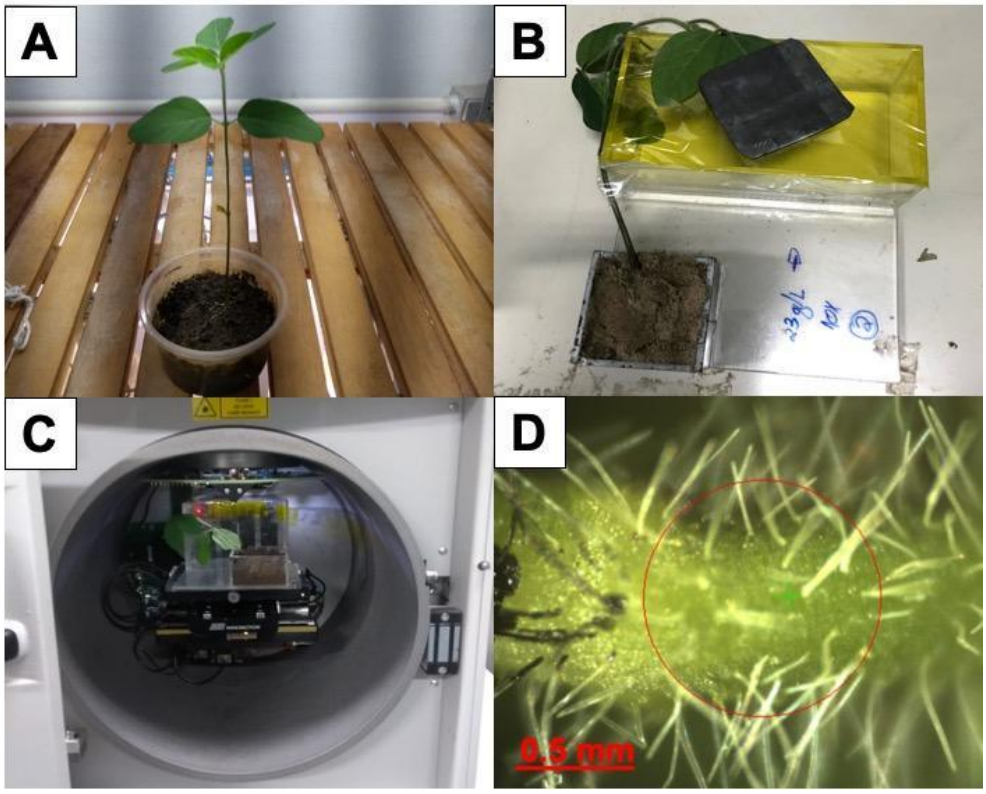

3.2.3 Scanning electron microscopy

To evaluate the effects of Zn fertilizer deposition on the leaf surface, 20-µL droplets of the above described treatments were applied on the abaxial surface of the middle leaflet of the third youngest leaf. The fertilizers were spread by using a brush, according to ordinary procedures for the kinetics assays. An additional application of water was performed to highlight possible injuries caused by the brush scratch. The leaves were collected after 24 h of foliar Zn application.

The samples were fixed in Karnovsky solutions.[21] The fixed samples were washed in 0.1 M phosphate buffer, post fixed in 1% osmium tetroxide in 0.1 M phosphate buffer (pH 7.2) and washed three times in deionized water. The leaves were sequentially dehydrated in graded water-acetone solutions (10% 1×, 30% 1×, 50% 1×, 70% 1×, 90% 1×, 100% 2×, for 15 min each), dried up to the critical point (Horridge and Tamm, 1969), glued on aluminum stubs and sputtered with gold using respectively the EM CPD 300 (LEICA, Wetzlar, Germany)

and SCD-050 (BAL-TEC, New York, USA) facilities. The measurements were performed at 20 kV using a JSM-IT300 (JEOL, Toquio, Japan) scanning electron microscope.

3.2.4 Chemical speciation

The Zn chemical environment during the redistribution process was *in vivo* evaluated using Zn-K XANES at the XRF beamline of the Brazilian Synchrotron National Laboratory (LNLS). The LNLS is a 1.37 GeV second-generation synchrotron facility. At the beamline, synchrotron radiation was generated by a bending-magnet dipole. The radiation was selected by a Si(111) monochromator and the beam was focalized on the sample by a KB mirror system resulting in a spot of ca. 20 x 22 μm^2. The spectra were recorded in fluorescence mode using a 30 mm^2 silicon drift detector (KETEK GmbH, Germany).

The leaves were treated following the same above-described procedure. The leaf was covered with a 1-mm Pb foil to avoid Zn fluorescence photons from the leaf surface (Figure 2). In order to prevent radiation damage in plant tissues, the measurements were taken in two 0.1 mm distant spots of the petiolule, 2 mm far from the leaf edge and approximately 24 h after the application of the fertilizer (Figure 3 illustrates these measured points). Between three to four XANES spectra were merged to improve the signal-to-noise ratio. Aiming at assessing possible radiation damage, simultaneously to the XANES measurements, we also recorded the Ca-Kα X-ray fluorescence and the intensity of scattered radiation.

Spectra for aqueous Zn-malate, Zn-citrate, $ZnSO_4$ and Zn-oxalate solutions at 1 Zn wt% were recorded as reference compounds according to Han et al.[22] The reference compounds measurements were performed in transmission mode using an acrylic cell assembled on a 25.4 μm polyamide film with 1 mm optical path (Figure 2 (D)). The pH of the references was 6.0 for Zn-malate, Zn-citrate and Zn-oxalate and 3.5 for $ZnSO_4$.

The spectra were merged, energy calibrated using a Zn foil and then normalized using the Athena software within the IFEFFIT package.[23]

Figure 2 - Experimental setup for the Zn chemical speciation analysis at the XRF beamline of the Brazilian Synchrotron National Laboratory (LNLS). (A) Spreading of the fertilizer solution on the half surface of a soybean leaf; (B) Soybean plant loaded in the beamline; (C) Region of the petiolule probed by the X-ray beam during measurements; (D) Acrylic cell assembled on a 25.4 μm polyamide film with 1 mm optical path used for the reference compounds analysis

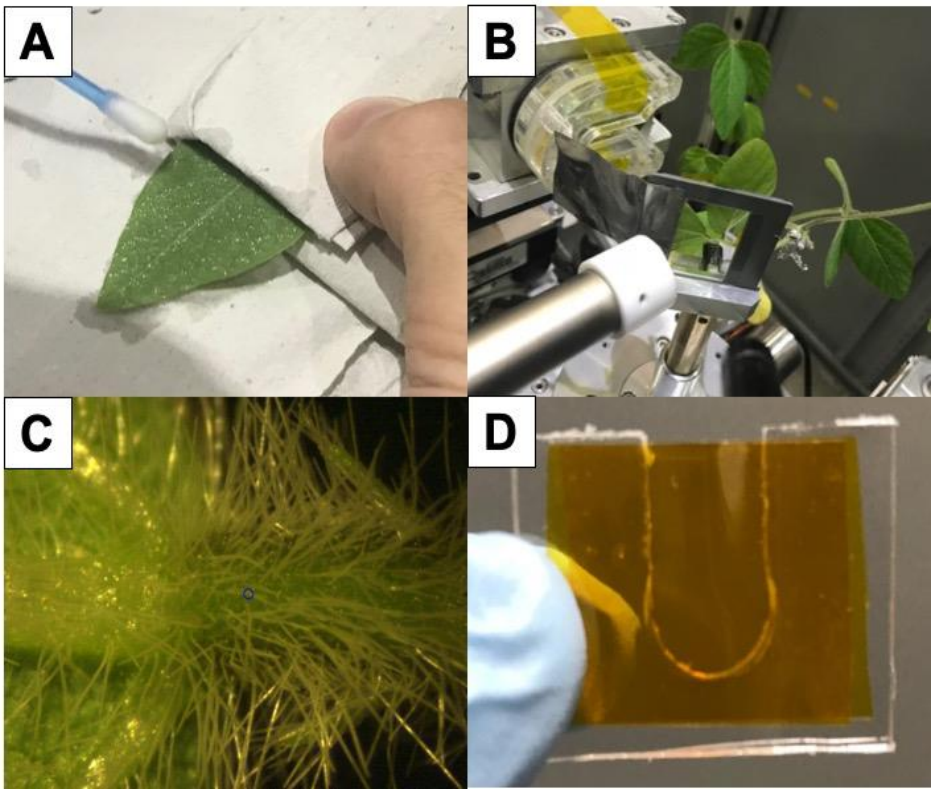

Figure 3 - Scheme of the two points of the leaflet petiolule where the XANES spectra were recorded

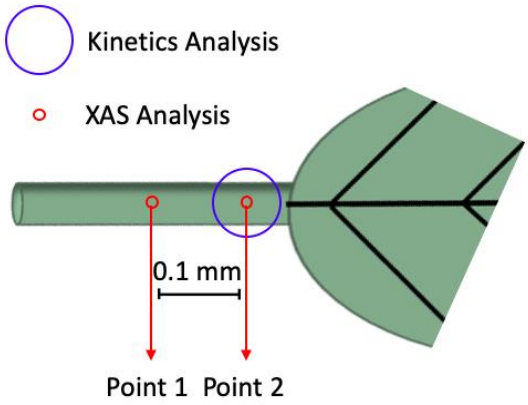

3.3 Results

3.3.1 *In vivo* redistribution kinetics of Zn

Since X-rays may damage fresh or living plant tissues, the impact of irradiation on the analyzed petiolules was firstly investigated. To this end, the content of other detected elements and the intensity of Compton scattering were monitored during the determination of Zn. Compton scattering can be an indicator of tissue dehydration since inelastic scattering decreases with the water content lessening. Using the benchtop equipment, Compton scattering, and the signals of Ca, K, Fe, and Mn underwent only slight modifications for all the plants without any trend (Figures 4-6). Thus, it demonstrates that the set instrumental conditions did not cause any artifact and, therefore, the method was adequate for tracing Zn in living tissues.

Figure 4 - XRF monitoring the intensities of Ca, K, Fe, Mn and the Compton scattering as function of time in the petiolule of soybean leaflet from plants whose leaves were exposed to Zn phosphite. The number of photon counts was normalized by the Rh photon counts

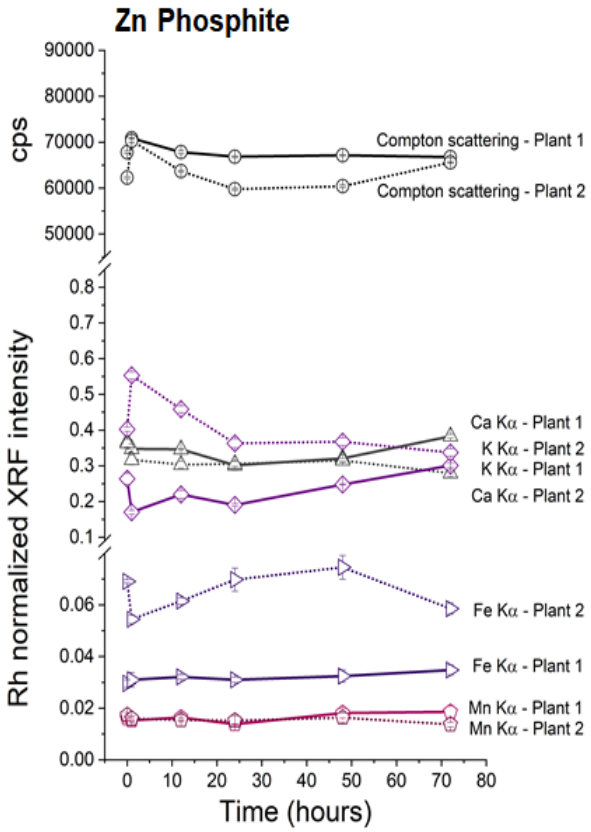

Figure 5 - XRF monitoring the intensities of Ca, K, Fe, Mn and the Compton scattering as function of time in the petiolule of soybean leaflet from plants whose leaves were exposed to Zn EDTA. The number of photon counts was normalized by the Rh photon counts

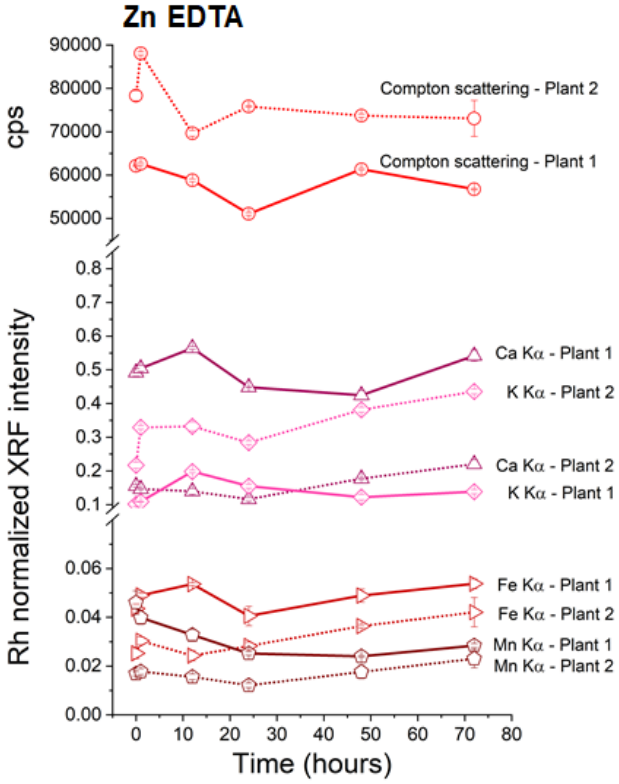

Figure 6 – XRF monitoring the intensities of Ca, K, Fe, Mn and the Compton scattering as function of time in the petiolule of leaflet of soybean control plants. The number of photon counts was normalized by the Rh photon counts

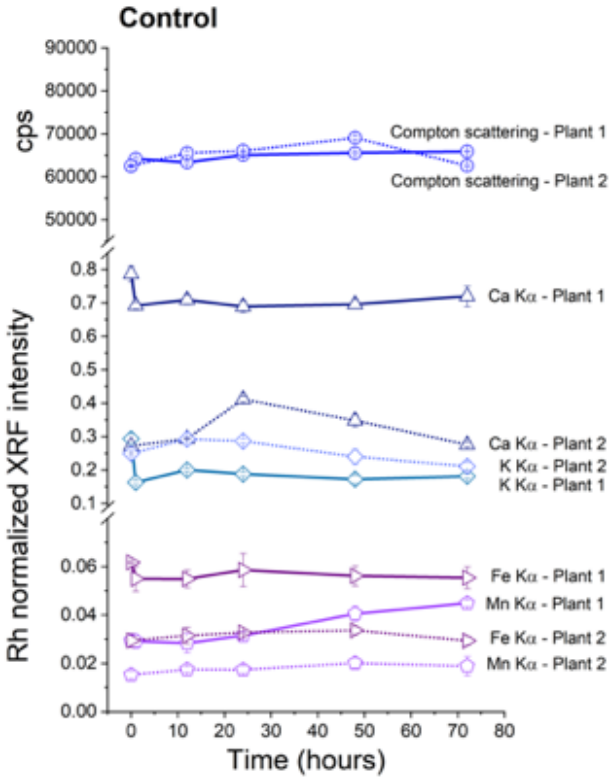

Figure 7 shows the average content of Zn in the petiolules as a function of time based on three measurements. A and B represent the two biological replicates composed of three plants. In order to avoid interferences of the petiolule thickness on the measurements, the Zn content is expressed as the number of Zn-Kα photon counts normalized by the rhodium scattering counts. Absorption and redistribution of Zn were higher for plants that received Zn phosphite. Despite the difference of Zn intensity between the two biological replicates, which reflects that different individuals may differently respond, they presented a similar behavior regarding the treatments. For both plants treated with Zn EDTA, the Zn concentration sharply increased after 12 h, then decreased after 24 h, and thereafter remained almost constant for 72 h.

Figure 7 – XRF monitoring the Zn concentration in the petiolule of soybean (*G. max*) as function of time. (A) and (B) represent two biological replicates with three plants each that received Zn phosphite and Zn EDTA treatments. The number of Zn photon counts was normalized by the Rh photon counts aiming to avoid interferences of the petiolule thickness on the measurements. Zinc absorption and redistribution were higher for Zn phosphite treatment compared to Zn EDTA. Error bars represent the standard deviation for three measurements

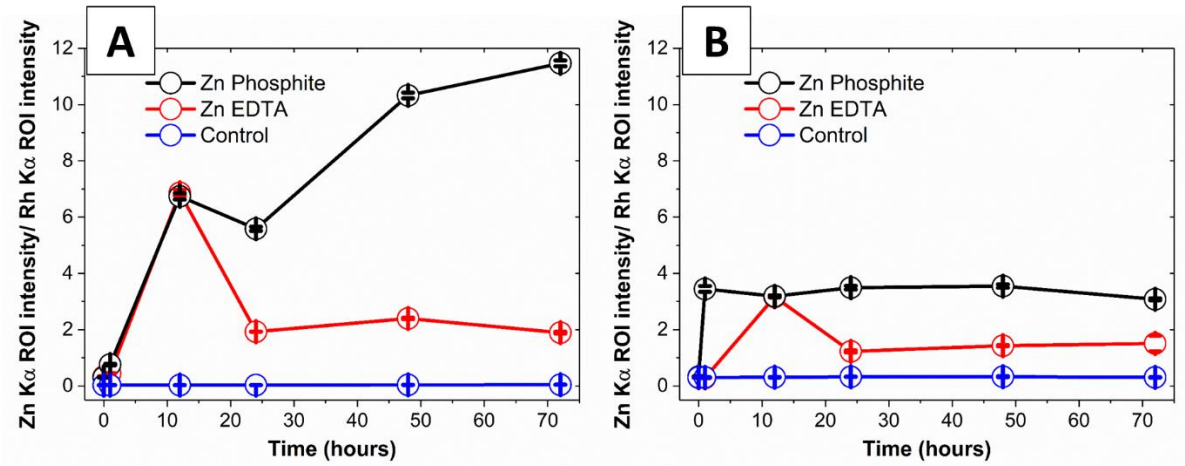

3.3.2 Scanning electron microscopy analysis

The control leaf (non-treated sample, Figure 8 (A-C)) revealed a dense and uniform layer of epicuticular wax crystals (EWC). Figure 8 (E-F) show that the water treatment with a brush was enough to remove mechanically part of the EWC. However, the application of Zn phosphite and Zn EDTA promoted higher EWC removals in comparison with water (Figure 8 (G-I) and Figure 8 (J-L)).

The treatments disintegrated most of EWC from the leaf surface possibly due to a chemical effect caused by the fertilizers. It was also observed that spots of Zn phosphite agglomerated along the leaf surface, mainly around the stomata (Figure 8 (H) and (I)),

whereas for Zn EDTA treatment, no evidence of accumulation was detected (Figure 8 (L)). Additional micrographs recorded for other leaves submitted to the same treatments are presented in Figure 9.

Figure 8 – SEM micrographs of the abaxial surface of soybean leaves at × 140, × 750, and × 1900 magnification. (A-C) Control sample; (D-F) water treatment; (G-I) Zn phosphite treatment; (J-L) Zn EDTA treatment. The control sample revealed epidermal cells covered by a uniform layer of epicuticular wax crystals. The water treatment with a brush was enough to remove mechanically part of the epicuticular wax crystals (EWC). However, the application of Zn phosphite and Zn EDTA promoted higher removal of EWC than water. The phosphite crystals were observed surrounding the stomata. PC – phosphite crystals, S – stomata of the leaf surface, SC – scalped areas by the brush

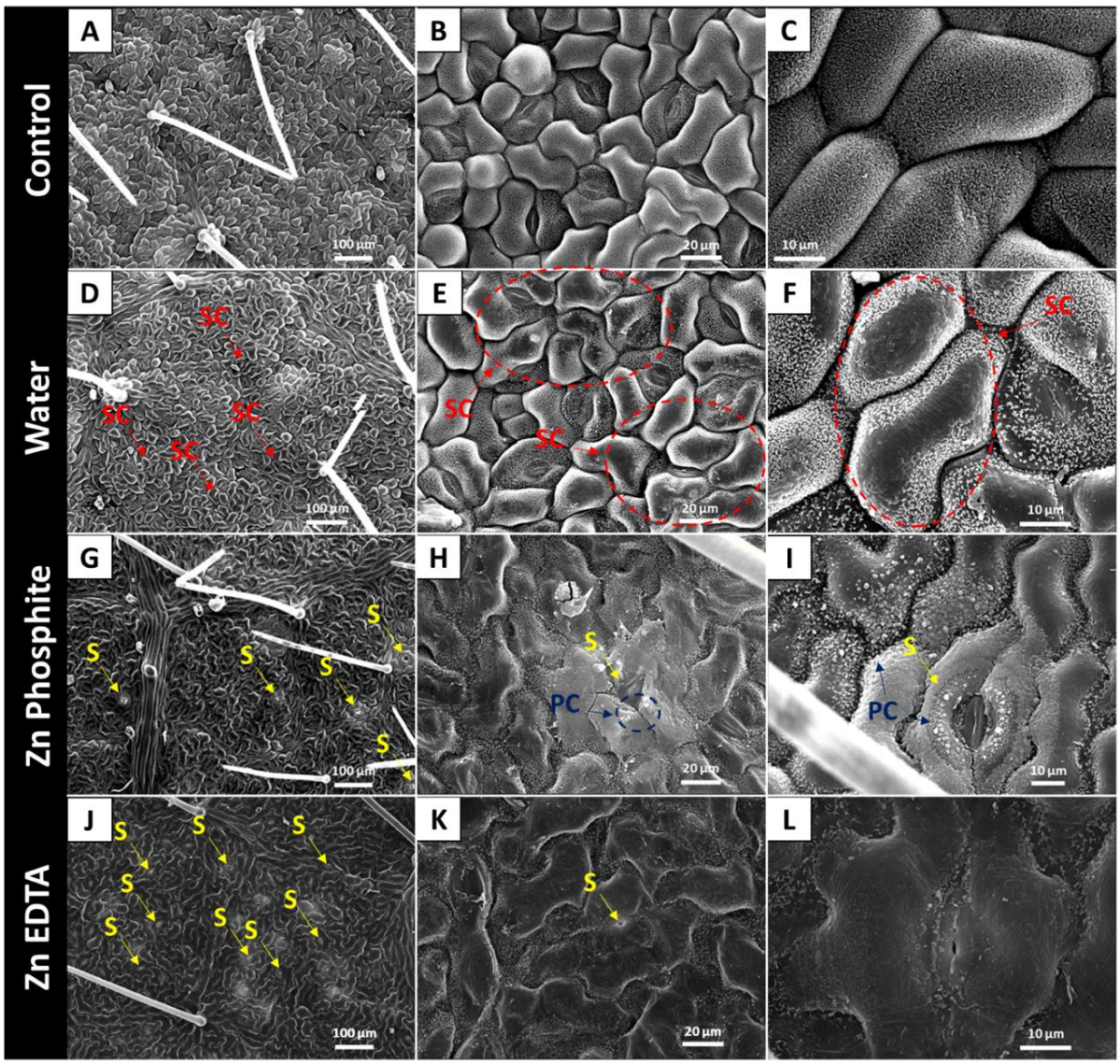

Figure 9 - SEM micrographs of the abaxial surface of soybean leaves at x 140, x 750 and x 1900 magnification. Zn-containing treatments disintegrated part of the wax crystals from the leaf surface. Zn phosphite accumulated around the stomata

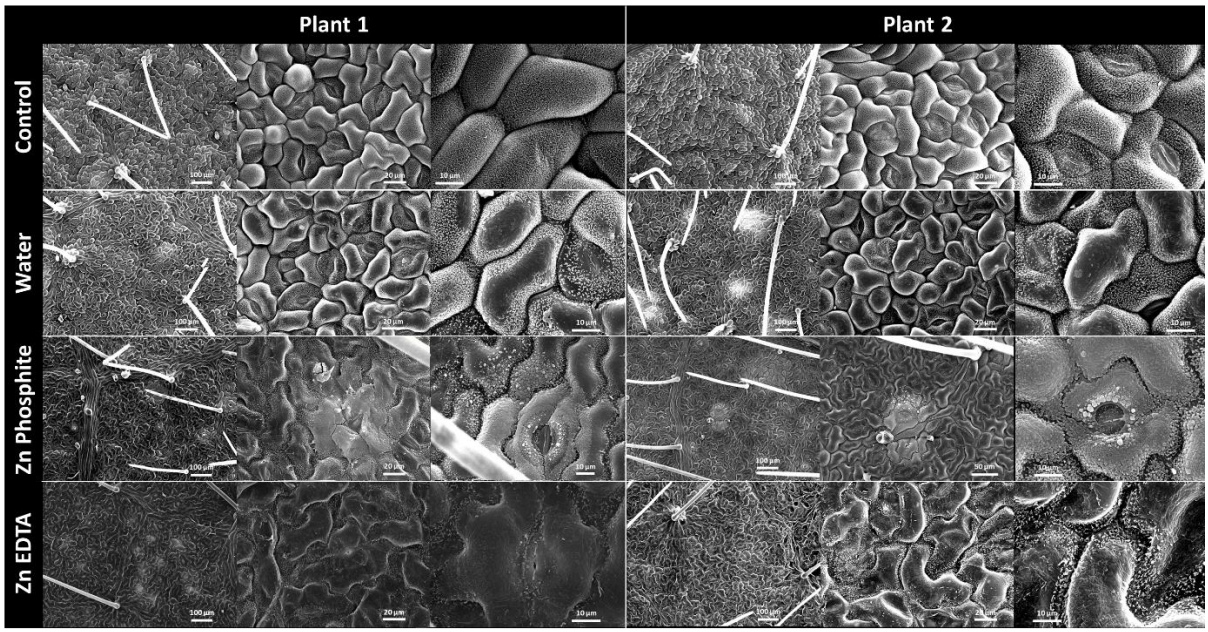

3.3.3 Chemical speciation

Figure 10 shows the non-normalized Zn-K XANES spectra recorded for the control plants. Despite the poor signal-to-noise ratio associated to the very low Zn concentration, no photoinduced spectral changes were noted. Similarly, the non-normalized Zn-K XANES spectra for plants treated with Zn phosphite (Figure 11 (A)) and Zn EDTA (Figure 11 (B)) did not show consistent spectral changes that could be assigned to radiation damage.

Figure 10 - Zn-Kα edge XANES spectra recorded for the petiolules of two control plants. Despite the noise, the data did not suggest spectral changes during the measurements

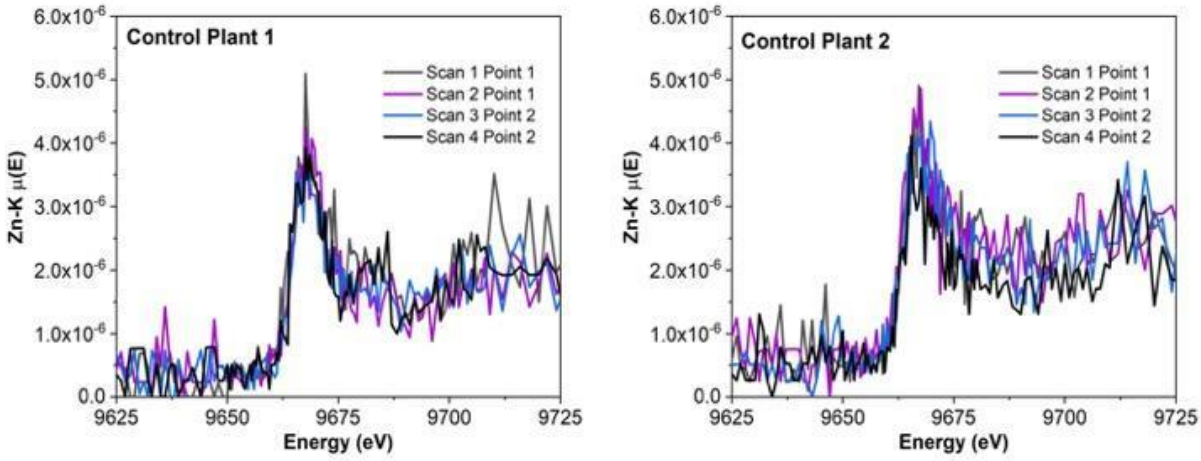

Figure 11 - Zn-Kα edge XANES spectra recorded for the petiolules of leaflets of (A) Zn phosphite and (B) Zn EDTA treatments. Zn chemical species was not affected by the radiation

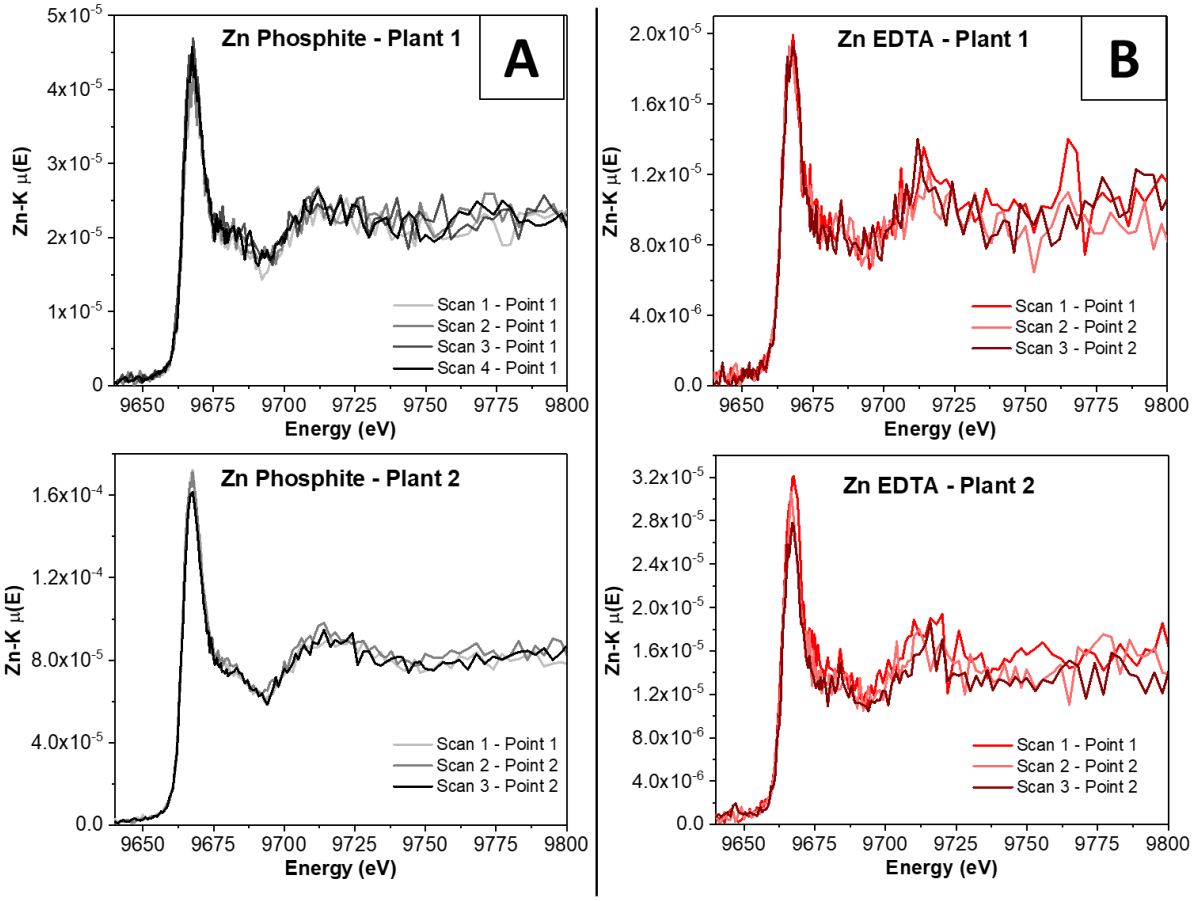

Concerning tissue dehydration, Figure 12 presents the Compton scattering intensity recorded during the XANES chemical speciation analysis. No significant changes were observed in the scattering intensities. Concomitantly, the intensity of Ca-Kα XRF (Figure 13) was also recorded, since Ca is one of the major constituents of plant tissues and stress signaler, thus a good radiation damage indicator. The data did not point out any significant signal variation for the Zn phosphite treated plants (Figure 13 (A)); however, a slight decrease, within error bar range, was noticed during the second scan in point 2 of plant 1, while in plant 2 it slightly increased (Figure 13 (B)).

Figure 12 - X-ray scattering normalized by the incident flux recorded for the petiolules of (A) Zn phosphite and (B) Zn EDTA treatments. The inelastic Compton scattering increases as function of the water content. As long as not changes were observed, we infer that dehydration did not occur during the XANES

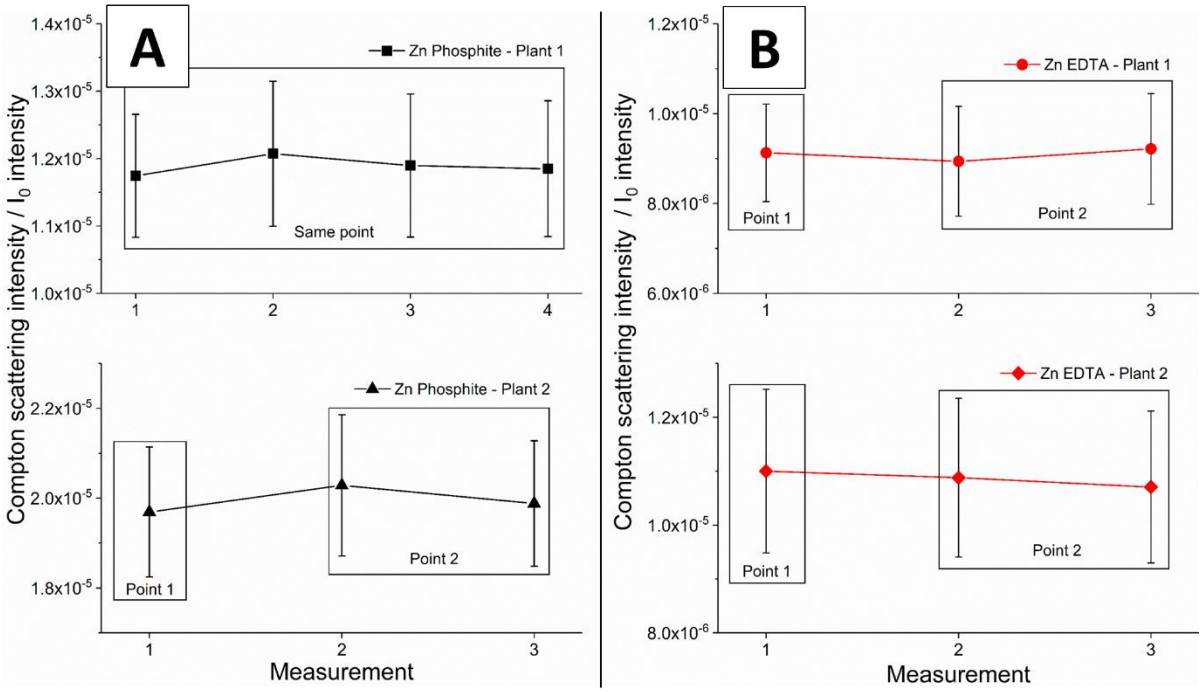

Figure 13 - Ca-Kα intensity normalized by the incident flux recorded for the petiolules of (A) Zn phosphite and (B) Zn EDTA treatments. The two plants from Zn EDTA treatment presented distinct behavior during the second scan in point 2

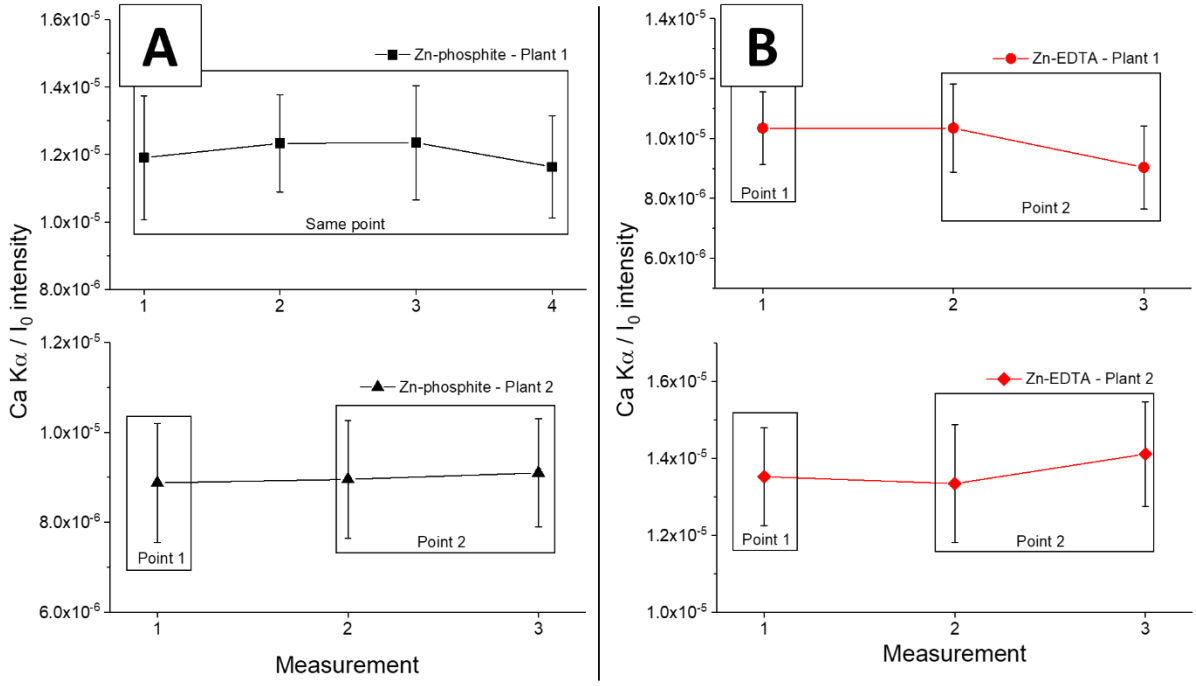

Figure 14 shows the stem of a soybean plant (A) prior to and after irradiation (B) by a ca. 30 μm focused beam during 20 min using an Rh anode operating at 45 kV and 900 μA. It is possible to note the scorching radiation damage caused by the X-ray beam.

Figure 14 - Region of the petiolule of leaflets probed by the X-Ray beam elapsed (A) prior and (B) after irradiation. Figure b presents a black spot which corresponds to injury caused by the beam. Figure C intends to show the energy wide spectrum used to irradiate the plant. It was obtained by the recoding the scattered energy from a Plexiglas cube

Figure 15 (A) and (B) present the XANES spectra recorded for Zn phosphite and Zn EDTA reference compound and for petiolules of two different plants whose leaves were treated with Zn phosphite. Analysis of the spectra associated to the standard compounds permits one to infer that Zn from Zn phosphite was transported as a compound different from that applied to the leaf. On the other hand, the spectra recorded for the petiolules of leaves treated with Zn EDTA overlapped that recorded for the pristine material. Figure 15 (C) presents the content of Zn in these plants in terms of XRF counts which represents the Zn concentration in the petiolule. The Zn content in the petiolule was higher for the Zn phosphite treatment, demonstrating the potential for higher absorption of Zn phosphite as compared with Zn EDTA. A similar finding was observed for the XRF approach (Figure 7).

Figure 15 - Zn-K XANES spectra recorded for petiolules of soybean after foliar application of a Zn phosphite and b Zn EDTA plus spectra registered for Zn phosphite and Zn EDTA reference compounds. Overlapping the spectra, one can observe that the Zn from Zn phosphite treatment has been transported as compounds different to that applied to the leaf, whereas the overlay between the spectra presented in b indicates that the Zn chemical environment in the petiolules and Zn EDTA reference compound were mostly the same. c Average XRF intensity from 9.78 to 9.84 KeV in the petiolules of these plants demonstrates higher concentration of Zn for Zn phosphite

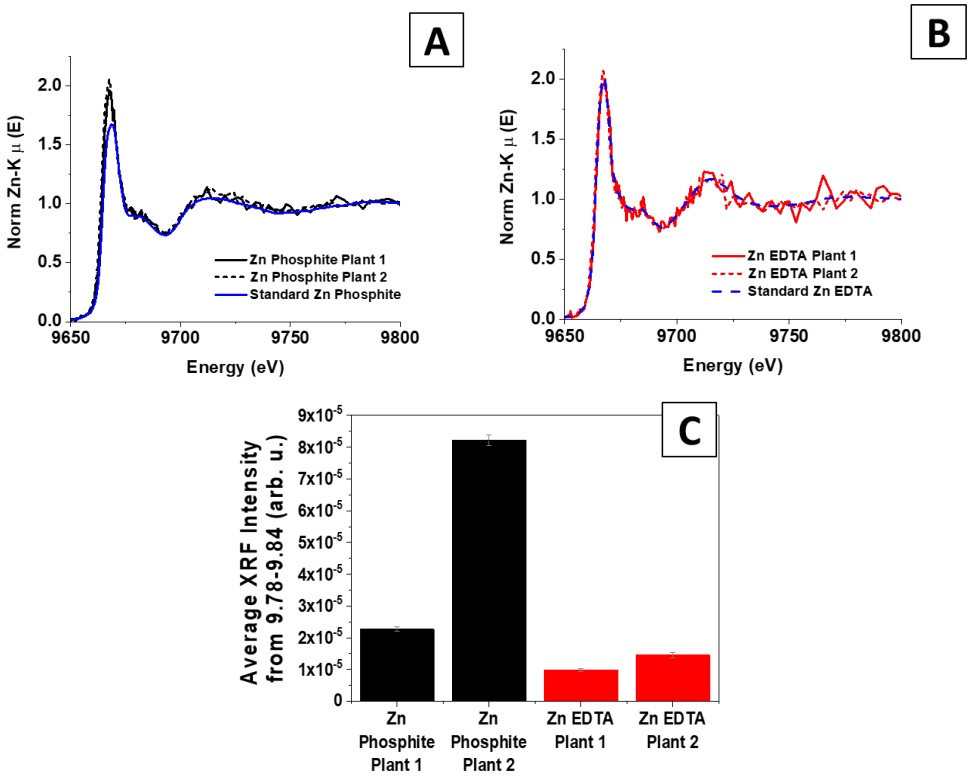

3.4 Discussion

The X-ray beam may modify the spatial distribution and chemical environment of the target element.[24] Changes in the chemical environment during in situ XANES measurements were reported by Smith et al.[25] during the speciation of arsenic in rice roots and by Scheckel et al.[24] in the analysis of thallium in *Iberis intermedia*. Differently from Zn^{2+}, both arsenic and thallium form compounds in multiple oxidation states and are more susceptible to photoreduction or oxidation than Zn^{2+}. The X-ray brilliance, thus the fluence on the sample, varies from one synchrotron beamline to another. This parameter should be then kept in mind during measurements in synchrotron sources. Additionally, recording a XANES spectrum usually subjects a certain point of the sample to longer exposure than that requested for XRF mapping or point analysis.[26] It is important highlighting that scorching symptoms were not observed in the plants submitted to the XRF LNLS beamline. The X-ray flux at this beamline

is in the order of 10^8 photons s^{-1} mm^{-2} at 10 keV. Nevertheless, differently from the Rh anode which supplied polychromatic beam (Figure 14 (C)), the XANES measurements were performed under monochromatic beam, resulting in a much shorter bandwidth. This is especially important, in relation to low energy photons, e.g., < 4 keV, which might modify the biological tissues since their interaction with matter is higher than those around Zn-K edge. Thus, as noted for the time-resolved XRF kinetic measurements, no radiation damage under the conditions used to register the XANES spectra was detected.

The Zn concentration commonly used in field applications is around 1 g Zn L^{-1}.[27] In order to overcome the limits of detection imposed by the in vivo XRF measurements, it was necessary to increase the dose to 23 g Zn L^{-1}. High concentrations of Zn may however negatively influence the uptake and transport of other nutrients such as K, P, Mg, Fe, Cu, and Mo.[28] In the present study, interference of Zn supply on the concentration of K, Ca, Mn, and Fe in plant petiolule was not observed, which suggests that even in higher concentrations, Zn was not interfering badly the metabolism of other nutrients. Under the set instrumental conditions, the limit of detection for Zn in the petiolule of living plants was estimated as 36 ± 1.3 mg kg^{-1}. The concentration of Zn in the leaves of soybean ranges from 50 to 80 mg kg^{-1} reaching up to ca. 600 mg kg^{-1} in plants grown in Zn-contaminated soil,[29] demonstrating that the experimental design adopted here allowed to quantitatively record the Zn concentration.

The observed agglomeration of Zn phosphite shown by SEM regards the precipitation as the solution dried and the mineral became solid. The inorganic particles of Zn phosphite agglomerated in the stomata may release ions under the influence of air humidity, thus increasing the uptake of Zn via the stomata pathway. A similar behavior was observed by Bala et al.[30] after applying ZnO nanoparticles in rice. Stomata may take up water and solutes, and even small particles may penetrate leaves through stomata. The mechanisms behind this process are still not fully understood.[31-33] It is possible that the uptake occurs by diffusion through a liquid water film in the stomata walls, which are formed by increasing the wettability of the stomata pores.[33; 34] Compared with the cuticular pathway, the stomatal pathway is characterized by higher size exclusion limits, which means that it is more accessible for larger molecules.[33] On the other hand, since higher stomata density did not lead to higher Zn foliar uptake after the application of $ZnSO_4$, Li et al.[35; 36] did not consider stomata the main foliar uptake pathway.

The disintegration of EWC followed the treatments with Zn phosphite and Zn EDTA was also in leaves exposed to abiotic stress, such as hygroscopic aerosols.[34] The EWC disintegration during the water treatment was caused mechanically by the brush. However, the

EWC disintegration caused by Zn phosphite and Zn EDTA can affect more epidermal cells than just the brush use, and it could be the mechanism responsible for the increased uptake of Zn compound through leaf cuticles. Moreover, both Zn phosphite and Zn EDTA are solubilized in a medium with low pH, and leaf cuticles exposed to acidic solutions presented lower fixation of cations such as Zn.[37] One can therefore conclude that the acidic condition of the Zn treatments may be a determinant factor associated Zn entrance trough the leaf.

The epicuticular wax damage caused by Zn EDTA and Zn phosphite raises a concern on possible stress induced by foliar fertilizers. The ability of EWC to recover from stress is dependent on the developmental stage, and, in some cases, it does not recover.[38] There is a compromise between Zn supplying and cuticle damage, this latter effect may bring undesirable consequences to plant health. From the abiotic stress standing point, the literature pointed out that the EWC has a minor influence in the rate of water movement across the cuticle membrane, in comparison with the intracuticular wax.[39] Conversely, the mechanical EWC removal may promote a moderate increase in water permeability.[39] In this context, no correlation between quantity of wax cuticular and epidermal water loss was noted for *Zea mays*.[40] Regarding biotic stress, it has been demonstrated that adjuvants may alter the epicuticular wax of Vitis vinifera and increase the susceptibility to *Botrytis cinerea*.[41] The soybean rust, caused by the fungus *Phakopsora pachyrhizi*, starts the leaf penetration by mechanical and enzymatic disruption of the cuticle.[42] Hence, one should wonder: Could the EWC damage promoted by Zn EDTA and Zn phosphite increase susceptibility to *P. pachyrhizi*? The present study highlights those investigations aiming at the development of novel foliar fertilizers should address the impacts of foliar fertilizer applications, the possible leaf stress, and the pathogen susceptibility.

The abaxial surface was chosen as an application site due to its presumed higher capacity to absorb nutrients. Preliminary XRF analysis indicated that Zn is more prone to be absorbed by the abaxial surface of soybean leaves than by the adaxial (data not shown here). Since the trichomes or stomata density seems to not affect Zn absorption,[35; 36] the higher absorption of the abaxial surface could be related to its thinner cuticle and epidermal cell wall. Compared with the adaxial application, Zn concentration in tomato and citrus leaves was nearly 2-fold higher when Zn nitrate or Zn hydroxide nitrate was applied to the abaxial leaf surface.[43]

One of the reasons why Zn EDTA behaved differently as Zn phosphite might be their different capacities of leaf penetration. In solution, Zn phosphite dissociates, releasing $Zn^{2+}_{(aq)}$ and presenting lower molecular weight than Zn EDTA, at least cuticular favored by smaller molecular size.[9] In addition, acidity might influence the uptake, and the pH values were 2.0 and 6.2 for Zn phosphite and Zn EDTA, respectively. The more effective absorption of Zn^{2+} from

Zn phosphite compared with the Zn EDTA agrees with previous reports. In fact, zinc-amino acid and $ZnSO_4$ increased the Zn concentration in rice grains more consistently when compared with Zn EDTA and Zn citrate.[14] Another study suggested that Fe EDTA reduced the size of aqueous pores from the leaf epidermis, decreasing the nutrient uptake.[44] In pea leaves treated with Zn EDTA and $ZnSO_4$, Zn was less absorbed as chelate than inorganic salt, whereas its translocation within the plant was higher with Zn EDTA.[45] Zn EDTA was also less mobile than $ZnSO_4$ in wheat leaves.[46] Chelated or organically complexed Zn was also less absorbed than inorganic salts, as demonstrated in a study of Peryea[47] who applied foliar fertilization in apple trees. Since part of the foliar-applied material inevitably falls on the ground, especially for crops with limited leaf area, one advantage that Zn EDTA might have over Zn phosphite is its higher mobility in soil, which leads to increased Zn uptake by roots.[48]

Our study partially agrees with Doolette et al.[46] that treated wheat leaves treated with Zn EDTA at 1000 mg L^{-1} Zn, their chemical speciation indicated that Zn EDTA was the dominant Zn species near the application point (from 66% to 60%). Their study did not measure the petiolule region; in some sites in the surrounding area of the application point, they found also Zn bonded to phytate, cysteine, and polygalacturonate.[46] In the present study, apparently all Zn was transported to the phloem as Zn EDTA. We employed that other four reference compounds were used to identify the chemical form of Zn in the petiolules from the Zn phosphite treatment. Figure 16 shows the XANES spectra recorded for Zn Malate (A), Zn sulfate (B), Zn oxalate (C), and Zn citrate (D), along with the spectra recorded for two plants that received Zn phosphite treatment. The features of the reference compounds spectra did not match with those observed for the samples. Although we the presence of these compounds were not found, one must keep in mind that in linear combination analysis of XAS, a fraction of Zn (less than 5%) would hardly be detectable, since the normalization itself can introduce errors in the order of 10%.

Figure 16 - XANES spectra recorded for petiolules of soybean leaflet of plants after foliar application of Zn phosphite and spectra registered for (A) Zn-Malate, (B) Zn-Sulphate, (C) Zn-Oxalate and (D) Zn-Citrate reference compounds

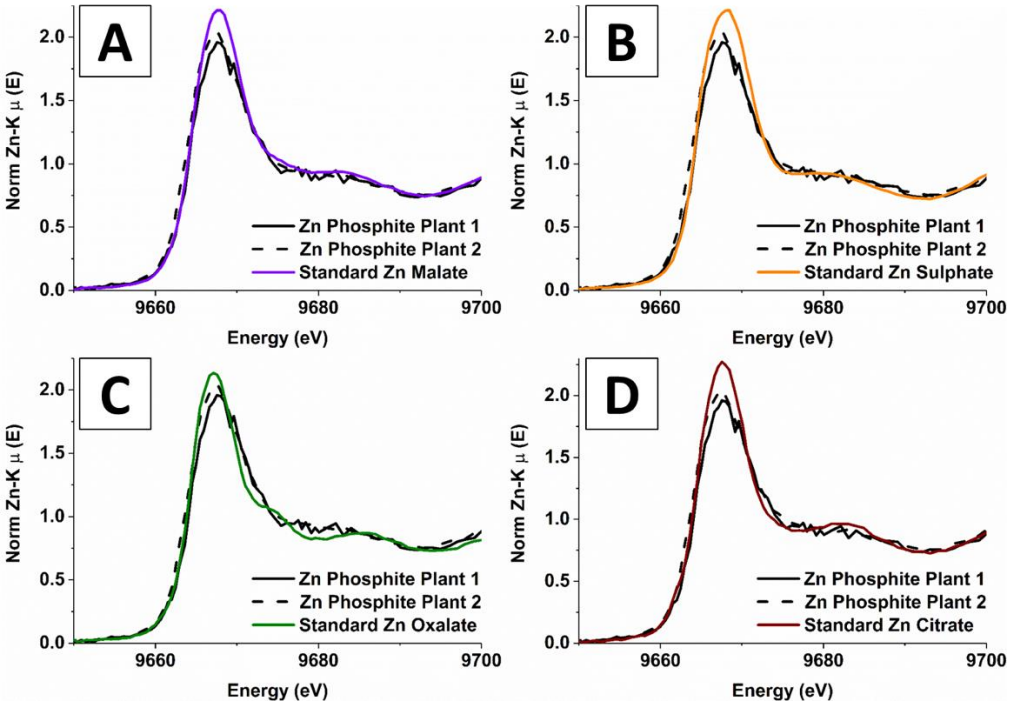

3.5 Conclusions

The combined absorption and transport rate for Zn phosphite were faster in comparison with Zn EDTA. Since both treatments promoted equivalent dissolution of leaf cuticle, the higher absorption-transport rate for Zn phosphite might be a consequence of the higher diffusion coefficient of the ionic Zn^{2+} forms from Zn phosphite. However, the accumulation of crystals from Zn phosphite fertilizer in the vicinity of stomata suggests the potential uptake of Zn by the stomata pathway, which could have accelerated the uptake. Of course other factors, such as ionic charge and pH, may also play a role on the absorption and transport velocity.

Inside the petiolule, the Zn supplied as Zn EDTA remained in its pristine form, whereas that from Zn phosphite was transformed and could not be identified. Hence, it is likely that Zn was loaded in the phloem as Zn EDTA; however, the mechanism that would allow a chelate to cross the cell membrane is not clear. Further studies using smaller X-ray beams in the nanometer range shall be performed to trace the chemical species along the Zn pathway. Additionally, it is still not clear in which moment, or tissue, the chelate is break down releasing the Zn^{2+} ions.

Finally, the present study draws the attention to the deleterious effects that foliar fertilizers may cause on the leaf cuticle. Hence, it would be keen to pursue the development of foliar fertilizers able to accomplish the task of nutrient supply while avoiding damages to leaf cuticle.

References

1 BROADLEY, M. et al. Function of nutrients: micronutrients. In: MARSCHNER, P. **Marschner's mineral nutrition of higher plants**. San Diego: Academic Press, 2012. p. 191–248.

2 GUILHERME, L. R. G. et al. Zinc availability in brazillian agroecosystems. In: International Zinc Symposium, 4., 2015, São Paulo. **Improving Crop Production and Human Health; proceedings.** São Paulo: Fertilizer Canada, 2015. p. 59-49.

3 CAULFIELD, L. E.; BLACK, R. E. Zinc deficiency. In: EZZATI, M., LOPEZ, A. D., RODGERS, A. A., MURRAY, C. J. L. **Comparative quantification of health risks:** global and regional burden of disease attribution to selected major risk factors. Geneva: WHO, 2004. p. 257–279.

4 MONTALVO, D. et al. Agronomic effectiveness of zinc sources as micronutrient fertilizer. **Advances in Agronomy**, v. 139, p. 215-267, 2016.

5 SLATON, N. A.; NORMAN, R. J.; WILSON, C. E. Effect of zinc source and application time on zinc uptake and grain yield of flood-irrigated rice. **Agronomy Journal,** v. 97, n. 1, p. 272-278, 2005.

6 CAKMAK, I. et al. Biofortification and localization of zinc in wheat grain. **Journal of Agricultural and Food Chemistry,** v. 58, n. 16, p. 9092-9102, 2010.

7 EICHERT, T.; FERNÁNDEZ, V. Uptake and release of elements by leaves and other aerial plant. In: MARSCHNER, P. **Marschner's mineral nutrition of higher plants**. San Diego: Academic Press, 2012. p. 71-84.

8 FERNANDEZ, V.; BROWN, P. H. From plant surface to plant metabolism: the uncertain fate of foliar-applied nutrients. **Frontiers in Plant Science,** v. 4, art. 289, 2013.

9 FERNANDEZ, V. et al. Physico-chemical properties of plant cuticles and their functional and ecological significance. **Journal of Experimental Botany,** v. 68, n. 19, p. 5293-5306, 2017.

10 AYTAC, S.; CIRAK, C.; OZCELIK, H. Foliar zinc application on yield and quality characters of soybean. **Asian Journal of Chemistry,** v. 19, n. 3, p. 2410-2418, 2007.

11 ZOU, C. Q. et al. Biofortification of wheat with zinc through zinc fertilization in seven countries. **Plant and Soil,** v. 361, n. 1-2, p. 119-130, 2012.

12 PHATTARAKUL, N. et al. Biofortification of rice grain with zinc through zinc fertilization in different countries. **Plant and Soil,** v. 361, n. 1-2, p. 131-141, 2012.

13 SINGH, P. et al. Zinc application enhances superoxide dismutase and carbonic anhydrase activities in zinc-efficient and zinc-inefficient wheat genotypes. **Journal of Soil Science and Plant Nutrition,** v. 19, n. 3, p. 477-487, 2019.

14 WEI, Y. Y.; SHOHAG, M. J. I.; YANG, X. E. Biofortification and bioavailability of rice grain zinc as affected by different forms of foliar zinc fertilization. **Plos One,** v. 7, n. 9, e45428, 2012.

15 BRENNAN, R. F. Effectiveness of different sources of manganese foliar sprays in alleviating manganese deficiency of *Lupinus angustifolius* L. grown on manganese deficient soils in western Australia. **Journal of Plant Nutrition,** v. 19, n. 2, p. 293-304, 1996.

16 KINACI, E.; GULMEZOGLU, N. Grain yield and yield components of triticale upon application of different foliar fertilizers. **Interciencia,** v. 32, n. 9, p. 624-628, 2007.

17 KAYAN, N.; GULMEZOGLU, N.; KAYA, M. D. The optimum foliar zinc source and level for improving Zn content in seed of chickpea. **Legume Research,** v. 38, n. 6, p. 826-831, 2015.

18 GHASAL, P. C. et al. Zinc accounting for different varieties of wheat (*Triticum aestivum*) under different source and methods of application. **Indian Journal of Agricultural Sciences,** v. 87, n. 9, p. 1111-1116, 2017.

19 GOZZO, F.; FAORO, F. Systemic acquired resistance (50 years after discovery): moving from the lab to the field. **Journal of Agricultural and Food Chemistry,** v. 61, n. 51, p. 12473-12491, 2013.

20 MCDONALD, A. E.; GRANT, B. R.; PLAXTON, W. C. Phosphite (phosphorous acid): its relevance in the environment and agriculture and influence on plant phosphate starvation response. **Journal of Plant Nutrition,** v. 24, n. 10, p. 1505-1519, 2001.

21 KARNOVSKY, M. J. A formaldehyde-glutaraldehyde fixative of high osmolality for use in electron microscopy. **Journal of Cell Biology,** v. 27, n. 2, p. 137-138, 1965.

22 HAN, F. et al. Organic acids promote the uptake of lanthanum by barley roots. **New Phytologist,** v. 165, n. 2, p. 481-492, 2005.

23 RAVEL, B.; NEWVILLE, M. ATHENA, ARTEMIS, HEPHAESTUS: data analysis for X-ray absorption spectroscopy using IFEFFIT. **Journal of Synchrotron Radiation,** v. 12, p. 537-541, 2005.

24 SCHECKEL, K. G. et al. In vivo synchrotron study of thallium speciation and compartmentation in *lberis intermedia*. **Environmental Science and Technology,** v. 38, n. 19, p. 5095-5100, 2004.

25 SMITH, E. et al. Localization and speciation of arsenic and trace elements in rice tissues. **Chemosphere,** v. 76, n. 4, p. 529-535, 2009.

26 LOMBI, E.; SCHECKEL, K. G.; KEMPSON, I. M. In situ analysis of metal(loid)s in plants: state of the art and artefacts. **Environmental and Experimental Botany,** v. 72, n. 1, p. 3-17, 2011.

27 CAKMAK, I.; KUTMAN, U. B. Agronomic biofortification of cereals with zinc: a review. **European Journal of Soil Science,** v. 69, n. 1, p. 172-180, 2018.

28 DOS SANTOS, L. R. et al. 24-epibrassinolide improves root anatomy and antioxidant enzymes in soybean plants subjected to zinc stress. **Journal of Soil Science and Plant Nutrition,** v. 20, n. 1, p. 105-124, 2020.

29 SILVA, M. L. D. S.; VITTI, G. C.; TREVIZAM, A. R. Heavy metal toxicity in rice and soybean plants cultivated in contaminated soil. **Revista Ceres,** v. 61, n. 2, p. 248-254, 2014.

30 BALA, R.; KALIA, A.; DHALIWAL, S. S. Evaluation of efficacy of ZnO nanoparticles as remedial zinc nanofertilizer for rice. **Journal of Soil Science and Plant Nutrition,** v. 19, n. 2, p. 379-389, 2019.

31 AVELLAN, A. et al. Nanoparticle size and coating chemistry control foliar uptake pathways, translocation, and leaf-to-rhizosphere transport in wheat. **ACS Nano,** v. 13, n. 5, p. 5291-5305, 2019.

32 EICHERT, T.; GOLDBACH, H. E. Equivalent pore radii of hydrophilic foliar uptake routes in stomatous and astomatous leaf surfaces - further evidence for a stomatal pathway. **Physiologia Plantarum,** v. 132, n. 4, p. 491-502, 2008.

33 EICHERT, T. et al. Size exclusion limits and lateral heterogeneity of the stomatal foliar uptake pathway for aqueous solutes and water-suspended nanoparticles. **Physiologia Plantarum,** v. 134, n. 1, p. 151-160, 2008.

34 BURKHARDT, J. Hygroscopic particles on leaves: nutrients or desiccants? **Ecological Monographs,** v. 80, n. 3, p. 369-399, 2010.

35 LI, C. et al. Effects of changes in leaf properties mediated by methyl jasmonate (MeJA) on foliar absorption of Zn, Mn and Fe. **Annals of Botany,** v. 120, n. 3, p. 405-415, 2017.

36 LI, C. et al. Absorption of foliar-applied Zn fertilizers by trichomes in soybean and tomato. **Journal of Experimental Botany,** v. 69, n. 10, p. 2717-2729, 2018.

37 FERNANDEZ, V.; STIROPOULOS, T.; BROWN, P. H. **Foliar fertilization:** scientific principles and field pratices. International Fertilizer Industry Association, 2013.

38 NEINHUIS, C.; KOCH, K.; BARTHLOTT, W. Movement and regeneration of epicuticular waxes through plant cuticles. **Planta,** v. 213, n. 3, p. 427-434, 2001.

39 GOODWIN, S. M.; JENKS, M. Plant cuticle function as a barrier to water loss. In: JENKS, M.; HASEGAWA, P. M. **Plant abiotic stress**. Oxford: Blackwell Publishing, 2005. p. 14-36.

40 RISTIC, Z.; JENKS, M. A. Leaf cuticle and water loss in maize lines differing in dehydration avoidance. **Journal of Plant Physiology,** v. 159, n. 6, p. 645-651, 2002.

41 ROGIERS, S. Y. et al. Effects of spray adjuvants on grape (*Vitis vinifera*) berry micro. ora, epicuticular wax and susceptibility to infection by *Botrytis cinerea*. **Australasian Plant Pathology,** v. 34, n. 2, p. 221-228, 2005.

42 EDWARDS, H. H.; BONDE, M. R. Penetration and establishment of *Phakopsora pachyrhizi* in soybean leaves as observed by transmission electron microscopy. **Phytopathology,** v. 101, n. 7, p. 894-900, 2011.

43 DU, Y. M. et al. In situ analysis of foliar zinc absorption and short-distance movement in fresh and hydrated leaves of tomato and citrus using synchrotron-based X-ray fluorescence microscopy. **Annals of Botany,** v. 115, n. 1, p. 41-53, 2015.

44 SCHLEGEL, T. K.; SCHONHERR, J.; SCHREIBER, L. Rates of foliar penetration of chelated Fe(III): Role of light, stomata, species, and leaf age. **Journal of Agricultural and Food Chemistry,** v. 54, n. 18, p. 6809-6813, 2006.

45 FERRANDON, M.; CHAMEL, A. R. Cuticular retention, foliar absorption and translocation of Fe, Mn and Zn supplied in organic and inorganic form. **Journal of Plant Nutrition,** v. 11, n. 3, p. 247-263, 1988.

46 DOOLETTE, C. L. et al. Foliar application of zinc sulphate and zinc EDTA to wheat leaves: differences in mobility, distribution, and speciation. **Journal of Experimental Botany,** v. 69, n. 18, p. 4469-4481, 2018.

47 PERYEA, F. J. Phytoavailability of zinc in postbloom zinc sprays applied to 'Golden Delicious' apple trees. **HortTechnology,** v. 16, n. 1, p. 60-65, 2006.

48 GANGLOFF, W. J. et al. Relative availability coefficients of organic and inorganic Zn fertilizers. **Journal of Plant Nutrition,** v. 25, n. 2, p. 259-273, 2002.

4 SOYBEAN ZN ABSORPTION AND DEVELOPMENT WITH NANOPARTICLE AND BEAD FERTILIZERS

Abstract

The kinetics of Zn absorption and subsequent incorporation is closely dependent on fertilizer efficiency. The hypothesis is that Zn fertilizers applied via nanotechnology and beads promote soybean development without a negative effect on plant metabolism. The aims were to monitor the kinetics of Zn absorption and desorption and influence on soybean Zn accumulation and reactive oxygen species. Experiments were settled with foliar application of Zn sulfate ($ZnSO_4$), Zn sulfate + Beads, and Zn oxide nanoparticle (nano ZnO). The kinetics of Zn absorption and desorption, soybean Zn accumulation, and reactive oxygen species were monitored. Results showed that Zn absorption and desorption of Zn were accentuated with posterior stabilization. Zn contents in plants and leaves were similar for all Zn fertilizers. $ZnSO_4$ + Beads presented the highest concentration in leaves. The malondialdeido, hydrogen peroxide, catalase, antioxidative enzyme superoxide dismutase, protein, guaiacol peroxidase, ascorbate peroxidase, and catalase were not influenced by Zn sources. The $ZnSO_4$ + Beads presented the highest intensity Zn without increases on reactive oxygen species. More studies are requested to understand the use of beads on fertilizers and the dynamic on release nutrients.

Keywords: Zn sulfate; beads; nanoparticles; Zn fertilizers; Zn oxide

4.1 Introduction

Brazil occupies a prominent position on grain production with 60.49 million hectares cultivated. Soybean responds for 33.89 million hectares representing 56% of the area planted.[1] Usually, a high-yield soybean field requires constant resupplying of exported micronutrients, such as zinc (Zn) which is carried out through foliar application or soil broadcasting, alone or in conjunction with NPK fertilizers.[2; 3]

Zinc is essential for plant metabolism, acting in (a) photosynthetic processes, intervening in the breaking down of water molecule and in the activity of carbonic anhydrase, responsible for fixation and CO_2;[4; 5] (b) nitrogen metabolism, participating in nitrate and nitrite reductases;[6; 7] (c) hormonal regulation, influencing the synthesis of indoleacetic acid, responsible for cell elongation;[8; 9] (d) attenuation of the oxidative degradation processes of cell structures.[10] Oliveira et al.[11] reported that the soil application of $ZnSO_4$ increased soybean

productivity by approximately 12%; and Heidarian et al.[12] noticed an increase of 25% soybean yield under foliar application.

Generally, micronutrient fertilizers present low use-efficiency in tropical agriculture. According to Cunha et al.[13] between 2009 and 2012, Brazilian agriculture applied 2.7-fold the amount of Zn exported by crops. The increase in use-efficiency of fertilizer application is fundamental not only from an economic standing point, but more importantly from an environmental one. The efficiency of Zn-based foliar fertilizers depends on source chemical features such as solubility and deliquescence point, crop demand, and environmental conditions, during the application (*i.e.*, air humidity, temperature, and wind). The main sources of Zn are sulfates, chlorides, oxides, and chelates which can be applied isolated or associated with granular NPK fertilizers.[14] In soluble sources (i.e. sulfates, chlorides, and chelates), the ions are readily available and subject to leaching, which can contaminate groundwater and watercourses.[15] On the other hand, oxides slow release the ions which may end up not supplying the plant demand.[16]

Nanotechnology and encapsulation represent alternatives to increase the use-efficiency of fertilizers. Nevertheless, these alternatives require studies to evaluate the kinetics of absorption and the subsequent incorporation in plants. The chemical and physical properties of fertilizer (such as, the nutrient's particle size) can affect its penetration into the leaf blade and consequently its absorption.[14] On the other hand, the use of micronutrient formulations based on nanoparticles can offer a new highly effective mechanism for the suppression of crop diseases, based on more targeted and strategic nutrition that enhances the plant's defense mechanisms. To take advantage of dissolution dependency on particle size, the oxide or carbonate particles must be finely ground until reaching the nanoparticle scale, this can be achieved using different methods.[17] Cruz et al.[18] exposed common bean (*Phaseolus vulgaris*) roots to ZnO colloidal dispersions at 1,000 mg L^{-1}, they reported that Zn uptake was faster for 40 nm compared to 20 and 60 nm. Prasad et al.[19] exposed peanut seeds (*Arachis hypogaea*) to 1,000 mg L^{-1} ZnO nanoparticles, observing increase in germination, chlorophyll, and stem and root growth. Regarding the foliar application of ZnO (25 nm diameter), the production of peanut pods increased by 29% compared to the foliar application of $ZnSO_4$.

In the present study, encapsulation refers to the loading of plant nutrients within micrometric beads, which are microparticles commonly made by plastic and applied in products (i.e., facial scrubs, hand-cleansers, and soaps) with a low biodegrade and persistence in aquatic environments.[20] Here, we are testing microbeads made from sodium alginate, proteins, and cellulose characterized as biodegradable particles.[21] There is little information about the plant

ability of taking up nutrients from such beads. One of the few studies was reported by Meurer et al.[22] that evaluated the uptake of Fe loaded within 933 nm microgel beads made of poly(allylamine) hydrochloride (PAH) and *N*,*N*′-methylene-bis(acrylamide). They showed that the Fe-loaded beads were able to correct iron chlorosis in cucumber leaves. Nevertheless, they did not compare their results against a positive control, for example a soluble Fe source.

The preset study hypothesizes that ZnO nanoparticle and Zn^{2+}-bead loaded can be absorbed by soybean leaves and promote plant development without negative effects on plant metabolism. Thus, the aim of the present study consisted in monitoring the kinetics of Zn absorption and desorption within cellulose microbeads, the kinetics of Zn foliar uptake, and the influence of the above-mentioned Zn sources on soybean Zn accumulation and reactive oxygen species.

4.2 Material and methods

4.2.1 Microbeads synthesis and characterization

Thirty-two grams of dried microcrystalline cellulose (MCC, Sigma-aldrich) were diluted in 280 ml of dimethyl sulfoxide (DMSO, Fisher) and left stirring for two hours. Subsequently, 120 ml of 1-ethyl-3-methylimidazolium acetate ionic liquid (Iolitec) was added and left stirring overnight. The cellulose microbeads were synthetized via membrane emulsification according to Obrien et al.[21]

Aiming at removing residual of DMSO and ionic liquid, they were rinsed with deionized water until it got clean. To certify the cleaning process, it was measured the electrical conductivity of the rinsing water. When it reached the same values of pure deionized water, the beads were considered clean. The diameter of the wet beads was determined by dynamic light scattering (DLS). The DLS analysis were performed using a Masterzize equipment (Malvern, USA).

To determine the Zn absorption by the beads, two grams of cleaned wet beads were soaked in 10 ml of $ZnSO_4.7H_2O$ (Scientific Laboratory Supplies, UK) at 20 g L^{-1} for 10 minutes. Zn concentration in the solution was determined by measuring the electrical conductivity of the solution over time. To convert the electrical conductivity of the solution to Zn concentration, it was previously built an external calibration. The Zn mass within the beads was determined by gravimetry. The Zn-loaded beads were dried at 60 ºC until reaching constant mass. Then, 0.1 g of dried beads were soaked in 10 ml of deionized water to determine the desorption kinetics. The Zn desorption rate was determined by measuring the electrical conductivity of the deionized water over time.

4.2.2 Transport kinetics

The kinetics of Zn transport was determined by measuring the Zn content on the petiole of a trefoil which received the treatments over 72 hours with five biological replicates. Treatments consisted of a solution of $ZnSO_4.7H_2O$ (positive control), an aqueous colloidal dispersion of 60 nm ZnO nanoparticles (Nanophase, USA), and an aqueous suspension of cellulose microbeads bearing $ZnSO_4$.

The cellulose microbeads suspension bearing $ZnSO_4$ was prepared by mixing 10 ml of $ZnSO_4.7H_2O$, concentration at 0.67 g L^{-1}, and 2 g of the cellulose microbeads. The 60 nm ZnO particles, hereafter called nano ZnO, were previously characterized by Cruz et al.[18] The treatments were applied on the abaxial face of the leaves using a Drigalski spatula (Figure 1). The employed concentration was 23 g L^{-1} of Zn and the volume spread on each trefoil was 70 µL. Measurements were performed using a portable X-ray fluorescence spectrometer (Bruker, Tracer III SD). The X-ray spot was *ca*. 3 mm^2 and generated by an Rh anode operating at 40 kV and 30 µA, using 12 mil Al + 1 mil Ti primary filter. X-ray fluorescence was detected by a silicon drift detector with a dwell of 60 s and a dead time smaller than 10%. During the trial, the plants were maintained in a growth room at 25º C and photoperiod of 12 h supplied by led lamps with a photon flux of 250 µmol m^{-2} s^{-1}.

Figure 1 - Design of the kinetics transport trial

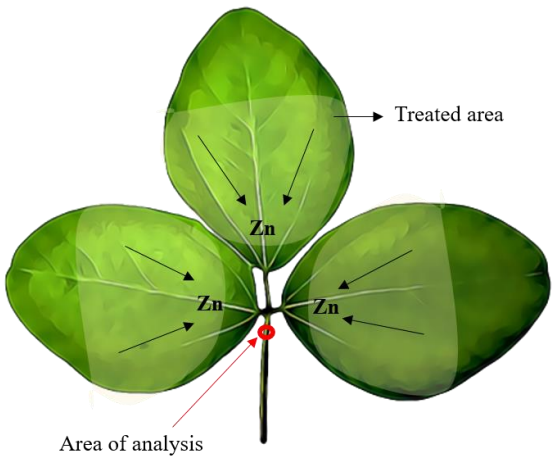

4.2.3 Greenhouse trial

A greenhouse trial was settled in a randomized blocks design. The foliar treatments consisted of the same materials above described. In addition to the positive control, two more controls were employed using (i) a control that received only 10% Zn requirement supplied trough root; (ii) and a root application that received 100% of the Zn requirement trough root

supply. Each treatment and control counted on five replications. Each pot was considered as an experimental unit and the whole experiment summed up 40 pots.

Soybean seeds (*Glycine max* L. Merril cv. 7739 (IPRO) were germinated in the organic substrate (Basaplant ®, Brazil) for ten days. In the VC phenological stage, two plants were transferred to 2 L plastic pot containing Hoagland's nutrient solution renewed every seven days. With exception of the root application treatment, plants were maintained at 10% of the regular Zn concentration.

During the trial, the plants were maintained in a growth room at 25 ºC, and a photoperiod of 12 h supplied by led lamps with a photon flux of 250 µmol m^{-2} s^{-1}. The Zn treatments were applied on the leaf surface at the V5, V7, and R2 phenological stages. The Zn dose was based on the recommendation of approximately 300 g ha^{-1} of Zn[3] split into three applications of 100 g ha^{-1} each. To calculate the Zn amount for each plant, it was considered a field population of 250,000 plants ha^{-1} (Figure 2). The Zn sources were diluted in 70 µL of distilled water and sprayed in the entire plant's shoot, using a CO_2-pressurized sprayer, in the three applications. During the first two applications (V5 and V7), there were two plants per pot, while in the third application (R2 phenological stage), there was one plant per pot due to the harvesting of one of the plants.

Figure 2 - Design of the greenhouse trial

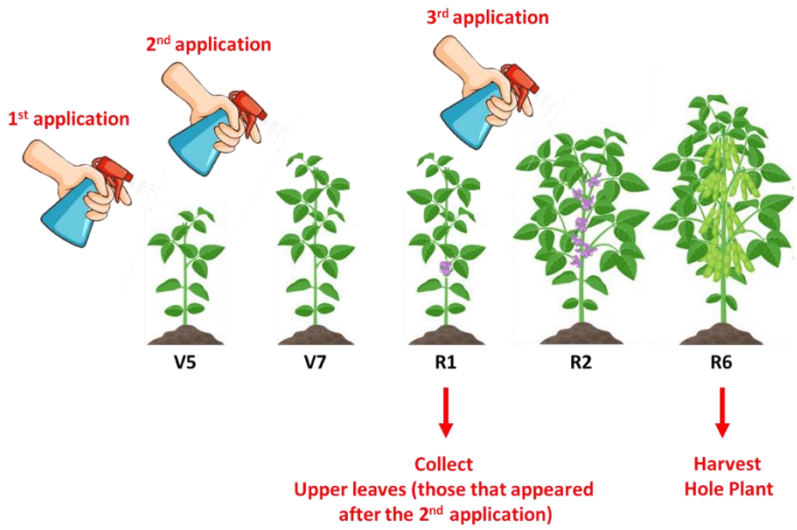

4.2.4 Determination of zinc content in leaves

Zinc content in leaves was monitored ten days after the second foliar application, at the R1 phenological stage. We collected one entire plant of each pot and analyzed the new leaves that emerged after the second foliar application (Upper Leaves). These leaves were washed

twice in a HCl solution (3 v%) and taken for drying in a laboratory oven at 60 ºC. In the R6 phenological stage, the whole plants were collected and separated into the leaves + stem + petioles (shoot), which were also washed twice in an HCl solution (3% vol/vol) and taken for drying in a laboratory oven at 60º C. The total Zn in the shoot was assessed by multiplying the shoot dry mass (kg) by the Zn content (mg kg^{-1}).

The dried leaves were ground in a ball mill (Retsch USA, MM400), till reaching 150 µm particle size. Then, the powders were analyzed in an energy dispersive X-ray fluorescence facility (Shimadzu Japan, EDX 720). The equipment was furnished with a Rh anode operating at 50 kV and 1,000 µA. The measurements were performed in triplicate under air with dwell time of 300 seconds and dead time below 10%.

4.2.5 Enzymatic activity and protein determination

The first fully expanded trifoliate leaf also was collected and stored in liquid nitrogen for further enzymatic analysis in the R6 phenological stage. The MDA (malondialdehyde) and antioxidative enzyme activity determination were performed at the first fully expanded trifoliate leaf of plants at the R6 phenological stage. Therefore, the leaves were collected, immediately stored in liquid N_2, and then transferred to a -80 ºC freezer. Later, the samples were ground under liquid nitrogen using plastic mortars and stored at -80 ºC for further analysis.

The lipid peroxidation (MDA) was determined according to Heath and Packer,[23] using TCA 20 % and 0.5 % of thiobarbituric acid (TBA). The soluble protein content and activity of the antioxidative enzyme superoxide dismutase (SOD), guaiacol peroxidase (GPOX), ascorbate peroxidase (APX), and catalase (CAT) were extracted following Azevedo et al.[24]

The protein content was determined with bovine serum albumin (BSA) using concentrations from 0.1 up to 1 mg L^{-1}.[25] The SOD activity was determined according to Giannopolitis and Ries[26] and Cembrowska-Lech et al.[27] using a solution containing 50 mM of potassium phosphate buffer (pH 7.8), 13mM methionine, 63 mM nitroblue tetrazolium (NBT), 0.1 mM EDTA, and 1.3 mM riboflavin. The GPOX activity was determined according to Matsuno and Uritani,[28] standardized in the laboratory of vegetal physiology of the Embrapa Temperate Climate, Brazil, with modifications, and using phosphate-citrate buffer (0.2 M of dibasic sodium phosphate and 0.1 M of citric acid, pH 5), 10 µL of the plant extracts, 50 µL of 0.2% guaiacol, and 50 µL of H_2O_2 9.8 mM.

The APX activity was determined according to Moldes et al.,[29] with modifications. Solutions of plant extract, potassium phosphate buffer (at pH 7), ascorbate, EDTA, H_2O_2 were used to determination. CAT activity was determined based on Kraus et al.[30] modifications

according to Azevedo et al.,[24] using potassium phosphate buffer (pH 7.5). Glutathione reductase (GR) was determined in a spectrophotometry at 30ºC, using a buffer solution (potassium phosphate; 100 mM at pH 7,5) with 2-nitrobenzoic acid (1mM), oxidized glutathione (1 mM), and NADPH (0.1 mM).[24] Hydrogen peroxide (H_2O_2) concentration was monitored according to Alexieva et al.,[31] using trichloroacetic acid (0.1% in a 1 g 10 mL^{-1}; w:v), potassium phosphate buffer (100 mM; pH 7.5) and potassium iodide (1 M) with reading in a spectrophotometer at 390 nm.

4.2.6 Microscopy analysis

Once stomata pathway represents an important mechanism of absorption for particles,[32] the stomatal density of leaves was determined. The measurements were taken on the adaxial face of the second fully expanded trefoil of two soybean plants. For this analysis, the leaflets were placed on slides and then a drop of water was pipetted onto the leaf surface, then the leaflets were covered with cover slips. The samples were taken to an epifluorescence microscope (Zeiss Axionscope) and images were recorded using an ultraviolet filter. The stomatal density was determined by counting the stomata in an area of 1 mm^2, two areas per leaflet were sampled, as shown in Figure 3.

Figure 3 - Design of the stomatal density counting method

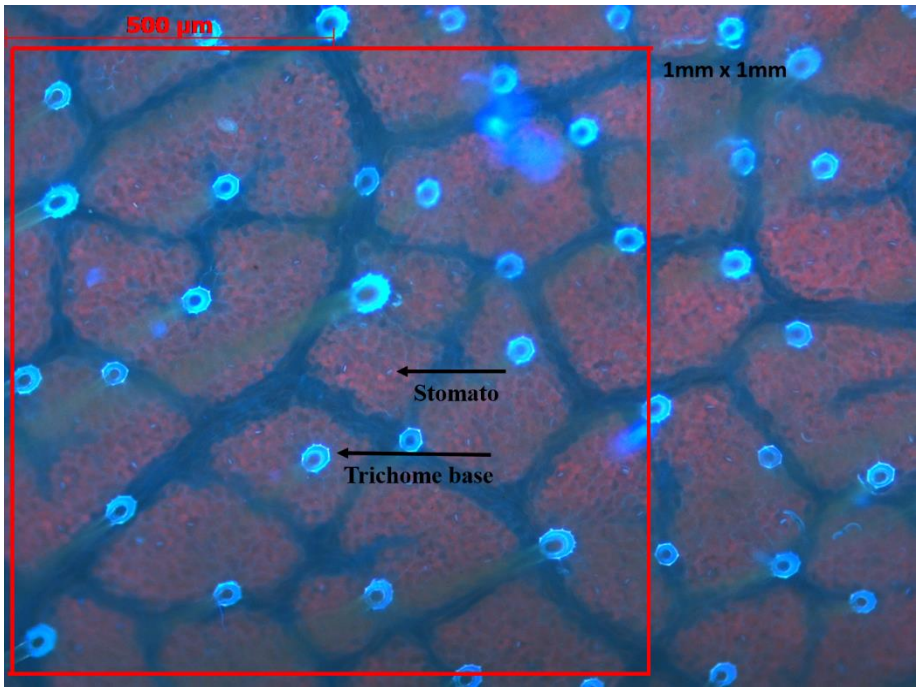

The deposition of the fertilizers on the leaf surface was evaluated by scanning electron microscopy images. Hence, 70 µL of the fertilizers were deposited on the surface of the leaflets at 23 g L^{-1} of Zn. Seventy-two hours after application, the leaves were immersed in Karnovsky fixative solution for 48 h. After this process, they were sequentially dehydrated by immersion in ethanol solutions from 10 to 90 vol% per 30 min each. Then, the samples were dehydrated in 100 vol% ethanol for 1 h and this step was done three times. The samples were then dried at their critical point (LEICA CPD 300), and then coated with gold (model Bal-tec 129 SCD 050) and examined with SEM (Jeol JSM IT 300).

4.2.7 Data analysis

The assumptions of normality and homogeneity of variance were evaluated by the Shapiro-Wilk test and the Oneillmathews test ($P \leq 0.05$), respectively. Outliers identified by Grubbs' test were removed when present. Data from each variable was submitted to ANOVA, based on the F-test. When the F-test was significant ($P \leq 0.1$), the Zn sources were tested by the LSD-test ($P \leq 0.05$).

The data of MDA, H_2O_2, catalase, SOD, protein, GR, GPOX, APX, and Zn accumulation were subjected to multivariate exploratory analysis by hierarchical clustering, using a similarity matrix constructed by the Euclidean distance. The Euclidean distance among accesses was calculated, distinguishing between the Zn sources and exposing the group structure contained within in the dendrogram. The correlations between variables also were monitored using the Pearson correlation ($P \leq 0.05$). The Zn absorption and desorption were compared between the first and last min, and correlated by Pearson correlation ($P \leq 0.05$).

4.3 Results

4.3.1 In vitro Zn absorption and release by the cellulose microbeads

The zinc incorporation by the beads was fast phenomenon, the content of zinc within the beads steeply increased in the first minute followed by stabilization (Figure 4 (A)). The Zn release presented a similar trend, although it was slower than the absorption (Figure 4 (B)). There was a positive correlation between Zn absorption and desorption (0.89; $p < 0.05$), indicating that Zn was desorped with consecutive absorption. The wet microbeads diameter (Dx90) was 10 µm ± 2.5 and a specific surface area of 223.5 $m^2\ kg^{-1}$.

Figure 4 - (A) Zn content in the beads (Zn absorption); (B) Zn concentration on the deionized water (Zn desorption) on time (minutes)

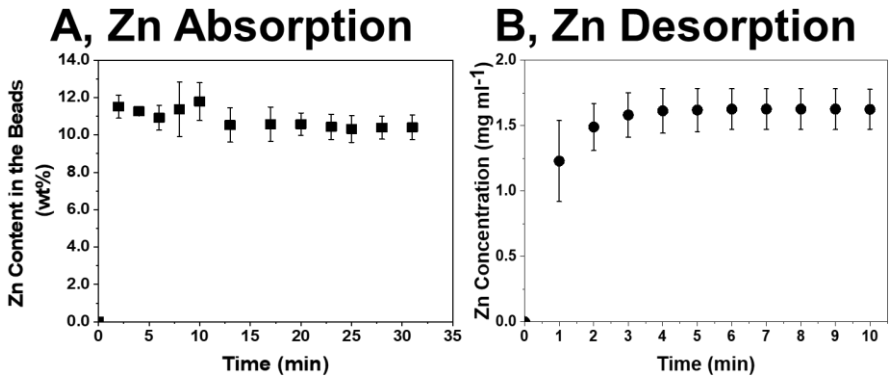

4.3.2 Transport kinetics

Using the handheld X-ray fluorescence spectrometer, we monitored the content of the Zn in the petiole of the treated leaves as function of time. This procedure revealed the transport kinetics and hence the ability of the Zn source in supplying this nutrient to the plant. Figure 5 (A) shows that the cellulose microbeads bearing $ZnSO_4$ ($ZnSO_4$ + Beads) presented the highest intensity Zn from the 1st to the 70th hour of the experiment. This also becomes clear by summing up the number of counts obtained throughout the experiment. Figure 5 (B) shows that the total number of counts for $ZnSO_4$ + Beads was 0.27 ± 0.08. This value was 51% higher than the control (Figure 5 (B)). On the other hand, the temporal and total Zn intensity measured for nano ZnO, $ZnSO_4$, and control presented a general average of 0.15 ± 0.02 (Figure 5 (B)).

Figure 5 - Temporal and total intensity Zn kα of fertilizers. Zn sources were tested by the LSD-test ($P \leq 0.05$), and results were represented by uppercase letters

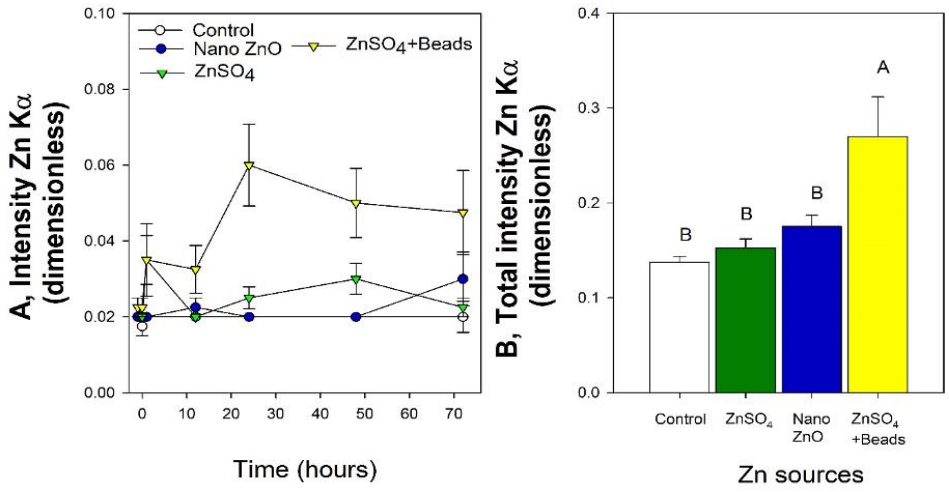

Figure 6 shows that no symptoms of phytotoxicity were observed in the leaves treated with $ZnSO_4$ + Beads and nano ZnO. In contrast, $ZnSO_4$ caused chlorosis in the treated leaves, highlighted by the red arrows, which became evident 72 h after the application. Additional pictures registered during the experiment are presented in supplementary Figure 7.

Figure 6 - The visual aspect of leaves with $ZnSO_4$, Zn sulfate + beads, nano ZnO after 24, 48, and 72 h of application

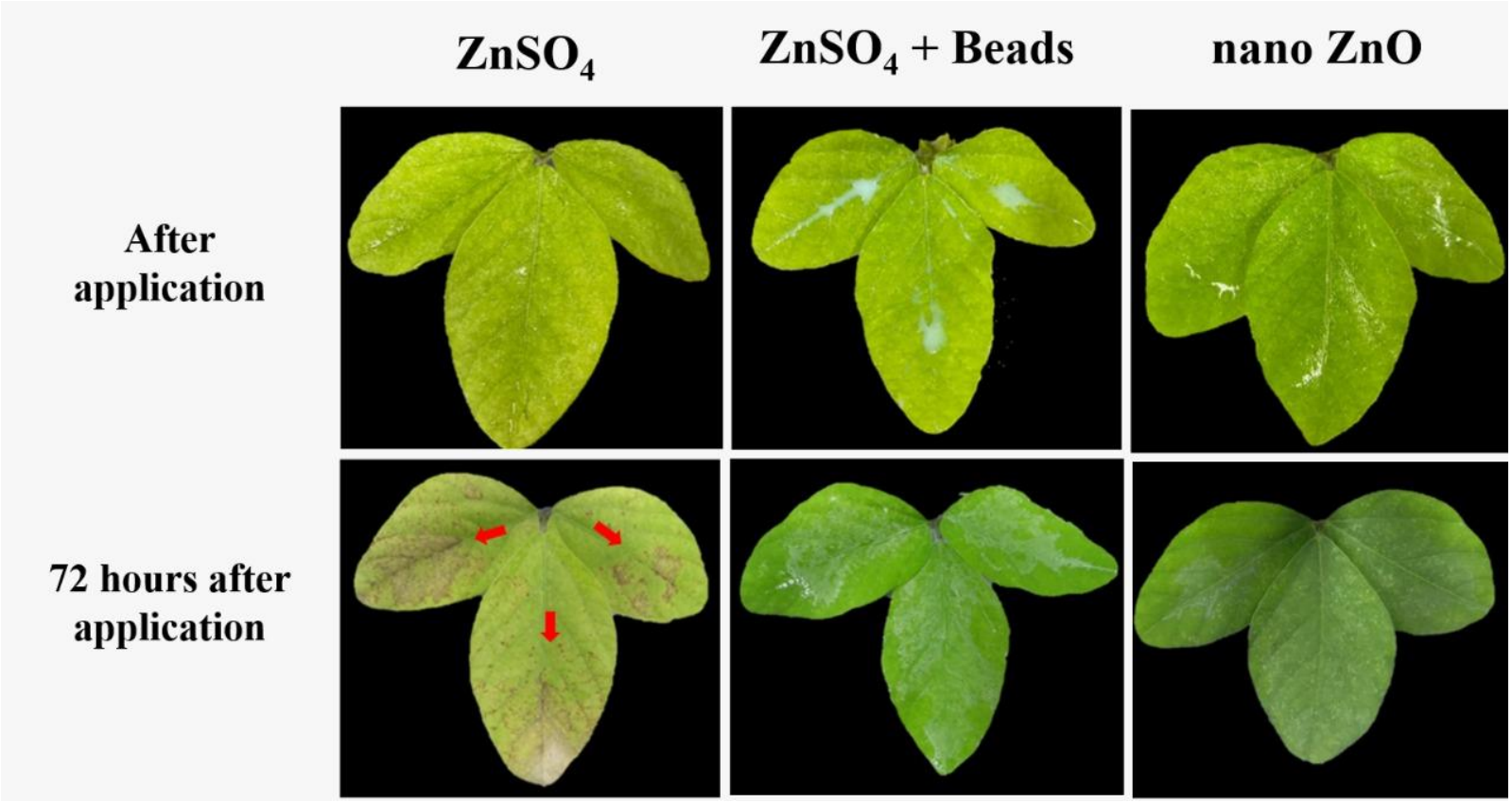

Figure 7 - The visual aspect of leaves with Zn sulfate ($ZnSO_4$), Zn sulfate + Beads, Zn oxid_Nano (ZnO_Nano) after 24, 48, and 72 h of application. R1, R2, and R3 represent replications 1, 2, and 3

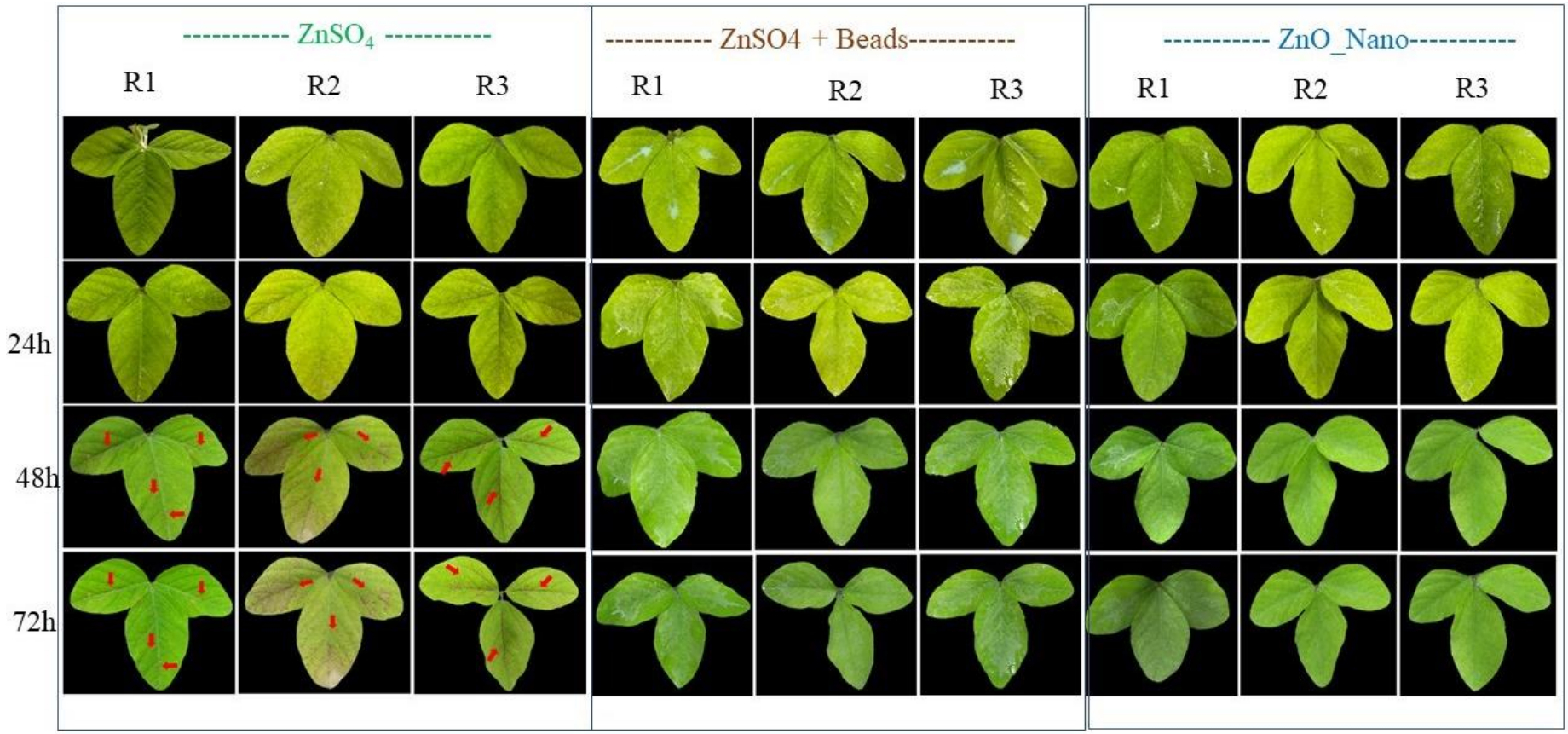

4.3.3 Greenhouse trial

Figure 8 (A) shows the concentration of Zn, at R1 stage, in the leaves that developed after two sprayings at V5 and V7 stage, they were called “upper leaves”. Figure 8 (B) presents the concentration of Zn in the hole plant at R6 stage previously treated at V5, V7 and R1 stage. The Zn content was similar between the Zn sources applied on leaves and roots with an average ranging from 24 to 32 mg kg^{-1}. The lowest Zn content was noticed in control with an average of 20 mg kg^{-1} (Figure 8 (B)).

In the “upper leaves”, the Zn content was higher under root application (47 mg kg^{-1}; Figure 8 (B)), while there was no difference between on the below leaves (general average of 36 mg kg^{-1}). It means that at despite the short-term experiments showed that $ZnSO_4$ + Beads readily transported Zn to other plant parts, in the long run the Zn sources performed equally. The treatments did not cause any difference on dry mass with an average of 23 g $plant^{-1}$ (Figure 8 (D)).

The Zn accumulation was higher under root application, in which we observed increase of 42% compared to control, indicating the plant absorption and translocation were more efficient under application on roots (Figure 8 (E)).

Figure 8 - Zn contents in the plant leaf, dry mass, and Zn accumulation in soybean with Zn sulfate, Zn sulfate + Beads, nano ZnO. Root application was performed with $ZnSO_4$. Zn sources were tested by the LSD-test ($P \leq 0.05$), and results were represented by uppercase letters. The treatment “Root Application” refers to the complete Hoagland solution positive control. Ns: not significant

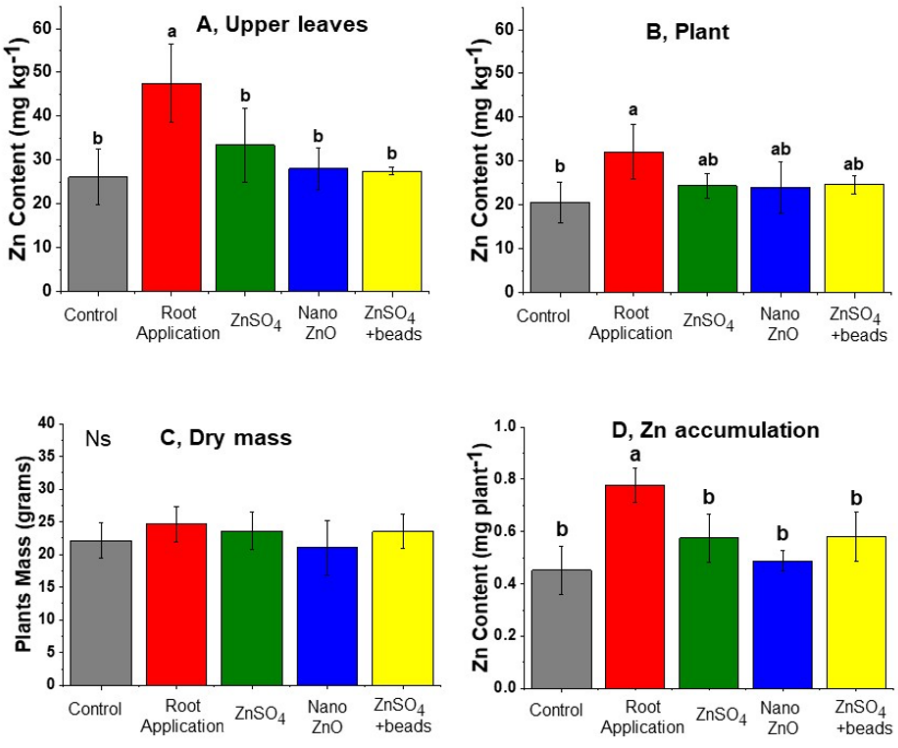

4.3.4 Effects of the treatments on the oxidative metabolism

The first fully expanded leaf at R6 stage, *i.e.*, after the three foliar applications of Zn sources at V5, V7, and R2 were subject to enzymatic activity analysis. Zn fertilizers did not influence MDA, H_2O_2, catalase, SOD, and protein in soybean with an average of 75 mmol g of fresh weight^{-1}, 7,024 µmol g of fresh weight^{-1}, 651 µmol min^{-1} protein mg^{-1}, 24.3 U protein mg^{-1}, and 5.1 g kg^{-1}, respectively (Figure 9 (A-E)). Note that the activity of glutathione reductase was higher for plants receiving zinc by root from a complete Hoagland solution (Figure 9 (F)).

Figure 9 - Malondialdehyde (MDA), hydrogen peroxide (H_2O_2), catalase, antioxidative enzyme superoxide dismutase (SOD), and glutathione reductase (GR) enzymatic activities and protein content. The plants were previously treated with $ZnSO_4$, $ZnSO_4$+Beads, nano ZnO. Control and Root Application were not subjected to any foliar treatment; they were grown in 10% and 100% Hoagland solution, respectively. The results were evaluated by the LSD-test ($P \leq 0.05$), and results were represented by uppercase letters. The treatment "Root Application" refers to the complete Hoagland solution positive control. Ns: not significant

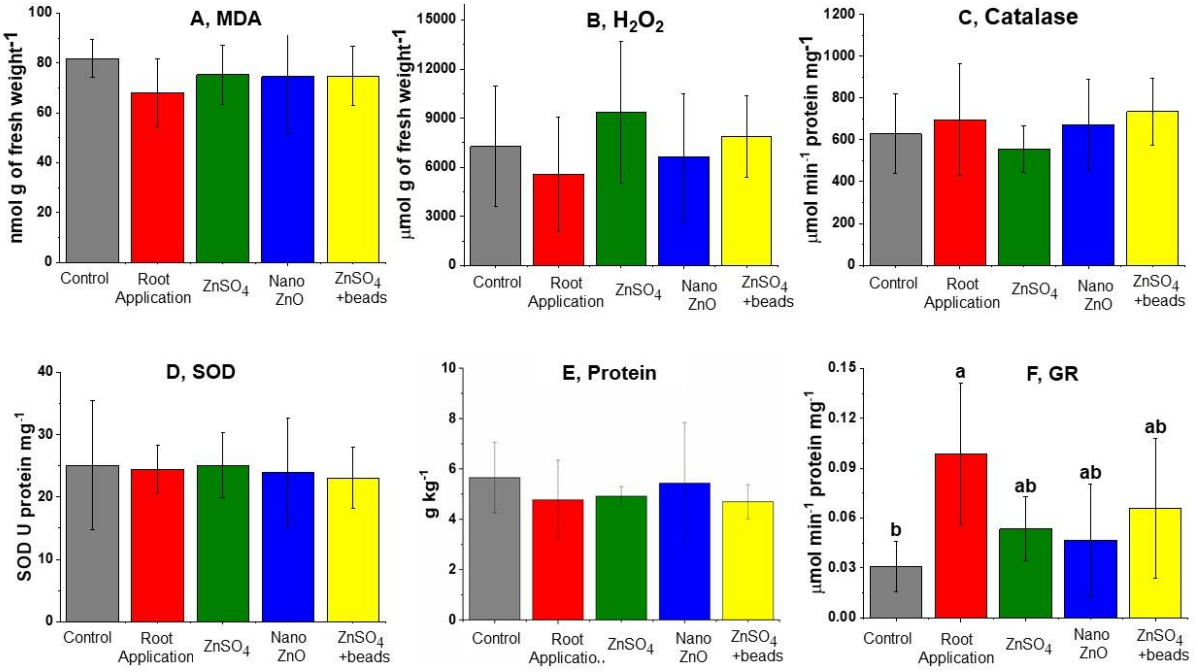

GPOX and APX also did not present significant difference between treatments, the average activity was 653 min^{-1} protein mg^{-1} and 3,027 mmol min^{-1} protein mg^{-1}, respectively (Figure 10). There was no linear Pearson correlation between Zn accumulation and enzymatic activities or protein, specifically the correlations were with MDA (r: -0.27; $P \leq 0.05$), H_2O_2 (r: -0.11; $P \leq 0.05$), catalase (r: -0.03; $P \leq 0.05$), SOD (r: -0.11; $P \leq 0.05$), protein (r: -0.02; $P \leq 0.05$), and GR (r: -0.41; $P \leq 0.05$).

Figure 10 - Guaiacol peroxidase (GPOX) and ascorbate peroxidase (APX) activities in R6 soybean leaves. The plants were previously treated with $ZnSO_4$, $ZnSO_4$+Beads, nano ZnO. Control and Root Application were not subjected to any foliar treatment; they were grown in 10% and 100% Hoagland solution, respectively. The results were evaluated by the LSD-test ($P \leq 0.05$), and results were represented by uppercase letters

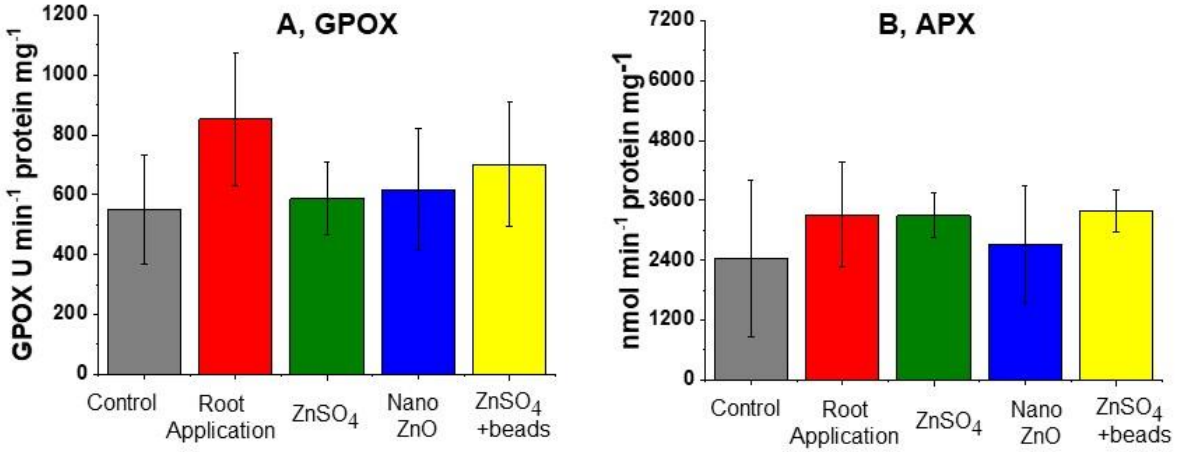

In the dendrogram, there was a clear difference between the Zn sources using the data set. When the plant received the complete Zn feeding by roots, it was fitted in the Group 1, which presented higher efficiency on Zn supply different from the Group 2 (others Zn sources), Figure 11. That difference is associated with higher Zn contents in plant and upper leaves with 100% of $ZnSO_4$ (Figure 8).

Figure 11 - Dendrogram with the results of Zn sulfate ($ZnSO_4$), Zn sulfate + Beads, Nano ZnO, and $ZnSO_4$ applied on roots; control, 10%_Zn is $ZnSO_4$

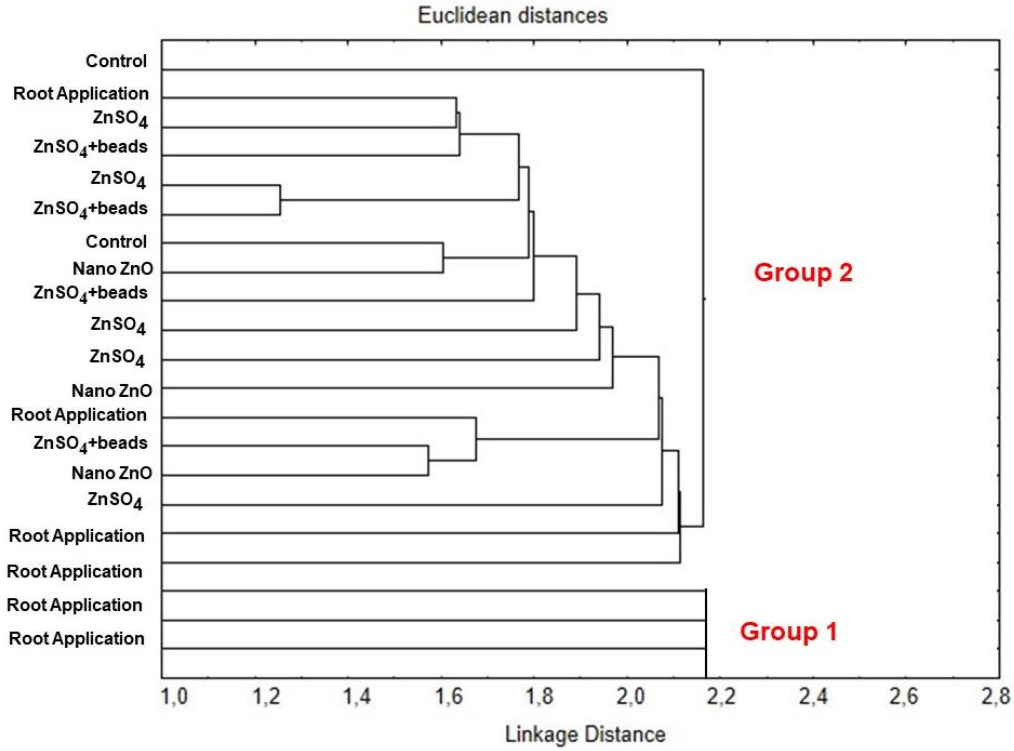

The stomatal density on the adaxial face of the soybean leaf is approximately 36 stomata mm^{-2}. The SEM images demonstrated the deposition of nanoparticles and entire beads on the leaves surface just after the application and elapsed 72 h (Figure 12).

Figure 12 - Soybean leaf surface images by Scanning Electron Microscope (SEM) with magnification of 140x

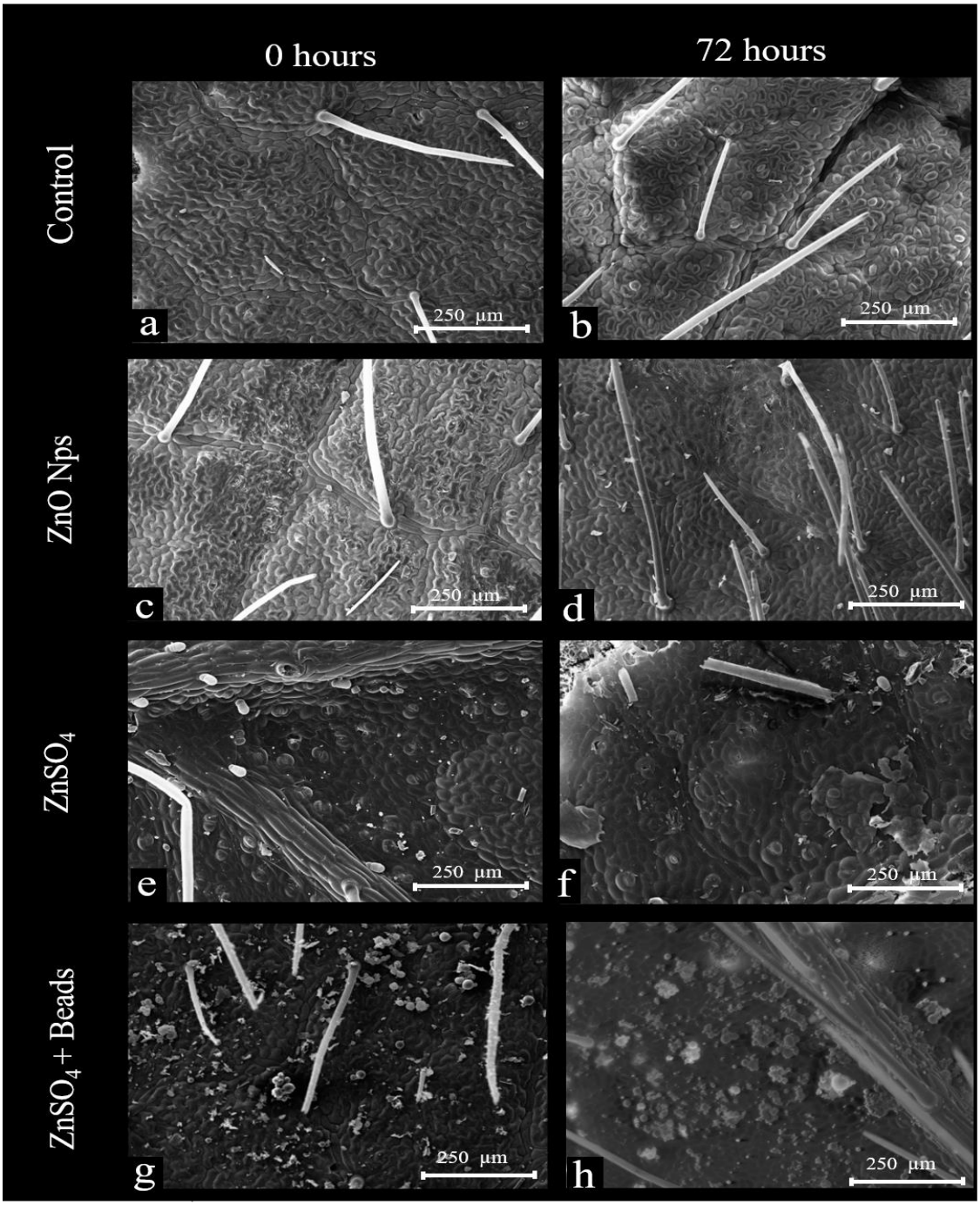

4.4 Discussion

4.4.1 Zn uptake as a function of source

The X-ray fluorescence-assisted experiment to Zn transport in the petiole showed that during the first 72 hours, the $ZnSO_4$ + Beads was more efficient in supplying Zn to plants. However, the long-term experiment showed that the Zn sources did not present statistical difference neither for Zn concentration nor for Zn content. It is important to recall that the concentration of Zn employed in the latter and the former were 4-fold apart. While $ZnSO_4$ quickly supplied Zn to leaf tissue, the dose of Zn was too high causing the toxic effects and making the tissue unable to continue absorbing. On the other hand, the $ZnSO_4$ + Beads offered a reduced Zn supply rate, compared to the $ZnSO_4$, but an increased one compared to nano ZnO. Thus, since the Zn release rate was intermediate, it ended up in being the Zn source able to deposit high Zn load on the surface, and effectively deliver it to the plants at the higher rates without any phytotoxic effects.

Generally, the rate of Zn absorption and transport from soluble sources ($ZnSO_4$) is higher than insoluble sources regardless the nutrient is taken up by roots, such as demonstrated by Cruz et al.,[18] or leaves as shown by Gomes et al.[16] who reveals that Zn solubility is the most important factor controlling Zn uptake. Since dependence between size the dissolution rate become highly evident below a certain particle size, nanoparticles are alternative forms to supply insoluble sources as ZnO and $ZnCO_3$, which are considered sources with low uptake velocity.[16; 33] The increase in fertilizer efficiency of insoluble sources as nanoparticles is well known in the literature,[34; 35] the solubility of nano ZnO is inversely proportional to the particle size.[16; 36] Positive effects of nano fertilizers on crop production have been presented by Du et al.[37] and Yusefi-Tanha et al.[38] However, there is a concern about the use of nano-based products in agriculture and possible negative effect on plant development.[36; 39] An important mechanism of nanotoxicity regards the overproduction of reactive oxygen species.[38; 40]

4.4.2 Oxidative metabolism

The reactive oxygen species can be a by-product of light reaction in chloroplasts during photosynthesis,[41] while the enzymatic antioxidant defense includes SOD, catalase, ascorbate peroxidase, and glutathione peroxidase.[42] In the present study, Zn sources did not influence MDA, H_2O_2, catalase, SOD, GPOX and APX, and protein. These enzymes and substances in plants are altered when the plants have stress conditions.[39]

Yusefi-Tanha et al.[38] showed that higher Zn concentration (400 mg kg^{-1}) increased the oxidative stress responses with the increase in H_2O_2, MDA, SOD, CAT, POX in soybean. In

contrast, Dimkpa et al.[43] testing a ZnO nanoparticle rate of 500 mg Zn kg^{-1} in wheat, and Liu et al.[44] testing a rate of 800 mg Zn kg $soil^{-1}$ in corn did not detect any negative effects. Probably, in the present study, the Zn inputs did not cause oxidative stress responses because the Zn rate, ie. of 300 g ha^{-1}, was split into three applications of 100 g each. As expected, the applied Zn contributed to maintain adequate Zn concentration in leaves (23 mg kg^{-1}) and plant accumulation (0.5 mg $plant^{-1}$). It is important to highlight that all these studies were performed under root exposure to the Zn sources.

Interestingly, glutathione reductase was increased by Zn with an increase of activities, mainly with the root application of $ZnSO_4$. The glutathione reductase is classified as a small intracellular thiol molecule considered as a strong non-enzymatic antioxidant,[45] which maintains the intracellular glutathione pool in the response to oxidative stress, functioning as an antioxidant that scavenges reactive oxygen species such as hydrogen peroxide and superoxide.[46] The balance between ascorbic acid and glutathione (found at high concentrations in chloroplasts) is maintained by glutathione reductase and considered crucial for plant defense against oxidative stress.[40] The increase in glutathione biosynthesis in chloroplasts can result in oxidative damage to cells rather than their protection.[40] Generally, plants increase the production of reactive oxygen species in mitochondria, chloroplasts, and peroxisomes as a response to abiotic stress and pathogenic defense.[39; 40] In the present study, there was no biotic or abiotic stress, except from zinc starvation in the Hoagland solution.

The present study also shows the treatments did not affect oxidative metabolism. Yusefi-Tanha et al.[38] testing the spherical 38, 59, and 500 nm ZnO noticed that the highest oxidative stress responses (H_2O_2 synthesis, MDA, SOD, CAT, POX) was found for 38 nm. While Dimkpa et al.[2] showed that 18 nm spherical ZnO did not affect the plant biomass, one the other hand, it increased chlorophyll content, shoot height, and grain yield in winter wheat.

4.5 Conclusion

The cellulose microbeads were able to absorb up to 12% of its own wet weigh in zinc. In vitro experiments showed that both zinc absorption and zinc release, in water, take place within few minutes.

The short-term experiments using portable X-ray fluorescence spectrometry indicate that the Zn transport depends on the source. The Zn transport supplied from cellulose microspheres ($ZnSO_4$ + Beads), was much higher than the Zn transport supplied from the $ZnSO_4$ and ZnO nanoparticles sources.

The Zn accumulation increased Zn by 42% compared to control when Zn is supplied in adequate amount exclusively through roots. This indicated that the plant absorption and translocation were more efficient under root *via*. In the long-term, the treatments applied at V5 and V7 stages neither statistically affected the biomass production nor the concentration of Zn in the upper leaves. Although the average Zn content in the plants that received the foliar treatments were slightly above the control, they were statistically the same. The reason for the absence of statistical significance might the high variability presented by the dataset. Nevertheless, since plants were grown under hydroponic media, one has to be careful in extrapolating the results here presented to field conditions. Under soil, root uptake efficiency is expected to be smaller than that observed in solution.

References

1 COMPANHIA NACIONAL DE ABASTECIMENTO. **Acompanhamento da safra brasileira:** grãos, safra 2020/2021, 11º levantamento. Brasília, DF: Conab, 2021.

2 DIMKPA, C. O. et al. Effects of manganese nanoparticle exposure on nutrient acquisition in wheat (*Triticum aestivum* L.). **Agronomy-Basel,** v. 8, n. 9, art. 158, 2018.

3 VITTI, G. C.; TREVISAN, W. **Manejo de macro e micronutrientes para alta produtividade da soja**. Piracicaba: POTAFOS, 2000. (Informações Agronômicas, n. 90).

4 CAO, M. L.; LI, Y. X.; DU, H. L. Effects of exogenous zinc on the photosynthesis and carbonic anhydrase activity of millet (*Setaria italica* L.). **Photosynthetica,** v. 58, n. 3, p. 712-719, 2020.

5 ESCUDERO-ALMANZA, D. J. et al. Carbonic anhydrase and zinc in plant physiology. **Chilean Journal of Agricultural Research,** v. 72, n. 1, p. 140-146, 2012.

6 BERGES, J. A. et al. Enzymes and nitrogen cycling. In: CAPONE, D. G. et al. **Nitrogen in the marine environment.** 2. ed. San Diego: Academic Press, 2008. p. 1385-1444.

7 RINALDO, S. et al. Nitrite reductases in denitrification. In: BOTHE, H.; FERGUSON, S.; NEWTON, W. E. **Biology of the nitrogen cycle**. Amsterdam: Elsevier, 2007. p. 37-55.

8 DEFEZ, R.; ANDREOZZI, A.; BIANCO, C. The overproduction of indole-3-acetic acid (IAA) in endophytes upregulates nitrogen fixation in both bacterial cultures and inoculated rice plants. **Microbial Ecology,** v. 74, n. 2, p. 441-452, 2017.

9 OUYANG, L. M.; PEI, H. Y.; XU, Z. H. Low nitrogen stress stimulating the indole-3-acetic acid biosynthesis of *Serratia* sp. ZM is vital for the survival of the bacterium and its plant growth-promoting characteristic. **Archives of Microbiology,** v. 199, n. 3, p. 425-432, 2017.

10 BHAT, A. P.; GOGATE, P. R. Degradation of nitrogen-containing hazardous compounds using advanced oxidation processes: a review on aliphatic and aromatic amines, dyes, and pesticides. **Journal of Hazardous Materials,** v. 403, p. 123657, 2021.

11 OLIVEIRA, F. C. et al. Diferentes doses e épocas de aplicação de zinco na cultura da soja. **Revista de Agricultura Neotropical,** v. 4, n. 5, p. 28–35, 2017.

12 HEIDARIAN, A. R. et al. Investigating Fe and Zn foliar application on yield and its components of soybean (*Glycine max* (L) Merr.) at different growth stages. **Journal of Agricultural Biotechnology and Sustainable Development,** v. 3, n. 9, p. 189 -197, 2011.

13 CUNHA, J. F.; FRANCISCO, E. A. B.; PROCHNOW, L. I. **Balanço de nutrientes na agricultura brasileira no período de 2013 a 2016**. Piracicaba: International Plant Nutrition Institute (IPNI), 2018.

14 FERNÁNDEZ, V.; SOTIROPOULOS, T.; BROWN, P. **Adubação foliar:** fundamentos científicos e técnicas de campo. São Paulo: Abisolo, 2015.

15 CASTRO, P. R. C. **Princípios da adubação foliar**. Jaboticabal: Funep, 2009.

16 GOMES, M. H. F. et al. In vivo evaluation of Zn foliar uptake and transport in soybean using X-ray absorption and fluorescence spectroscopy. **Journal of Agricultural and Food Chemistry,** v. 67, n. 44, p. 12172-12181, 2019.

17 SERVIN, A. et al. A review of the use of engineered nanomaterials to suppress plant disease and enhance crop yield. **Journal of Nanoparticle Research,** v. 17, art. 92, 2015.

18 CRUZ, T. N. M. et al. Shedding light on the mechanisms of absorption and transport of ZnO nanoparticles by plants via in vivo X-ray spectroscopy. **Environmental Science-Nano,** v. 4, n. 12, p. 2367-2376, 2017.

19 PRASAD, T. et al. Effect of nanoscale zinc oxide particles on the germination, growth and yield of peanut. **Journal of Plant Nutrition,** v. 35, n. 6, p. 905-927, 2012.

20 VAN CAUWENBERGHE, L.; JANSSEN, C. R. Microplastics in bivalves cultured for human consumption. **Environmental Pollution,** v. 193, p. 65-70, 2014.

21 OBRIEN, J. C. et al. Continuous production of cellulose microbeads via membrane emulsification. **ACS Sustainable Chemistry & Engineering,** v. 5, n. 7, p. 5931-5939, 2017.

22 MEURER, R. A. et al. Biofunctional microgel-based fertilizers for controlled foliar delivery of nutrients to plants. **Angewandte Chemie-International Edition,** v. 56, n. 26, p. 7380-7386, 2017.

23 HEATH, R. L.; PACKER, L. Photoperoxidation in isolated chloroplasts: I. Kinetics and stoichiometry of fatty acid peroxidation. **Archives of Biochemistry and Biophysics,** v. 125, n. 1, p. 189-198, 1968.

24 AZEVEDO, R. A. et al. Response of antioxidant enzymes to transfer from elevated carbon dioxide to air and ozone fumigation, in the leaves and roots of wild-type and a catalase-deficient mutant of barley. **Physiologia Plantarum,** v. 104, n. 2, p. 280-292, 1998.

25 BRADFORD, M. M. A rapid and sensitive method for the quantitation of microgram quantities of protein utilizing the principle of protein-dye binding. **Analytical Biochemistry,** v. 72, n. 1, p. 248-254, 1976.

26 GIANNOPOLITIS, C. N.; RIES, S. K. Superoxide dismutases: 1. Occurrence in higher-plants. **Plant Physiology,** v. 59, n. 2, p. 309-314, 1977.

27 CEMBROWSKA-LECH, D.; KOPROWSKI, M.; KEPCZYNSKI, J. Germination induction of dormant Avena fatua caryopses by KAR_1 and GA_3 involving the control of reactive oxygen species (H_2O_2 and $O_2.^-$) and enzymatic antioxidants (superoxide dismutase and catalase) both in the embryo and the aleurone layers. **Journal of Plant Physiology,** v. 176, p. 169-179, 2015.

28 MATSUNO, H.; URITANI, I. Physiological behavior of peroxidase isozymes in sweet potato root tissue injured by cutting or with black rot. **Plant and Cell Physiology,** v. 13, n. 6, p. 1091-1101, 1972.

29 MOLDES, C. A. et al. Biochemical responses of glyphosate resistant and susceptible soybean plants exposed to glyphosate. **Acta Physiologiae Plantarum,** v. 30, n. 4, p. 469-479, 2008.

30 KRAUS, T. E.; MCKERSIE, B. D.; FLETCHER, R. A. Paclobutrazol-induced tolerance of wheat leaves to paraquat may involve increased antioxidant enzyme-activity. **Journal of Plant Physiology,** v. 145, n. 4, p. 570-576, 1995.

31 ALEXIEVA, V. et al. The effect of drought and ultraviolet radiation on growth and stress markers in pea and wheat. **Plant Cell and Environment,** v. 24, n. 12, p. 1337-1344, 2001.

32 FERNANDEZ, V.; BROWN, P. H. From plant surface to plant metabolism: the uncertain fate of foliar-applied nutrients. **Frontiers in Plant Science,** v. 4, art. 289, 2013.

33 MACHADO, B. A. et al. X-ray spectroscopy fostering the understanding of foliar uptake and transport of Mn by soybean (*Glycine max* L. Merril): kinetics, chemical speciation, and effects of glyphosate. **Journal of Agricultural and Food Chemistry,** v. 67, n. 47, p. 13010-13020, 2019.

34 DIMKPA, C. O. et al. Composite micronutrient nanoparticles and salts decrease drought stress in soybean. **Agronomy for Sustainable Development,** v. 37, art. 5, 2017.

35 LIU, R. Q.; ZHANG, H. Y.; LAL, R. Effects of stabilized nanoparticles of copper, zinc, manganese, and iron oxides in low concentrations on lettuce (*Lactuca sativa*) seed germination: nanotoxicants or nanonutrients? **Water Air and Soil Pollution,** v. 227, art. 42, 2016.

36 YOON, S. J. et al. Zinc oxide nanoparticles delay soybean development: a standard soil microcosm study. **Ecotoxicology and Environmental Safety,** v. 100, p. 131-137, 2014.

37 DU, W. et al. Comparison study of zinc nanoparticles and zinc sulphate on wheat growth: from toxicity and zinc biofortification. **Chemosphere,** v. 227, p. 109-116, 2019.

38 YUSEFI-TANHA, E. et al. Zinc oxide nanoparticles (ZnONPs) as a novel nanofertilizer: influence on seed yield and antioxidant defense system in soil grown soybean (*Glycine max* cv. Kowsar). **Science of The Total Environment,** v. 738, art. 140240, 2020.

39 COMAN, V. et al. Soybean interaction with engineered nanomaterials: a literature review of recent data. **Nanomaterials,** v. 9, n. 9, art. 1248, 2019.

40 MITTLER, R. Oxidative stress, antioxidants and stress tolerance. **Trends in Plant Science,** v. 7, n. 9, p. 405-410, 2002.

41 HUANG, H. L. et al. Mechanisms of ROS regulation of plant development and stress responses. **Frontiers in Plant Science,** v. 10, art. 800, 2019.

42 APEL, K.; HIRT, H. Reactive oxygen species: metabolism, oxidative stress, and signal transduction. **Annual Review of Plant Biology,** v. 55, p. 373-399, 2004.

43 DIMKPA, C. O. et al. CuO and ZnO nanoparticles: phytotoxicity, metal speciation, and induction of oxidative stress in sand-grown wheat. **Journal of Nanoparticle Research,** v. 14, n. 9, art. 1125, 2012.

44 LIU, X. Q. et al. Bioavailability of Zn in ZnO nanoparticle-spiked soil and the implications to maize plants. **Journal of Nanoparticle Research,** v. 17, n. 4, art. 175, 2015.

45 HASANUZZAMAN, M. et al. Glutathione in plants: biosynthesis and physiological role in environmental stress tolerance. **Physiology and Molecular Biology of Plants,** v. 23, n. 2, p. 249-268, 2017.

46 YOUSUF, P. Y. et al. Role of glutathione reductase in plant abiotic stress. In: AHMAD, P.; PRASAD, M. N. V. **Abiotic stress responses in plants:** metabolism, productivity and sustainability. New York: Springer, 2012. p. 149-158.

5 CONCLUSION

The investigation of absorption, transport and metabolism of Zn applied on soybean leaves from the sources described in this study, allows us to make some conclusions.

In vivo XRF assays demonstrated faster absorption and transport of Zn when applied as $ZnSO_4$ aqueous solution compared to a ZnO commercial suspension. The major factor driving the Zn absorption was the higher solubility of the $ZnSO_4$. The XANES analysis demonstrated that zinc was transported through plant petiole coordinated by organic acids, *i.e*. as Zn-malate and Zn-citrate.

The combined absorption and transport rate for Zn-phosphite were faster than those of Zn EDTA. Both fertilizers caused dissolution of leaf cuticle and the higher absorption of Zn-phosphite might be a consequence of the higher diffusion coefficient of zinc from this source. The accumulation of Zn-phosphite crystals in the proximity of leaf stomata may occasion later Zn uptake stomata pathway. Once in the petiolule, the Zn from Zn-phosphite was transformed and could not be identified while that from Zn-EDTA remained in its pristine form.

Cellulose microbeads were able to absorb and release Zn, in water, within few minutes. In a short period of time the Zn transport was much higher when supplied by a mixture of $ZnSO_4$ and cellulose microspheres compared to ZnO nanoparticles and pristine $ZnSO_4$. It seems that the elevated dose of $ZnSO_4$ induced toxicity to plant tissue, while the same dose supplied as $ZnSO_4$+Beads did not cause collateral effects. It happened because the Zn within the beads was slowly released to the plant. Here it is important to highlight; the release profile of Zn from the beads was intermediate, between the $ZnSO_4$ and ZnO. Thus it motivates further studies to tune the technology transforming it in a controlled release fertilizer. In principle, the concept can be extended to other micronutrients. In longer trials, Zn accumulation in plant shoot was higher for the root application compared to leaf application. Once again, one should consider that these experiments were carried out under hydronic condition, in which root uptake faces no barrier or difficulty as compared to soil. At long-term, none of the foliar treatments statistically affected the biomass production, concentration of Zn in the upper leaves, Zn concentration in the whole shoot, and the oxidative enzymatic metabolism.

The development of new nutrients sources as well as new techniques for plant analysis are fundamental for an environmentally friend agriculture able to deliver the necessary high yields. They allow the increase of nutrient employment avoiding environmental issues *e.g* leaching, volatilization and accumulation. Furthermore, they increase nutrient absorption and utilization by plants, which enhance their development, yield and quality. More studies are necessary on this context for better understanding of all the processes involved on the absorption, transport and metabolization of nutrients by plans.

Appendix or Annex

In Vivo Evaluation of Zn Foliar Uptake and Transport in Soybean Using X-ray Absorption and Fluorescence Spectroscopy

Author: Marcos H. F. Gomes, Bianca A. Machado, Eduardo S. Rodrigues, et al

Publication: Journal of Agricultural and Food Chemistry

Publisher: American Chemical Society

Date: Nov 1, 2019

SPRINGER NATURE LICENSE

TERMS AND CONDITIONS

Aug 27, 2021

This Agreement between Mr. Marcos Henrique Feresin Gomes ("You") and Springer Nature ("Springer Nature") consists of your license details and the terms and conditions provided by Springer Nature and Copyright Clearance Center.

License Number	5137110631349
License date	Aug 27, 2021
Licensed Content Publisher	Springer Nature
Licensed Content Publication	Journal of Soil Science and Plant Nutrition
Licensed Content Title	Foliar Application of Zn Phosphite and Zn EDTA in Soybean (Glycine max (L.) Merrill): In Vivo Investigations of Transport, Chemical Speciation, and Leaf Surface Changes
Licensed Content Author	Marcos Henrique Feresin Gomes et al
Licensed Content Date	Sep 16, 2020
Type of Use	Thesis/Dissertation
Requestor type	academic/university or research institute
Format	print and electronic
Portion	full article/chapter
Will you be no translating?	
Circulation/distribution	200 - 499
Author of this Springer Nature content	yes

Title : Characterization of the foliar uptake of zinc sources by soybean (Glycine max L.)

Institution name	University of Sao Paulo
Expected presentation Date:	Oct 2021
Requestor Location:	Mr. Marcos Henrique Feresin Gomes Rua Padre Galvão PIRACICABA, São Paulo 13416008 - Brazil Attn: Agriculture

Total 0.00 USD

Terms and Conditions

Springer Nature Customer Service Centre GmbH
Terms and Conditions

This agreement sets out the terms and conditions of the licence (the **Licence**) between you and **Springer Nature Customer Service Centre GmbH** (the **Licensor**). By clicking 'accept' and completing the transaction for the material (**Licensed Material**), you also confirm your acceptance of these terms and conditions.

GRANT OF LICENSE

1. 1. The Licensor grants you a personal, non-exclusive, non-transferable, world-wide licence to reproduce the Licensed Material for the purpose specified in your order only. Licences are granted for the specific use requested in the order and for no other use, subject to the conditions below.

1. 2. The Licensor warrants that it has, to the best of its knowledge, the rights to license reuse of the Licensed Material. However, you should ensure that the material you are requesting is original to the Licensor and does not carry the copyright of another entity (as credited in the published version).

1. 3. If the credit line on any part of the material you have requested indicates that it was reprinted or adapted with permission from another source, then you should also seek permission from that source to reuse the material.

SCOPE OF LICENCE

2. 1. You may only use the Licensed Content in the manner and to the extent permitted by these Ts&Cs and any applicable laws.

2. 2. A separate licence may be required for any additional use of the Licensed Material, e.g. where a licence has been purchased for print only use, separate permission must be obtained for electronic re-use. Similarly, a licence is only valid in the language selected and does not apply for editions in other languages unless additional translation rights have been granted separately in the licence. Any content owned by third parties are expressly excluded from the licence.

2. 3. Similarly, rights for additional components such as custom editions and derivatives require additional permission and may be subject to an additional fee.
Please apply to
Journalpermissions@springernature.com/bookpermissions@springernature.com for these rights.

2. 4. Where permission has been granted **free of charge** for material in print, permission may also be granted for any electronic version of that work, provided that the material is incidental to your work as a whole and that the electronic version is essentially equivalent to, or substitutes for, the print version.

2. 5. An alternative scope of licence may apply to signatories of the STM Permissions Guidelines, as amended from time to time.

DURATION OF LICENCE

3. 1. A licence for is valid from the date of purchase ('Licence Date') at the end of the relevant period in the below table:

	Duration of Licence
Post on a website	12 months
Presentations	12 months
Scope of Licence	
Books and journals Lifetime of the edition in the language purchased	

ACKNOWLEDGEMENT

4. 1. The Licensor's permission must be acknowledged next to the Licenced Material in print. In electronic form, this acknowledgement must be visible at the same time as the figures/tables/illustrations or abstract, and must be hyperlinked to the journal/book's homepage. Our required acknowledgement format is in the Appendix below.

RESTRICTIONS ON USE

5. 1. Use of the Licensed Material may be permitted for incidental promotional use and minor editing privileges e.g. minor adaptations of single figures, changes of format, colour and/or style where the adaptation is credited as set out in Appendix 1 below. Any other changes including but not limited to, cropping, adapting, omitting material that affect the meaning, intention or moral rights of the author are strictly prohibited.

5. 2. You must not use any Licensed Material as part of any design or trademark.

5. 3. Licensed Material may be used in Open Access Publications (OAP) before publication by Springer Nature, but any Licensed Material must be removed from OAP sites prior to final publication.

OWNERSHIP OF RIGHTS

6. 1. Licensed Material remains the property of either Licensor or the relevant third party and any rights not explicitly granted herein are expressly reserved.

WARRANTY

IN NO EVENT SHALL LICENSOR BE LIABLE TO YOU OR ANY OTHER PARTY OR ANY OTHER PERSON OR FOR ANY SPECIAL, CONSEQUENTIAL, INCIDENTAL OR INDIRECT DAMAGES, HOWEVER CAUSED, ARISING OUT OF OR IN CONNECTION WITH THE DOWNLOADING, VIEWING OR USE OF THE MATERIALS REGARDLESS OF THE FORM OF ACTION, WHETHER FOR BREACH OF CONTRACT, BREACH OF WARRANTY, TORT, NEGLIGENCE, INFRINGEMENT OR OTHERWISE (INCLUDING, WITHOUT LIMITATION, DAMAGES BASED ON LOSS OF PROFITS, DATA, FILES, USE, BUSINESS OPPORTUNITY OR CLAIMS OF THIRD PARTIES), AND WHETHER OR NOT THE PARTY HAS BEEN ADVISED OF THE POSSIBILITY OF SUCH DAMAGES. THIS LIMITATION SHALL APPLY NOTWITHSTANDING ANY FAILURE OF ESSENTIAL PURPOSE OF ANY LIMITED REMEDY PROVIDED HEREIN.

LIMITATIONS

8. 1. ***BOOKS ONLY:*** Where **'reuse in a dissertation/thesis'** has been selected the following terms apply: Print rights of the final author's accepted manuscript (for clarity, NOT the published version) for up to 100 copies, electronic rights for use only on a personal website or institutional repository as defined by the Sherpa guideline (www.sherpa.ac.uk/romeo/).

8. 2. For content reuse requests that qualify for permission under the STM Permissions Guidelines, which may be updated from time to time, the STM Permissions Guidelines supersede the terms and conditions contained in this licence.

TERMINATION AND CANCELLATION

9. 1. Licences will expire after the period shown in Clause 3 (above).

9. 2. License reserves the right to terminate the Licence in the event that payment is not received in full or if there has been a breach of this agreement by you.

Appendix 1 - Acknowledgements:

For Journal Content:

Reprinted by permission from [**the Licensor**]: [**Journal Publisher** (e.g. Nature/Springer/Palgrave)] [**JOURNAL NAME**] [**REFERENCE CITATION** (Article name, Author(s) Name), [**COPYRIGHT**] (year of publication)

For **Advance Online Publication papers:**

Reprinted by permission from [**the Licensor**]: [**Journal Publisher** (e.g. Nature/Springer/Palgrave)] [**JOURNAL NAME**] [**REFERENCE CITATION** (Article name, Author(s) Name), [**COPYRIGHT**] (year of publication), advance online publication, day month year (doi: 10.1038/sj. [JOURNAL ACRONYM].)

For Adaptations/Translations:

Adapted/Translated by permission from [**the Licensor**]: [**Journal Publisher** (e.g. **Nature/Springer/Palgrave)] [**JOURNAL NAME**] [**REFERENCE CITATION
(Article name, Author(s) Name), [**COPYRIGHT**] (year of publication)

Note: For any republication from the British Journal of Cancer, the following credit line style applies:

Reprinted/adapted/translated by permission from [**the Licensor**]: on behalf of Cancer Research UK:- [**Journal Publisher** (e.g. Nature/Springer/Palgrave)] [**JOURNAL NAME**] [**REFERENCE CITATION** (Article name, Author(s) Name), [**COPYRIGHT]** (year of publication) For **Advance Online Publication** papers: Reprinted by permission from The [**the Licensor**]: on behalf of Cancer Research UK: [**Journal Publisher** (e.g. Nature/Springer/Palgrave)] [**JOURNAL NAME**]
[**REFERENCE CITATION** (Article name, Author(s) Name), [**COPYRIGHT**] (year of publication), advance online publication, day month year (doi: 10.1038/sj.
[JOURNAL ACRONYM])

For Book content:

Reprinted/adapted by permission from [**the Licensor**]: [**Book Publisher** (e.g. Palgrave Macmillan, Springer etc) [**Book Title**] by [**Book author**(s)] [**COPYRIGHT**] (year of publication)

Other Conditions:

Version 1.3

Questions? customercare@copyright.com or +1-855-239-3415 (toll free in the US) or +1-978-646-2777.